Environmental Laboratory

US Army Corps
of Engineers®
Engineer Research and
Development Center

Hydroacoustic Evaluation of Fish Passage Through Bonneville Dam in 2000

Gene R. Ploskey, Carl R. Schilt, Michael E. Hanks,
John R. Skalski, William T. Nagy, Peter N. Johnson,
Deborah S. Patterson, Jina Kim, and Larry R. Lawrence

May 2002

Hydroacoustic Evaluation of Fish Passage Through Bonneville Dam in 2000

by   Gene R. Ploskey

Pacific Northwest National Laboratory
902 Battelle Boulevard
Richland, WA   99352

Carl R. Schilt, Michael E. Hanks, Peter N. Johnson, Jina Kim

Mevatec Corporation
1525 Perimeter Parkway
Huntsville, AL   35806

William T. Nagy

U.S. Army Engineer District, Portland
P.O. Box 2946
Portland, OR   97208-2946

Deborah S. Patterson

DynTel Corporation
3530 Manor Drive, Suite 4
Vicksburg, MS 39180

Larry R. Lawrence

Environmental Laboratory
U.S. Army Engineer Research and Development Center
3909 Halls Ferry Road
Vicksburg, MS 39180-6199

Final report

Contents

List of Figures

List of Tables

Preface

This report was prepared by the Fisheries Engineering Team (FET), Water Quality and Contaminant Modeling Branch (WQCMB), Environmental Processes and Effects Division (EPED), Environmental Laboratory (EL), U.S. Army Engineer Research and Development Center (ERDC), with support from the Pacific Northwest National Laboratory, Richland, WA, Mevatec Corporation, Huntsville, AL, DynTel Corporation, Vicksburg, MS, AScI, Inc., McLean, VA, the U.S. Army Engineer District, Portland (CENWP), and the University of Washington, Seattle. The research was conducted under the general supervision of Dr. Mark Dortch, Chief, WQCMB; Dr. Richard Price, Chief, EPED; and Dr. Edwin Theriot, Director, EL. Blaine Ebberts, CENWP, provided technical oversight.

Many people made valuable contributions to this study. Toni Schneider managed interagency transfers and allocation of funds. Riggers from the Bonneville Project helped with the installation, repair, and removal of hydroacoustic equipment. Schlosser Machine fabricated transducer mounts. Alan Wirtz and Michael Macaulay of Precision Acoustic Systems in Seattle, WA, supplied and calibrated the hydroacoustic equipment. A hard working team of AScI, Inc., technicians (Nathan Barret, Kyle Bouchard, Charlie Escher, Theresa Kuhnhausen, Craig Smith, Keri Taylor, Kevin Thornburg, and Erin Wright) deployed hardware, maintained hydroacoustic systems, and aided with data processing.

At the time of publication of this report the Commander and Executive Director of ERDC was COL John W. Morris III, EN, and the Director was Dr. James R. Houston.

This report should be cited as follows:

> Ploskey, G. R., Schilt, C. R., Hanks, M. E., Skalski, J. R., Nagy, W. T., Johnson, P. N., Patterson, D. S., Kim, J., and Lawrence, L. R. (2002). "Hydroacoustic evaluation of fish passage through Bonneville Dam in 2000," ERDC/EL TR-02-8, U.S. Army Engineer Research and Development Center, Vicksburg, MS.

Conversion Factors, Non-SI to SI Units of Measurement

Non-SI units of measurement used in this report can be converted to SI units as follows:

Multiply	By	To Obtain
cubic feet	0.0283	cubic meters
degrees (angle)	0.01745329	radians
feet	0.3048	meters
inches	25.4	millimeters

Summary

2000 Research

This study was one of many investigations of the U.S. Army Engineer District, Portland (CENWP), involving monitoring and assessment of juvenile fish passage at Bonneville Dam. The program is described in detail in a comprehensive Monitoring and Evaluation Plan developed by the District. Other research efforts in 2000 included a joint study by the U.S. Army Engineer Research and Development Center (ERDC), Environmental Laboratory (EL), and Pacific Northwest National Laboratory (PNNL) to evaluate the performance of a Prototype Surface Collector (PSC) and the fish passage efficiency (FPE) of the extended-length submerged bar screen (ESBS) at Unit 8. The U.S. Geological Survey (USGS) used radio telemetry to study the passage of tagged yearling chinook and steelhead. The PNNL evaluated approach behavior and fish distributions using multi-beam and split-beam sonar techniques in front of the PSC entrance at Unit 5. A joint effort by PNNL, USGS, and EL investigated behavior of tagged yearling chinook as they approached the project using acoustic sonic tag technologies (i.e., acoustic telemetry).

Goal

The goal of this study was to report the first project-wide estimates of FPE, spill efficiency, and spill effectiveness for the Bonneville Project. These data provide a valuable baseline for evaluating the performance of future management efforts to improve juvenile fish passage. Other fish-passage measures include FPE by powerhouse, fish-guidance efficiency (FGE) by turbine, and horizontal and vertical distributions of fish passage at both powerhouses and spillway. Project-wide FPE, spill efficiency, and spill effectiveness have never been empirically determined for Bonneville Dam. It has been assumed that passage is directly related to the amount of flow through each route.

Objectives

Objectives of this study were to:

a. Estimate the proportion of juvenile salmon that pass the project by non-turbine routes, including the proportion of fish that pass at the spillway, above screens or the floor of the PSC at Powerhouse 1.

b. Determine whether spill efficiency and effectiveness measures differ significantly between two levels of spill that occur during the day and at night.

c. Characterize the vertical and lateral distribution of fish passing through Powerhouses 1 and 2 and the spillway.

d. Characterize diel changes in vertical and lateral distributions of smolt-sized fish passing Powerhouse 1 and 2 and the spillway.

e. Determine the vertical distribution of fish at two locations (3-15 ft[1] and 100 ft upstream of Units 12 and 14 at Powerhouse 2) and compare the distributions among locations.

Materials and Methods

Equipment and Calibrations

Samples were taken from PSC Units 1-6 and turbines 7-10 with nine hydroacoustic systems, the spillway with three systems, and Powerhouse 2 turbines and forebay with four systems. Each system consisted of an echosounder, cables, transducers, an oscilloscope, and a computer system. The 420 kHz, circular, single-, or split-beam Precision Acoustic Systems (PAS) transducers were controlled by PAS 103 echosounders and Hydroacoustic Assessments' HARP software running on Pentium-class computers.

Before deployment, all hydroacoustic equipment was transported to Seattle, WA, where PAS electronically checked the echosounders and transducers and calibrated the transducers using a standard transducer from the U.S. Navy. After calibration, receiver gains were calculated to equalize the output voltages among transducers for on-axis targets ranging in hydroacoustic size from –56 to –36 dB $\| 4\boldsymbol{p}\,m^2$. Lengths of fish corresponding to that acoustic size range would be about 1.3 and 15 inches, respectively, for fish insonified within 21 deg of dorsal aspect (Love 1977).

---

[1] A table of factors for converting U.S. customary units of measure to metric (SI) can be found on page xii.

Sampling the PSC

Two different approaches were used to sample smolt passage at the PSC units (1–6). The first was based upon in-turbine deployments and sampling with single-beam transducers and the second relied on split-beam deployments and sampling in the forebay immediately upstream of the PSC slot entrances.

In each of 18 intakes downstream of the PSC, one 7 deg single-beam transducer was mounted at the top of trash rack 1 and aimed straight down 11 deg off the plane of the trash racks. Fish passing through the beam above an elevation located 0.5 m below the top of the PSC floor were classified as collected by the PSC and those passing through the beam at greater ranges were classified as passing under the PSC. The down-looking beams had a blanking distance of 1 m, limited detectability in the first 3 m, and could not sample the sluice opening inside the center slot of every PSC unit.

Slot entrances at center intakes of PSC Units 1, 2, 4, 5, and 6 were sampled with 6 deg split-beam transducers. A team of PNNL researchers sampled the slot entrance at Unit 3. Opposing split-beam transducers were mounted at the top and bottom of the 45-ft tall frame. The lateral position of the transducer pair on the frame was chosen at random so that the pair would sample the north, center, or south third of the 20-ft slot entrance. The frames were deployed by crane and rested on horizontal crossbeams that tied the front of the A and C modules of the PSC together at several elevations. At each slot entrance, one transducer was aimed 6 deg upstream of the plane of slot entrance to count fish near the upper half of the slot. The other transducer was aimed downward 6 deg upstream of the lane of the entrance to count fish entering the bottom half of the slot. Fish passage estimates through every slot were based on counts of traces with trajectories into the PSC, each with an average displacement ≥ 1 cm/ping.

Counts from the PSC slots were considered to be guided fish as an alternative to the guided counts derived from the upper portion of the single-beam transducers within each turbine slot. Thus, there were two competing estimators of collection efficiency depending on the source of the estimate of guided numbers. Unguided numbers were always obtained from counts of fish passing through the deep portion of the in-turbine beams. Vertical distribution estimates in the forebay were obtained by counting fish within 1-m strata in the upper portion of the up-looking split-beam > 6.5 m from that transducer and in 1-m strata in the down-looking split-beam from 6.5 to 25 m from the down-looking transducer. All split-beam transducers had a pulse repetition rate of 10 pings per second and sampled 20 1-minute intervals per hour.

Sampling Units 7, 9, and 10

At turbine Units 7, 9, and 10, hydroacoustic sampling was performed within one of three randomly selected intake slots per turbine. In Units 7 and 9, 7 deg single-beam transducers, one upward- and one downward-angled, were placed in the selected slots to monitor guided and unguided passage, respectively. An identical deployment was made in Unit 10, except that the transducers were 6 deg

split-beams. Sampling was for 20 1-minute intervals per hour per transducer location, and the pulse repetition rate was 14 pings per second for each transducer.

Sampling Unit 8

At Unit 8, the center slot with an ESBS was sampled with an upward- and a downward-angled, 6 deg split-beam transducer to estimate guided and unguided numbers, respectively. Sampling was continuous, 60 minutes per hour, and the pulse repetition rate was 16.7 pings per second for each transducer.

Sampling the Spillway

Spillway Bays 2, 4, 6, 8, 10, 12, 14, and 16 were each sampled with one down-looking, 10 deg single-beam transducer, and Spill Bay 17 was sampled with one down-looking, 12 deg split-beam transducer. Bays were selected to allow interpolation of fish passage to bays that were not sampled and to emphasize sampling at gates that would pass the most water according to the 1999 Fish Passage Plan. Transducers were mounted 28 ft below the tops of spill gates and aimed 8 deg upstream. Transducers were at elevation (EL) 56.5 ft when the gate was closed and at EL 69 ft when the gate was opened 12.5 ft (7 dogs). Maximum ranges from the transducer to the ogee were about 44.7 ft (10 deg beam diameter = 7.9 ft) when a gate was opened 12.5 ft above the ogee and 32.5 ft (10 deg beam diameter = 5.7 ft) when a gate was closed. Dam operations data were used to determine spill gate positions and to estimate range to the ogee for automated processing of data. Based upon fish trajectories and speeds through the split-beam deployed at Spill Bay 17, most fish passed down through the hydroacoustic beam at ranges 8-25 ft from transducers at speeds of 6-12 feet per second (fps) and would have been committed to passing by the time they were detected. Fish approaching at the elevation of the ogee were traveling 13-15 fps as they passed through the beam. Transducers transmitted at 30 pings per second for 12 1-minute periods per hour.

Sampling Powerhouse 2

At Powerhouse 2, one of three intakes at every turbine unit was randomly selected for sampling. A pair of transducers was mounted on the downstream side of trash racks 1 and 4 at each sampled intake. One transducer of each pair was mounted near the top of the uppermost trash rack and aimed downward to sample unguided fish passing below the tip of the traveling screen. The second transducer of each pair was mounted near the bottom of the fourth trash rack from the top and aimed upward to sample fish passing above the tip of the screen. Each transducer transmitted sound pulses at 14 pings per second, and pairs of transducers were fast multiplexed so that each pair sampled 15 1-minute periods per hour, 23 hours per day. The two transducers deployed in Unit 18 were split beams. Three transceivers and computers were used to control the 16 transducers. The locations of transducers within intakes also were randomized among north, center, and south locations. Vertical distributions of fish upstream of Units 14 and 17 at Powerhouse 2 were also sampled. At each unit, an up-looking 6 deg

single-beam transducer was deployed on a clump anchor 100 ft upstream of the turbine intake extensions (TIEs), and a pair of up- and down-looking 6 deg split-beam transducers were used on a pier adjacent to the upstream side of intake trash racks.

Fish Tracking

Since the hydroacoustic sampling effort on Bonneville Dam was so extensive and generated such a large volume of data (156 Gigabytes) in 2000, it was impossible to manually track enough data to make reliable fish-passage estimates with available staff. Therefore, autotracking software developed over the last 3 years by the Fisheries Field Unit and ERDC was relied upon to process raw data into tracked fish observations. Although the autotracker was a very efficient analysis tool, its performance had to be continually verified with respect to trained human trackers. Five human trackers were employed. They received extensive training on raw hydroacoustic data from previous years before the 2000 tracking season began. The autotracker was evaluated by comparing its counts to those of several human trackers who all processed the same sample data sets. This approach was used because fish counts, even for the same files, can vary widely among human trackers.

To evaluate inter-tracker differences, all of the human trackers tracked the same daily samples of all systems from five different days scattered throughout the passage seasons, three in spring and two in summer. Human and autotracked counts were compared for each transducer (channel) because there are important differences in passage characteristics, ranges of interest, trace slopes and lengths, and noise conditions for each deployment site and aiming.

Dam Operations and Fish Passage

All data on project operations and total spill and powerhouse discharge were entered into a data set and integrated with fish passage data. Fish passage was set to zero when passage routes were closed. Turbine discharge at Powerhouse 1 was estimated from megawatts (MW) and head (the difference between the forebay and tailwater elevations) using multiple regression equations. Data files were obtained listing MW, head, and other operations data by 5-minute intervals throughout the season. Another equation was used to estimate discharge through the PSC slot from PSC unit discharge and forebay elevation.

Missing Data

All hydroacoustic systems were operated continuously (> 23 hours/day), except for a 15-45 minute period every morning when data were copied from the acquisition computers, or when equipment failed and data from the affected routes were not collected. Short equipment failures lasting up to 45 minutes were not a problem because fish counts and associated variances could still be estimated from the remaining within-hour samples. Computer lock ups usually were fixed within an hour because staff were on duty from 0800 to 1700 hours and

contractors monitored systems from 1700 to 0800 hours. Missing hourly data that resulted from equipment outages > 45 minutes were estimated by temporal linear interpolation for periods < 6 hours and by spatial interpolation or linear regression for periods > 6 hours.

Detectability Modeling and Spatial Expansions

The count of every fish was expanded based upon the ratio of the opening width to beam diameter at the range of detection:

$$EXP\_NUM = \frac{OW}{[MID\_R \times TAN(\frac{EBA}{2}) \times 2]} \tag{1}$$

where OW is opening width in meters, MID_R is the mid-point range of a trace in meters, TAN is the tangent, and EBA is effective beam angle in degrees.

Effective beam angle depends upon the detectability of fish of different sizes in the acoustic beam and is a function of nominal beam width, ping rate, trace criteria, and fish size, aspect, trajectory, velocity, and range. Detectability for every transducer deployment was modeled to determine effective beam angle as a function of range from a transducer. Target-strength estimates were obtained from the average split-beam transducers and flow data by 1-m depth strata from a physical or computational fluid design (CFD) model. These data and other hydroacoustic-acquisition data were entered into a stochastic detectability model. Model output consisted of effective beam angle as a function of range from a transducer. Polynomials fitted to those data were substituted for EBA in Equation 1 to correct for differences in detectability by range among transducers and locations.

Statistical Estimators and Comparisons

Detailed statistical methods are presented under Materials and Methods in the body of the report.

Results and Discussion

Hydroacoustic Detectability

In spring, most deployments had effective beam angles > 4 deg for the ranges that were sampled. Exceptions included deployments where sampling had to begin at relatively short ranges < 4 m (e.g., those at Unit 8 and up-looking beams on clump anchors 100 ft upstream of TIEs) or where fish and flow moved rapidly through the relatively narrow portions of hydroacoustic beams (e.g., 4-5 m from up-looking transducers in Units 11-18). In summer, curves for effective-beam

angle by range had similar shapes to those modeled in spring, although angles at all ranges tended to be narrower because target strength based upon the average backscattering cross section of summer-run juvenile fish were lower than those of spring-run fish.

The driving force behind efforts to improve detectability modeling is the desire to provide hydroacoustic estimates that are quantitative as well as reliable relative indices to fish passage. Ratio estimators like the FGE of the PSC, ESBSs, and submerged traveling screens (STSs) only require that hydroacoustic beams sampling guided and unguided fish have equal detectability so that ratios of counts, not necessarily the counts themselves, are accurate. Similarly, combining counts from different locations such as powerhouses and a spillway also requires equalization of detectability so that counts from different locations are comparable, although the counts themselves may not be accurate. Nevertheless, accurate counts estimated by proper expansion of detected fish in known sample volumes has the potential to provide estimates with inherent quantitative value as well as providing acceptable relative estimates.

Quality Control on Automated Processing

The autotracker count for each transducer channel proved to be a reasonably good predictor of the mean human count, with the autotracker count explaining about 81 percent of the variation in the mean human tracker count for the 222 transducer channel samples. Different individuals were found to have a tendency toward characteristic biases that manifest themselves in different counts of fish from the same hydroacoustic data sets. Consequently, it is recommended that the data are distributed in such a way that the bias-induced differences are averaged over time.

Project and Powerhouse FPE, Spill Efficiency, and Spill Effectiveness

The proportion of all fish to pass the dam by non-turbine routes (Project FPE) was estimated to be 0.79 in both spring and summer. Although Project FPE was the same in spring and summer, Powerhouse FPE declined by about 6 percent at Powerhouse 1 and by about 19 percent at Powerhouse 2 from the spring estimate to the summer estimate. For Project FPE, the seasonal decline in fish passage efficiency at the screened units (Units 7-18) was offset by increased spillway passage and continued high PSC guidance efficiency through summer, when screen guidance efficiencies were much lower.

In both seasons, fish passage through the spillway was the largest component of project passage (44 percent in spring, 49 percent in summer). Whereas total and daily volumes of water spilled were lower in summer than in spring, the proportion of the total project discharge allotted to spill was lower in spring (average = 33 percent for spring days) than in summer (average = 49 percent for summer days), which explains summer's lower spill effectiveness (1.03 compared to 1.36 in spring). Closing off most of Powerhouse 2 in summer allowed a higher

fraction of total flow for spill and reduced fish passage by the STS-equipped turbines at Powerhouse 2.

The PSC played a major role in improving Project FPE over what it might have been with screened units alone. Adjusting FPE based on the calculated guided passage for Units 1-6 using each day's mean FGE for the three STSs on Powerhouse 1 instead of the mean for the PSC would reduce FPE an average of 6 percent in spring and about 12 percent in summer. Using the daily FGE values from Unit 8's ESBS slightly improves the project-wide FPE in late spring slightly (Unit 8 FGE average = 0.73 for spring days) but the ESBS performs nearly as poorly as the STSs in summer (Unit 8 FGE average = 0.50 for summer days).

Adjustment of PSC efficiency in spring and summer to compensate for not having sampled sluiceways inside the PSC would mean that the PSC really increased Project FPE by 21 percent in spring and 27 percent in summer. According to radio telemetry results, about 50 percent of tagged fish in the PSC passed through the sluice gates of the center intake where hydroacoustics could not sample. If that percentage held for run-of-the-river (untagged) fish, then in-turbine sampling with hydroacoustics would have underestimated PSC efficiency by 15 percent, which would put spring and summer PSC efficiencies at 83 and 84 percent, respectively.

Conservative estimates of PSC performance indicate that it was a highly used route in 2000. The PSC guided an estimated 18 percent of the total Bonneville Dam passage (guided, unguided, and spilled fish combined) in spring and 21 percent of the total detected passage in summer.

Effect of Spill Volume on Major Fish Passage Metrics

Increases in Project FPE and spill efficiency and decreases in spill effectiveness with increasing spill volume were consistent but small. Statistically significant positive relationships were found between Project FPE and spill volume in spring and summer; between spill efficiency and spill in spring but not in summer (although the slope was positive). The slope of the relation between spill effectiveness and spill volume was negative and significant in summer but not in spring. The hypothesis tests on the equality of means of the same metrics detected significant differences between "high spill" and "low spill" means for Project FPE in spring but not summer. Additionally, significant differences were detected for spill efficiency in both spring and summer, but not for spill effectiveness in either season. It is important to note that, whether statistically significant or not, the difference between "high spill" and "low spill" mean daily Project FPE in spring was only about 5 percent and the difference between "high spill" and "low spill" spill efficiency in spring was 7.3 percent. The related mean daily spill volumes associated with those daily FPE improvements involved an increase of 45 percent from the "low spill" mean of about 86,000 ft^3/second to the "high spill" mean of 125,000 ft^3/second. Similarly, the significant difference in summer daily spill efficiency means was 8 percent and associated with a "low spill" mean to "high spill" mean increase of 25 percent (84,500 to 106,000 ft^3/second).

The relationship between estimated passage and spill bay discharge through the same spillway through both seasons showed that a wide range of fish passage estimates were associated with the same discharge level during the day or at night. This result led us to conclude that higher passage is likely a function of some factor other than discharge. In fact, rather than higher spill correlating well with higher passage through single spill bays, it seems that the highest discharge values that are near 15,000 ft^3/second for any spill bay are never associated with the highest passage estimates.

Horizontal Distribution

Relative proportional discharge through the primary passage routes was generally a poor indicator for relative proportional passage among those same routes. The overall lateral distribution of fish passage through Bonneville Dam during the spring was not consistently related to project flow patterns except that about 35 percent of the fish and 32 percent of the water that passed the project passed through Powerhouse 1. Fish passage through Powerhouse 2 and the spillway, by contrast, were not closely related to the flow through each respective structure. Powerhouse 2 passed 21 percent of the fish with 36 percent of the flow, and the spillway passed 44 percent of the fish with only 32 percent of the flow in spring.

Fish passage by spill bay was not entirely a function of discharge by spill bay. Although both fish passage and discharge were lowest through Spill Bays 5-7, the bays that passed the most water did not pass the most fish. More water was spilled through Bays 2-4, relative to other sections of the spill bay, yet the density of fish passage was highest at Bays 11-14 during both spring and summer.

Vertical Distribution

The vertical distribution of fish in front of the PSC at Powerhouse 1 serves well the concept of surface collection. Sample volumes upstream of the PSC were located only about 1-3 m from the face of the PSC. At this distance, from 92 to 99 percent of fish detected upstream of the PSC during the spring and from 85 to 96 percent of summer fish were above the elevation of the PSC floor.

The great majority of fish 100 ft upstream of Powerhouse 2 were distributed above the elevation of the top of the turbine intakes during both spring and summer. Immediately upstream of the trash racks at intakes 14B and 17C, summertime fish distributions were lower in the water column than those observed 100 ft upstream, but most fish were still in a favorable position for diversion by the submerged traveling screens. From 66 to 72 percent of all fish were detected above the elevation of the top of the intake, and from 85 to 93 percent of detected fish were higher in the water column than the tip of the screens.

Temporal Trends in Fish Passage

Perhaps the most significant finding of this study was the summer decline in FGE of turbines with screens while the efficiency of the PSC remained high and relatively stable. Even the efficiency of the ESBS in Unit 8 was as poor as that of STSs in other turbines in late summer. Two factors may contribute to the continued success of the PSC in summer. First, the interception location of the PSC was upstream of the Powerhouse, and second; the PSC was open to the sky and passed relatively more fish during the day than at night. The success of the PSC also probably has a lot to do with depth (45 ft), entrance velocities, and upstream hydraulics. In contrast, most fish passage through Powerhouse 1 turbines occurred at night. The diel pattern of smolt passage through Powerhouse 2 turbines was more corpuscular in spring and summer than nocturnal.

Project FPE did not decline precipitously in summer like the FGE of turbines with screens (Units 7-18) likely due to the following factors: First, Powerhouse 2 with poor FGE in summer was only operating at 25-38 percent of capacity because 5-6 of the units were off most of the time. Second, the efficiency of the PSC did not decline in summer and contributed more to Project FPE in late spring and summer than it did for most of spring. Third, on some days in summer, spill efficiency accounted for a greater proportion of FPE than it did in spring, although overall seasonal trends in both Project FPE and spill efficiency were relatively stable throughout both seasons. Fourth, the proportion of fish relative to the proportion of water passed was relatively constant in spring and summer at the PSC, although spill the effectiveness declined slightly during summer.

Fish Guidance Efficiencies

The STSs performed worse than either the ESBS at Unit 8 or the PSC on Units 1-6 in spring. The FGE of the STSs on Powerhouse 2 averaged only 52 percent in spring although most of the interior units on that powerhouse were somewhat higher. Unit 11's STS performed most poorly. On Powerhouse 1 the PSC and the ESBS performed equally well in spring with estimated FGEs of 72 percent. The southernmost two units of the PSC performed best with FGEs of over 80 percent.

In summer, Powerhouse 2 was largely idle but when interior units were operated their STSs produced relatively high FGEs. Unit 11 again performed poorly but Unit 18 at the southern end did better with an FGE of about 50 percent. STS performance was also lower at Powerhouse 1 (except for Unit 7, which improved slightly), with Units 9 and 10 scoring well below 50 percent. Unit 8's ESBS also performed much more poorly. It went from spring's 72 to 50 percent, or about the same as Unit 7's STS, in summer. In stark contrast, the PSC continued to guide an estimated 72 percent of the fish that passed south of the wing wall, with Units 5 and 6 guiding with over 80 percent efficiency. In-turbine sampling shows that the PSC performed as well as the ESBS did in spring and much better than the ESBS in summer.

Comparing FGE Sampling Methods for the PSC and Unit 8

No significant correlations were found for fish counts in turbine intakes downstream of the PSC with fish counts upstream of 20-ft wide PSC slots, unlike in 1999 when a significant correlation was observed for the 5-ft wide PSC slot treatments. Although counts from split-beam sampling upstream from the PSC were not correlated with the in-turbine single-beam counts, those data can still be used to evaluate the availability of fish for collection. Expanded counts showed that there were twice as many fish above the level of the floor at night and an even higher proportion above the floor during the daytime hours.

The correlation of hydroacoustic and netting estimates of FGE at Unit 8 (r^2=0.65) was better than those for guided and unguided components of FGE. The assumption of equal detectability of guided and unguided smolts must have been reasonable most of the time given correlations between hydroacoustic and netting estimates of FGE with a correlation slope approaching 1. A near 1:1 ratio was found for numbers of guided fish netted in the gatewell to hydroacoustic counts above the ESBS and of numbers of unguided, fyke-netted fish to hydroacoustic counts below the ESBS. Paired t-tests indicated that mean estimates of FGE by the two sampling methods did not differ significantly in spring, and, although differences were significant for both seasons combined, means only differed by 3 percent and probably were biologically meaningless. In summer, the mean hydroacoustic estimate was 6 percent higher than the mean netting estimate.

PSC Guidance Efficiency by Different Methods

Average collection efficiency of the PSC, adjusted by radio telemetry estimates of the proportion of smolts in the PSC that used the center-slot sluiceways in the PSC instead of entering the turbine, averaged 83 percent in spring and 84 percent in summer. Radio telemetry data indicated that approximately half of all radio tagged fish in the PSC passed through the sluiceway. Accordingly, hydroacoustic estimates of total passage at the PSC would have been 15 percent low in 2000. Radio-telemetry and acoustic-telemetry estimates of PSC efficiency for all species combined in spring 2000 were 83 percent and 92 percent, respectively, and those estimates agree with an 83-84 percent hydroacoustic estimate corrected for sluiceway passage. In 1998, hydroacoustic estimates of PSC collection efficiency for 20-ft slot openings in PSC Units 3 and 5 were 87.8 percent in spring and 92 percent in summer. A radio telemetry estimate for 1998 was 97.5 percent for the 20-ft slot treatment. In 1999, hydroacoustic estimates for a 20-ft slot entrance at Unit 5 were 84.4 percent in spring and 75.2 percent in summer. Radio telemetry studies in 1999 estimated 20-ft slot efficiency at 65 percent, the lowest of any estimates by any method.

The PSC was more efficient than a prototype ESBS based upon 1998 and 2000 studies using hydroacoustics and radio telemetry at the PSC and hydroacoustics and netting at Unit 8, and the PSC was clearly more efficient than existing STSs. In spring 1998, PSC collection efficiency for a 20-ft wide slot was estimated as 87.8 percent by hydroacoustics and as 97.5 percent by radio telemetry compared with estimates of about 72 percent FGE for the ESBS

according to National Marine Fisheries Service (NMFS) netting and 80 percent FGE according to hydroacoustics. In summer 1998, the hydroacoustic estimate of PSC FGE was 92 percent compared with 40 and 50 percent for the ESBS by NMFS netting and hydroacoustic sampling. In spring 2000, PSC collection efficiency was estimated to be 83 percent by radio telemetry, 92 percent by acoustic telemetry, and 83-84 percent by hydroacoustic sampling with a radio telemetry adjustment for sluiceway passage compared with an estimate of 69.6 percent and 72.0 percent for the ESBS by NMFS netting and hydroacoustics, respectively. In summer, NMFS netting provided an average ESBS efficiency of 47.6 percent (which was close to the hydroacoustic estimate of 50 percent) compared with a PSC efficiency of 83-84 percent by hydroacoustic sampling.

1 Introduction

Background

The U.S. Army Engineer District, Portland (CENWP) is striving to meet the goal, set in the Biological Opinion, of maximizing fish passage efficiency (FPE) and obtaining 95 percent survival for juvenile salmon passing the Bonneville Project. Project FPE is the percent of all juvenile salmon passing the project by non-turbine routes. To estimate project FPE and survival, the proportions of juvenile salmon that pass through all major routes must be estimated.

The goal of maximizing FPE largely influences operation of the project. Large volumes of spill are presumed to be necessary to compensate for the low fish guidance efficiency (FGE) of screens at both powerhouses, particularly in summer. However, spill volumes are limited to between 50,000 and 75,000 ft^3/second during the day and up to 120 percent of the gas cap set to control total dissolved gas supersaturation. Spill under 50,000 ft^3/second creates eddies and slack water areas. Excessive predation is assumed in the tailrace where currents do not quickly carry fish downstream. Spill levels above 75,000 ft^3/second during the day can lead to high numbers of adult salmon falling back through the spillway, as adults exit the Bradford Island ladder and follow the shoreline around to the forebay of the spillway. Adult salmon do not pass through the ladder at night; therefore, spill can be increased in an attempt to reach 80 percent FPE for a 24-hour period. However, spill above 120,000 ft^3/second typically causes total dissolved gas (TDG) levels to exceed 120 percent saturation. State water-quality standard wavers allow supersaturation up to 120 percent. TDG above this level may result in greater fish mortality than would occur if spill was reduced and more fish were passed through the turbines.

Giorgi and Stevenson (1995) indicated that available biological information was inadequate to design and locate successful surface collector prototypes at Bonneville Dam. They found that information on the vertical and lateral distributions of juvenile salmon in the forebay areas of both powerhouses and the spillway was very limited. No mobile hydroacoustic sampling had been collected before 1996, and the proportion of juvenile salmon approaching Powerhouse 1, the spillway, and Powerhouse 2 had not been estimated.

The Portland District acquired mobile hydroacoustic data on fish distributions in both forebays in 1996 (Ploskey et al. 1998) and 1997 (BioSonics, Incorporated 1998). For Powerhouse 1, these data indicated that higher average fish densities occurred upstream of Units 4-6 in spring and upstream of Units 4-6, 8, and 9 in summer. For Powerhouse 2, average fish densities were highest upstream of Units 11-13 adjacent to the south eddy and sluice chute in spring and in summer. Fish densities also were high upstream of Unit 18 in 1996 but not in 1997. Vertical distribution data showed that most fish were in the upper 15 m of the water column. The low FGE of many submerged traveling screens (STSs) at Bonneville Dam would not be expected from an examination of the vertical distribution data collected within 10 m of the dam. If fish did not alter their vertical distribution from what was observed in forebay areas, data from 1996 and 1997 would suggest that FGE usually would exceed 80 percent.

Diel (24-hour) patterns of smolt passage are not uniform regardless of whether passage is estimated in sluiceways (Uremovich et al. 1980; Willis and Uremovich 1981) or the juvenile bypass system (JBS), Hawkes et al. 1991; Wood et al. 1994). Diel passage through the JBS often has a bimodal distribution with a major peak occurring just after dark and a minor peak after sunrise. In contrast, passage through sluiceways usually is higher during the day than at night (Willis and Uremovich 1981). However, patterns apparently are influenced by the operation of sluice gates (Uremovich et al. 1980), flow, unit outages, and species (Willis and Uremovich 1981). Netting required to estimate FGE is intensive but limited to a few hours per day and therefore does not provide diel information. Diel patterns of passage have important implications for statistical designs to estimate FPE for all three structures at Bonneville. Diel patterns of turbine passage above and below screens were estimated in spring and summer 1996 for randomly selected intakes of every turbine at Powerhouse 2 and every intake of Units 3 and 5 at Powerhouse 1.

Available data indicate that the horizontal distribution of smolt passage among intakes is not uniform. Gatewell sampling has indicated that the number and location of operating units and sluice gates as well as the species of smolt determine lateral distributions of juvenile salmon at Powerhouse 1 (Willis and Uremovich 1981). Interactions among factors may account for a lack of consistency in measures of horizontal patterns by Uremovich et al. (1980), who found fish concentrated at Units 6, 7, and 10; Willis and Uremovich (1981), who found variable patterns depending on operations; and Krcma et al. (1982), who observed most passage at Units 4-6. Considerable amount of FGE data collected at Powerhouse 2 with in-turbine hydroacoustics (e.g., Magne et al. 1989; Stansell et al. 1990) and netting (Gessel et al. 1988; Muir et al. 1989) are of limited value for evaluating the horizontal distribution of passage because they typically focus on one or two units at a time. The Fishery Field Unit attempted hydroacoustic sampling of juvenile salmon passing through several spillway gates in the mid-1980s. Transducers were mounted on the bottom of gates and aimed upward and out from the gate. Apparently, noise generated by sound echoing off of vortices at some gates masked echoes from juvenile salmon and prevented equalized sampling effort among gates. BioSonics tested several methods for sampling spillway passage in 1997 (BioSonics, Incorporated 1998). Their best approach

was to mount transducers on piers and aim them toward the ogee just upstream of the gates. BioSonics also designed a mount to deploy transducers and estimate passage through the second powerhouse sluice chute. Transducers were placed at the bottom center of the upstream bulkhead slot and aimed vertically and slightly upstream.

Vertical distributions of juvenile salmon sampled by fixed-aspect hydro-acoustics also vary seasonally and daily but this information has not been considered for improving juvenile fish passage at Powerhouse 2. For example, late spring and summer operations at Powerhouse 2 now prioritize the use of Turbines 11 and 18 for adult salmon attraction. However, previous studies clearly showed that these units have the lowest FGE for juveniles passing downstream and that juvenile passage through Unit 11 is exceptionally high relative to other units at Powerhouse 2. The FGE of traveling screens was highest at units near the center of the second powerhouse. If Units 11 and 18 did not have turbines, or had turbines with much more benign passage conditions than current turbines have, the current operations would benefit both adults and juveniles. Given the low FGE at Units 11 and 18 in summer, however, 85-90 percent of the juvenile fish passing Powerhouse 2 are passing through turbines rather than the bypass.

Hydroacoustics also has been used on limited spatial and temporal scales to evaluate sampling potential or relative passage among a few routes. Thorne and Kuehl (1989) evaluated the effects of noise on hydroacoustic assessment of passage within several turbines of Powerhouse 1. Results showed that acoustic sampling is feasible at the units they tested. Magne et al. (1986, 1989), Magne (1987), and Stansell et al. (1990) compared smolt passage through turbine Units 11 and 17 with passage estimates obtained by fyke netting.

A corner collector is being designed for the south end of the second power-house. Ploskey et al. (1998) and BioSonics, Incorporated (1998) found high densities of fish upstream of Units 11-13, and Unit 11 had the highest passage of any intake sampled in 1996. Like Fish Farmers Union (FFU) in previous years, BioSonics found that large numbers of fish passed through the sluice chute when that route was available. However, it is not known what contribution the sluice chute or a corner collector could make to Powerhouse 2 or project-wide FPE. Data from Ploskey et al. (1998) indicated that the combined FGE of Units 11, 12, and 13 was only 35 percent. However, operation of the chute increased the com-bined FGE to 87 percent after sluice passage was added to the guided fish terms. This finding could be significant because 1996 mobile hydroacoustic sampling indicated that there was a 2:1 skew in the distribution of passage toward the south end of Powerhouse 2. An important factor contributing to successful fish passage in 1998 was removal of one-half of the turbine intake extensions (TIEs) which reduce lateral flows that carry juvenile migrants toward the sluice chute.

Estimates of FPE can be made by radio telemetry, but only for tagged fish and under the assumption that tagged fish behave like untagged fish in the run at large. Radio telemetry provides species-specific information that hydroacoustics cannot, but it cannot provide the robust horizontal and vertical distribution information that is critical for assessing changes in fish passage or for suggesting improve-ments in interception facilities. Telemetry sample sizes are too small when

divided among 18 turbine units and 16 spill bays or among vertical depth strata. Hydroacoustic sampling not only provides overall measures of project performance, but also can indicate where improvements can be made and what kind and how much of a change might be required. For example, vertical distribution data of fish passing through turbines can provide estimates of FGE for existing screens or for proposed screens assuming that the interception point was lower in the water column. The ability to ask such "what if" questions for run-of-river fish is a unique strength of hydroacoustic sampling. In addition, continuous hydroacoustic sampling allows for regression of performance measures (such as spill efficiency) on continuous operations data such as spill volume. These types of regressions can suggest project operations to optimize juvenile fish passage at a project. Continuous sampling of a large percentage of the out-migrating fish is unique to hydroacoustic sampling.

Site Description

Estimation of FPE and quantification of any enhancement by surface collectors or intake screens is difficult because the Bonneville Project is among the most complex on the Columbia River. From the Oregon shore north toward Washington, the project is composed of a navigation lock, 10-unit Powerhouse 1, Bradford Island, an 18-gate spillway, Cascades Island, and 8-unit Powerhouse 2 (Figure 1). Principal passage routes include the spillway and two powerhouses, but within each powerhouse, fish passage can be through ice/trash sluiceways, turbines, or the JBS. Smolts enter the JBS after they encounter screens in the upper part of turbine intakes and are diverted to gatewell slots and orifices opening to a bypass channel. In 2000, Units 1-6 at Powerhouse 1 were modified to create a prototype surface collector (PSC) for testing the efficacy of deep-slot surface collection. The PSC tested in 2000 was not designed to bypass fish from turbines, and most fish passing into the PSC ultimately passed into turbines or the sluiceway.
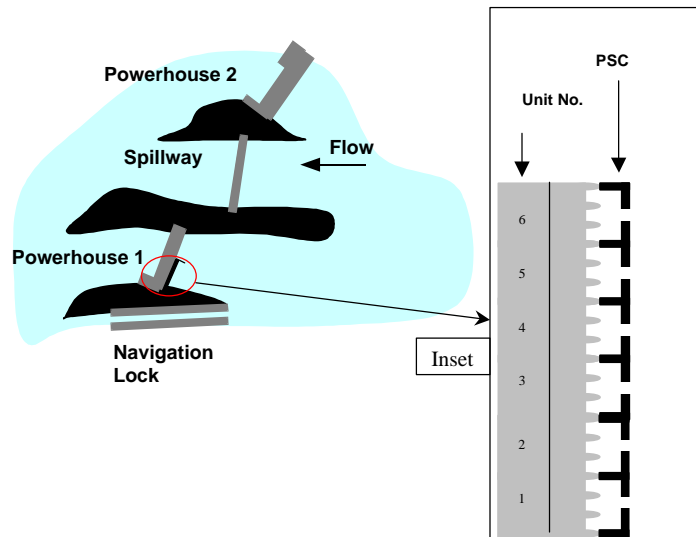
Figure 1.   Plan view of the Bonneville Dam Project. The inset shows the
            Prototype Surface Collector (PSC) that was present in 2000

2000 Research

This study was one of many investigations of the CENWP involving monitoring and assessment of juvenile fish passage at Bonneville Dam. The program is described in detail in a comprehensive Monitoring and Evaluation Plan developed by the District. Other research efforts in 2000 included a joint study by the Engineer Research and Development Center (ERDC), Environmental Laboratory (EL), and the Pacific Northwest National Laboratory (PNNL) to evaluate the performance of a PSC and the FGE of the extended submersible bar screen (ESBS) at Unit 8. The U.S. Geological Survey (USGS) used radio telemetry to study the passage of tagged yearling chinook and steelhead. PNNL evaluated approach behavior and fish distributions using multi-beam and split-beam sonar techniques in front of the PSC entrance at Unit 5. A joint effort by PNNL, USGS, and EL investigated behavior of tagged yearling chinook as they approached the project using acoustic tags (i.e., acoustic telemetry).

Goal

The goal of this study was to report the first project-wide estimates of FPE, spill efficiency, and spill effectiveness for run-of-river juvenile salmon at the Bonneville Project. These data provide a valuable baseline for evaluating the performance of future management efforts to improve juvenile fish passage. Other fish-passage measures include FPE by powerhouse, FGE by turbine, and horizontal and vertical distributions of fish passage at both powerhouses and the spillway.

Objectives

a. Estimate the proportion of juvenile salmon that pass the project by non-turbine routes, including the proportion of fish that pass at the spillway, above screens or above the floor of the PSC at Powerhouse 1.

b. Determine whether spill efficiency and effectiveness measures differ significantly between two levels of spill that occur during the day and at night.

c. Characterize the vertical and lateral distribution of fish passing through the powerhouses and the spillway.

d. Characterize diel changes in the rate of passage of smolt-sized fish passing the powerhouses and the spillway.

e. Determine the vertical distribution of fish at two locations (3-15 ft and 100 ft upstream of Units 14 and 17 at Powerhouse 2) and compare the distributions among locations.

2   Materials and Methods

Equipment

Samples were taken from PSC Units 1-6 and Turbines 7-10 with nine hydroacoustic systems, the spillway with three systems, and Powerhouse 2 turbines and forebay with four systems. Each system consisted of an echosounder, cables, transducers, an oscilloscope, and a computer system. Each echosounder and computer was plugged into an uninterruptible power supply. An echosounder generates electric signals of specific amplitude and at the required pulse repetition rates, and cables conduct those transmit signals from the echosounder to transducers and return data signals from transducers. Transducers convert voltages into sound on transmission and sound into voltages after echoes return to the transducer. The oscilloscopes were used to display echo voltages and calibration tones as a function of time, and the computer system controlled echosounder activity and recorded data to a hard disk. The 420 kHz, circular, single- or split-beam Precision Acoustic Systems (PAS) transducers were controlled by PAS 103 echosounders and Hydroacoustic Assessments' HARP software running on Pentium-class computers.

Calibrations

Before deployment, all hydroacoustic equipment was transported to Seattle, WA, where PAS electronically checked the echosounders and transducers and calibrated the transducers using a standard transducer from the U.S. Navy. After calibration, receiver gains were calculated to equalize the output voltages among transducers for on-axis targets ranging in hydroacoustic size from –56 to –36 dB $\parallel$ $4p\,m^2$ (Tables 1-5). Lengths of fish corresponding to that acoustic size range would be about 1.3 and 15 inches, respectively, for fish insonified within 21 deg of dorsal aspect (Love 1977). Inputs for receiver-gain calculations included calibration data [i.e., echosounder source levels and 40 log (range) receiver sensitivities for specific transducers and cable lengths] and acquisition equipment data and settings (installed cable lengths, maximum output voltage, and on-axis target strengths of the smallest and largest fish of interest). In most instances, calibrated and installed cable lengths were identical. When those cable lengths proved to be different because cable was insufficient for a deployment, an empirically derived

Table 1
Calibration Data, Acquisition Settings, and Calculated Receiver Gains for Single-beam Transducers to Provide Equal Detectability for On-axis Targets Ranging From –36 to –56 dB in Acoustic Size at Powerhouse 1

Echo-sounder Number	Transducer Number and Phase (if split beams)	Calibrated Cable Length (ft)	Source Level (dB)	Maximum Output Voltage (dB)	40 logR Receiver Sensitivity (dB)	Target Strength of largest on-axis target of interest (db)	Calculated Receiver gain (dB)	Installed Cable Length (ft)	Difference in Cable Length Between Calibrated Cable and Installed Cable (ft)	Receiver Gain Adjusted for Difference in Cable Length (dB)	Source Level Adjusted for Difference in Cable Length (dB)	Receiver Sensitivity Adjusted for Difference in Cable Length (dB)	Target Strength of Smallest On-axis Target (dB)	Voltage of Smallest On-axis Target (dB)	Voltage of Smallest On-axis Target at 20 dB per Volt (V)
3	8	650	214.82	70	-112.25	-36	3.43	650	0	3.43	214.82	-112.25	-56	50	2.5
3	7	650	215.25	70	-111.91	-36	2.66	650	0	2.66	215.25	-111.91	-56	50	2.5
3	6	650	214.61	70	-112.81	-36	4.20	674	-24	4.41	214.52	-112.93	-56	50	2.5
3	5	650	215.25	70	-111.83	-36	2.58	625	25	2.36	215.35	-111.70	-56	50	2.5
3	4	650	214.82	70	-112.35	-36	3.53	677	-27	3.77	214.72	-112.49	-56	50	2.5
3	3	650	214.21	70	-113.05	-36	4.84	650	0	4.84	214.21	-113.05	-56	50	2.5
3	2	650	214.88	70	-112.27	-36	3.39	646	4	3.35	214.90	-112.25	-56	50	2.5
3	1	650	214.97	70	-112.05	-36	3.08	647	3	3.05	214.98	-112.03	-56	50	2.5
3	66	650	213.95	70	-113.37	-36	5.42	650	0	5.42	213.95	-113.37	-56	50	2.5
4	67	650	215.40	70	-111.79	-36	2.39	650	0	2.39	215.40	-111.79	-56	50	2.5
4	19	650	215.55	70	-111.87	-36	2.32	650	0	2.32	215.55	-111.87	-56	50	2.5
4	18	650	215.43	70	-111.75	-36	2.32	650	0	2.32	215.43	-111.75	-56	50	2.5
4	17	650	215.49	70	-111.87	-36	2.38	625	25	2.16	215.59	-111.74	-56	50	2.5
4	13	650	214.74	70	-112.75	-36	4.01	648	2	3.99	214.75	-112.74	-56	50	2.5
4	12	650	214.76	70	-112.79	-36	4.03	617	33	3.73	214.89	-112.62	-56	50	2.5
4	11	650	214.97	70	-112.45	-36	3.48	621	29	3.22	215.08	-112.30	-56	50	2.5
4	10	650	215.01	70	-112.17	-36	3.16	681	-31	3.44	214.89	-112.33	-56	50	2.5
4	9	650	214.86	70	-112.33	-36	3.47	651	-1	3.48	214.86	-112.33	-56	50	2.5
4	65	650	214.68	70	-112.99	-36	4.31	650	0	4.31	214.68	-112.99	-56	50	2.5
5	29	650	215.53	70	-111.71	-36	2.18	650	0	2.18	215.53	-111.71	-56	50	2.5
5	28	650	214.76	70	-112.61	-36	3.85	650	0	3.85	214.76	-112.61	-56	50	2.5
5	27	650	215.34	70	-112.05	-36	2.71	649	1	2.70	215.34	-112.04	-56	50	2.5
5	26	650	215.54	70	-111.71	-36	2.17	650	0	2.17	215.54	-111.71	-56	50	2.5
5	23	650	215.49	70	-111.65	-36	2.16	648	2	2.14	215.50	-111.64	-56	50	2.5
5	22	650	215.38	70	-111.91	-36	2.53	648	2	2.51	215.39	-111.90	-56	50	2.5
5	21	650	215.34	70	-111.83	-36	2.49	653	-3	2.52	215.33	-111.84	-56	50	2.5
5	20	650	215.29	70	-111.95	-36	2.66	650	0	2.66	215.29	-111.95	-56	50	2.5
6	24	650	216.09	70	-111.09	-36	1.00	650	0	1.00	216.09	-111.09	-56	50	2.5
6	25	650	215.81	70	-111.39	-36	1.58	650	0	1.58	215.81	-111.39	-56	50	2.5
6	33	650	215.45	70	-112.13	-36	2.68	650	0	2.68	215.45	-112.13	-56	50	2.5
6	32	650	215.44	70	-112.25	-36	2.81	650	0	2.81	215.44	-112.25	-56	50	2.5
6	31	650	215.30	70	-112.37	-36	3.07	650	0	3.07	215.30	-112.37	-56	50	2.5
6	30	650	215.53	70	-111.69	-36	2.16	651	-1	2.17	215.53	-111.69	-56	50	2.5

Table 2
Calibration Data, Acquisition Settings, and Calculated Receiver Gains for Split-beam Transducers to Provide Equal Detectability for On-axis Targets Ranging From –56 to –36 dB in Acoustic Size at Powerhouse 1. Results for each transducer are presented for the x phase, y phase, and mean of x and y phases

Echo-sounder Number	Transducer Number and Phase (if split beams)	Calibrated Cable Length (ft)	Source Level (dB)	Maximum Output Voltage (dB)	40 logR Receiver Sensitivity (dB)	Target Strength of largest on-axis target of interest (db)	Calculated Receiver gain (dB)	Installed Cable Length (ft)	Difference in Cable Length Between Calibrated Cable and Installed Cable (ft)	Receiver Gain Adjusted for Difference in Cable Length (dB)	Source Level Adjusted for Difference in Cable Length (dB)	Receiver Sensitivity Adjusted for Difference in Cable Length (dB)	Target Strength of Smallest On-axis Target (dB)	Voltage of Smallest On-axis Target (dB)	Voltage of Smallest On-axis Target at 20 dB per Volt (V)
1	105 (x)	387	214.53	80	-106.01	-36	7.48	430	-43	7.86	214.36	-106.23	-56	60	3.0
1	105 (y)	387	214.52	80	-106.13	-36	7.61	430	-43	7.99	214.35	-106.35	-56	60	3.0
1	105	387	214.53	80	-106.07	-36	7.54	430	-43	7.93	214.36	-106.29	-56	60	3.0
1	53 (x)	387	214.60	80	-105.91	-36	7.31	387	0	7.31	214.60	-105.91	-56	60	3.0
1	53 (y)	387	214.62	80	-105.93	-36	7.31	387	0	7.31	214.62	-105.93	-56	60	3.0
1	53	387	214.61	80	-105.92	-36	7.31	387	0	7.31	214.61	-105.92	-56	60	3.0
21	400 (x)	627	214.89	80	-108.13	-36	9.24	627	0	9.24	214.89	-108.13	-56	60	3.0
21	400 (y)	627	214.90	80	-108.11	-36	9.21	627	0	9.21	214.90	-108.11	-56	60	3.0
21	400	627	214.90	80	-108.12	-36	9.23	627	0	9.23	214.90	-108.12	-56	60	3.0
21	401 (x)	627	214.83	80	-108.11	-36	9.28	627	0	9.28	214.83	-108.11	-56	60	3.0
21	401 (y)	627	214.83	80	-108.17	-36	9.34	627	0	9.34	214.83	-108.17	-56	60	3.0
21	401	627	214.83	80	-108.14	-36	9.31	627	0	9.31	214.83	-108.14	-56	60	3.0
21	402 (x)	627	214.91	80	-108.19	-36	9.28	627	0	9.28	214.91	-108.19	-56	60	3.0
21	402 (y)	627	214.93	80	-108.19	-36	9.26	627	0	9.26	214.93	-108.19	-56	60	3.0
21	402	627	214.92	80	-108.19	-36	9.27	627	0	9.27	214.92	-108.19	-56	60	3.0
21	403 (x)	627	214.91	80	-108.07	-36	9.16	627	0	9.16	214.91	-108.07	-56	60	3.0
21	403 (y)	627	214.89	80	-108.11	-36	9.22	627	0	9.22	214.89	-108.11	-56	60	3.0
21	403	627	214.90	80	-108.09	-36	9.19	627	0	9.19	214.90	-108.09	-56	60	3.0
22	404 (x)	627	214.83	80	-107.27	-36	8.44	627	0	8.44	214.83	-107.27	-56	60	3.0
22	404 (y)	627	214.82	80	-107.31	-36	8.49	627	0	8.49	214.82	-107.31	-56	60	3.0
22	404	627	214.83	80	-107.29	-36	8.47	627	0	8.47	214.83	-107.29	-56	60	3.0
22	405 (x)	627	214.82	80	-107.47	-36	8.65	627	0	8.65	214.82	-107.47	-56	60	3.0
22	405 (y)	627	214.82	80	-107.47	-36	8.65	627	0	8.65	214.82	-107.47	-56	60	3.0
22	405	627	214.82	80	-107.47	-36	8.65	627	0	8.65	214.82	-107.47	-56	60	3.0
23	408 (x)	627	214.68	80	-107.51	-36	8.83	627	0	8.83	214.68	-107.51	-56	60	3.0
23	408 (y)	627	214.70	80	-107.51	-36	8.81	627	0	8.81	214.70	-107.51	-56	60	3.0
23	408	627	214.69	80	-107.51	-36	8.82	627	0	8.82	214.69	-107.51	-56	60	3.0
23	409 (x)	627	214.76	80	-107.57	-36	8.81	627	0	8.81	214.76	-107.57	-56	60	3.0
23	409 (y)	627	214.75	80	-107.57	-36	8.82	627	0	8.82	214.75	-107.57	-56	60	3.0
23	409	627	214.76	80	-107.57	-36	8.82	627	0	8.82	214.76	-107.57	-56	60	3.0
23	407 (x)	627	214.79	80	-107.51	-36	8.72	627	0	8.72	214.79	-107.51	-56	60	3.0
23	407 (y)	627	214.75	80	-107.53	-36	8.78	627	0	8.78	214.75	-107.53	-56	60	3.0
23	407	627	214.77	80	-107.52	-36	8.75	627	0	8.75	214.77	-107.52	-56	60	3.0
23	411 (x)	627	214.64	80	-107.69	-36	9.05	627	0	9.05	214.64	-107.69	-56	60	3.0
23	411 (y)	627	214.65	80	-107.69	-36	9.04	627	0	9.04	214.65	-107.69	-56	60	3.0
23	411	627	214.65	80	-107.69	-36	9.05	627	0	9.05	214.65	-107.69	-56	60	3.0
24	413 (x)	387	215.02	80	-103.71	-36	4.69	387	0	4.69	215.02	-103.71	-56	60	3.0
24	413 (y)	387	215.01	80	-103.75	-36	4.74	387	0	4.72	215.01	-103.75	-56	60	3.0
24	413	387	215.02	80	-103.73	-36	4.72	387	0	4.80	215.02	-103.73	-56	60	3.0
24	412 (x)	387	215.05	80	-103.85	-36	4.80	387	0	4.84	215.05	-103.85	-56	60	3.0
24	412 (y)	387	215.01	80	-103.85	-36	4.84	387	0	4.84	215.01	-103.85	-56	60	3.0
24	412	387	215.03	80	-103.85	-36	4.82	387	0	4.82	215.03	-103.85	-56	60	3.0

Table 3
Calibration Data, Acquisition Settings, and Calculated Receiver Gains for Single-beam Transducers to Provide Equal Detectability for On-axis Targets Ranging From –56 to –36 dB in Acoustic Size at the Spillway

Echo-sounder Number	Transducer Number and Phase (if split beams)	Calibrated Cable Length (ft)	Source Level (dB)	Maximum Output Voltage (dB)	40 logR Receiver Sensitivity (dB)	Target Strength of largest on-axis target of interest (dB)	Calculated Receiver gain (dB)	Installed Cable Length (ft)	Difference in Cable Length Between Calibrated Cable and Installed Cable (ft)	Receiver Gain Adjusted for Difference in Cable Length (dB)	Source Level Adjusted for Difference in Cable Length (dB)	Receiver Sensitivity Adjusted for Difference in Cable Length (dB)	Target Strength of Smallest On-axis Target (dB)	Voltage of Smallest On-axis Target (dB)	Voltage of Smallest On-axis Target at 20 dB per Volt (V)
16	41	500	210.84	80	-102.99	-36	8.15	500	0	8.15	210.84	-102.99	-56	60	3.0
16	42	500	212.37	80	-101.97	-36	5.60	500	0	5.60	212.37	-101.97	-56	60	3.0
16	43	500	212.60	80	-102.17	-36	5.57	500	0	5.57	212.60	-102.17	-56	60	3.0
16	44	500	212.24	80	-101.75	-36	5.51	500	0	5.51	212.24	-101.75	-56	60	3.0
16	45	500	212.48	80	-101.95	-36	5.47	500	0	5.47	212.48	-101.95	-56	60	3.0
16	46	500	212.14	80	-101.65	-36	5.51	500	0	5.51	212.14	-101.65	-56	60	3.0
16	47	500	212.01	80	-101.97	-36	5.96	500	0	5.96	212.01	-101.97	-56	60	3.0
16	48	500	212.59	80	-101.35	-36	4.76	700	-200	4.73	211.82	-102.37	-56	60	3.0
17	49	500	211.86	80	-102.05	-36	6.10	700	-200	5.85	211.08	-103.07	-56	60	3.0
17	50	500	212.40	80	-101.89	-36	5.49	500	0	5.49	212.40	-101.89	-56	60	3.0
17	51	500	211.91	80	-102.57	-36	6.66	500	0	6.66	211.91	-102.57	-56	60	3.0
17	53	500	212.24	80	-101.93	-36	5.69	500	0	5.69	212.24	-101.93	-56	60	3.0
17	54	500	212.77	80	-101.65	-36	4.88	500	0	4.88	212.77	-101.65	-56	60	3.0
17	55	500	212.43	80	-102.35	-36	5.92	500	0	5.92	212.43	-102.35	-56	60	3.0
17	56	500	212.10	80	-102.49	-36	6.39	500	0	6.39	212.10	-102.49	-56	60	3.0
17	57	500	212.38	80	-101.53	-36	5.15	500	0	5.15	212.38	-101.53	-56	60	3.0

Table 4

Calibration Data, Acquisition Settings, and Calculated Receiver Gains for Single-beam Transducers to Provide Equal Detectability for On-axis Targets Ranging From –56 to –36 dB in Acoustic Size at Powerhouse 2

Echo-sounder Number	Transducer Number and Phase (if split beams)	Calibrated Cable Length (ft)	Source Level (dB)	Maximum Output Voltage (dB)	40 logR Receiver Sensitivity (dB)	Target Strength of largest on-axis target of interest (db)	Calculated Receiver gain (dB)	Installed Cable Length (ft)	Difference in Cable Length Between Calibrated Cable and Installed Cable (ft)	Receiver Gain Adjusted for Difference in Cable Length (dB)	Source Level Adjusted for Difference in Cable Length (dB)	Receiver Sensitivity Adjusted for Difference in Cable Length (dB)	Target Strength of Smallest On-axis Target (dB)	Voltage of Smallest On-axis Target (dB)	Voltage of Smallest On-axis Target at 20 dB per Volt (V)
7	44	650	215.16	70	-112.25	-36	3.09	650	0	3.09	215.16	-112.25	-56	50	2.5
7	43	650	215.00	70	-112.13	-36	3.13	650	0	3.13	215.00	-112.13	-56	50	2.5
7	42	650	215.74	71	-111.77	-36	2.03	650	0	2.03	215.74	-111.77	-56	50	2.5
7	41	650	215.37	70	-112.43	-36	3.06	650	0	3.06	215.37	-112.43	-56	50	2.5
7	40	650	215.92	70	-111.83	-36	1.91	650	0	1.91	215.92	-111.83	-56	50	2.5
7	39	650	215.65	71	-111.77	-36	2.12	650	0	2.12	215.65	-111.77	-56	50	2.5
7	38	650	215.59	70	-111.87	-36	2.28	650	0	2.28	215.59	-111.87	-56	50	2.5
7	37	650	214.97	70	-112.23	-36	3.26	650	0	3.26	214.97	-112.23	-56	50	2.5
7	36	650	215.23	70	-112.37	-36	3.14	650	0	3.14	215.23	-112.37	-56	50	2.5
7	35	650	215.77	70	-112.07	-36	2.30	650	0	2.30	215.77	-112.07	-56	50	2.5
7	34	650	215.66	70	-111.85	-36	2.19	652	-2	2.21	215.65	-111.86	-56	50	2.5
8	55	650	215.67	70	-111.73	-36	2.66	1000	-350	5.19	214.33	-113.51	-56	50	2.5
8	56	650	214.74	70	-113.09	-36	4.35	800	-150	5.69	214.16	-113.85	-56	50	2.5
8	57	650	214.82	71	-112.85	-36	4.03	650	0	4.03	214.82	-112.85	-56	50	2.5
8	57	650	214.82	70	-112.85	-36	4.03	800	-150	5.37	214.24	-113.61	-56	50	2.5
8	58	650	216.00	70	-111.99	-36	1.99	650	0	1.99	216.00	-111.99	-56	50	2.5
8	59	650	214.71	71	-112.83	-36	4.12	650	0	4.12	214.71	-112.83	-56	50	2.5
8	60	650	215.21	70	-112.21	-36	3.00	648	2	2.98	215.22	-112.20	-56	50	2.5
8	61	650	215.18	70	-112.27	-36	3.09	650	0	3.09	215.18	-112.27	-56	50	2.5
8	63	650	214.63	70	-113.27	-36	4.64	650	0	4.64	214.63	-113.27	-56	50	2.5
8	64	650	215.70	70	-111.59	-36	1.89	650	0	1.89	215.70	-111.59	-56	50	2.5
8	69	650	214.76	71	-113.05	-36	4.29	651	-1	4.30	214.76	-113.05	-56	50	2.5
8	69	650	214.76	70	-113.65	-36	4.29	651	-1	4.30	214.76	-113.05	-56	50	2.5

Table 5
Calibration Data, Acquisition Settings, and Calculated Receiver Gains for Split-beam Transducers to Provide Equal Detectability for On-axis Targets Ranging From –56 to –36 dB in Acoustic Size at the Spillway (System 15) and Powerhouse 2 (Other Systems). Results for each transducer are presented for the x phase, y phase, and the mean of x and y phases

Echo-sounder Number	Transducer Number and Phase (# split beams)	Calibrated Cable Length (ft)	Source Level (dB)	Maximum Output Voltage (dB)	40 logR Receiver Sensitivity (dB)	Target Strength of largest on-axis target of interest (db)	Calculated Receiver gain (dB)	Installed Cable Length (ft)	Difference in Cable Length Between Calibrated Cable and Installed Cable (ft)	Receiver Gain Adjusted for Difference in Cable Length (dB)	Source Level Adjusted for Difference in Cable Length (dB)	Receiver Sensitivity Adjusted for Difference in Cable Length (dB)	Target Strength of Smallest On-axis Target (dB)	Voltage of Smallest On-axis Target (dB)	Voltage of Smallest On-axis Target at 20 dB per Volt (V)
15	112 (x)	200	211.34	80	-113.09	-36	17.75	200	0	17.75	211.34	-113.09	-56	60	3.0
15	112 (y)	200	211.34	80	-112.97	-36	17.63	200	0	17.63	211.34	-112.97	-56	60	3.0
15	112	200	211.34	80	-113.03	-36	17.69	200	0	17.69	211.34	-113.03	-56	60	3.0
9	51 (x)	309	216.58	80	-103.49	-36	4.91	309	0	4.91	216.58	-103.49	-56	60	3.0
9	51 (y)	309	216.59	80	-105.51	-36	4.92	309	0	4.92	216.59	-105.51	-56	60	3.0
9	51	309	216.59	80	-105.50	-36	4.91	309	0	4.91	216.59	-105.50	-56	60	3.0
9	52 (x)	200	217.24	80	-105.19	-36	3.95	480	-280	6.45	216.16	-106.62	-56	60	3.0
9	52 (y)	200	217.23	80	-105.15	-36	3.92	480	-280	6.42	216.15	-106.58	-56	60	3.0
9	52	200	217.24	80	-105.17	-36	3.94	480	-280	6.44	216.16	-106.60	-56	60	3.0
18	414 (x)	705	214.72	80	-108.27	-36	9.55	705	0	9.55	214.72	-108.27	-56	60	3.0
18	414 (y)	705	214.73	80	-108.29	-36	9.56	705	0	9.56	214.73	-108.29	-56	60	3.0
18	414	705	214.73	80	-108.28	-36	9.55	705	0	9.55	214.73	-108.28	-56	60	3.0
18	415 (x)	705	214.77	80	-108.57	-36	9.80	705	0	9.80	214.77	-108.57	-56	60	3.0
18	415 (y)	705	214.74	80	-108.55	-36	9.81	705	0	9.81	214.74	-108.55	-56	60	3.0
18	415	705	214.76	80	-108.56	-36	9.80	705	0	9.80	214.76	-108.56	-56	60	3.0
18	416 (x)	705	214.69	80	-108.51	-36	9.82	705	0	9.82	214.69	-108.51	-56	60	3.0
18	416 (y)	705	214.64	80	-108.55	-36	9.91	705	0	9.91	214.64	-108.55	-56	60	3.0
18	416	705	214.67	80	-108.53	-36	9.86	705	0	9.86	214.67	-108.53	-56	60	3.0
18	417 (x)	705	214.79	80	-108.33	-36	9.54	705	0	9.54	214.79	-108.33	-56	60	3.0
18	417 (y)	705	214.78	80	-108.39	-36	9.61	705	0	9.61	214.78	-108.39	-56	60	3.0
18	417	705	214.79	80	-108.36	-36	9.57	705	0	9.57	214.79	-108.36	-56	60	3.0

correction factor was used to compensate for cable length effects on source levels, receiver sensitivity, and receiver gain settings.

Transducer Deployments and Sampling

This section describes hydroacoustic deployments and sampling schemes. Table 6 provides details of transducer locations and aiming angles for sampling to estimate guided and unguided numbers of fish passing the PSC, Units 7, 9, and 10 with STSs, and Unit 8 with an extended-length submerged bar screen (ESBS). Spillway and Powerhouse 2 transducer locations and aiming angles are presented in Table 7.

Table 6
Transducer Locations at Bonneville Powerhouse 1

System	Transducer	Unit	Intake	Lateral Position	Struc-ture	Description of Location on Structure	E-coord[2]	N-coord	Elev-ation (ft)	Aim	Aiming Angle[1] (Deg.)
3	1	1	A	North	Rack 1[3]	4.4 ft below top; 8.8 ft S of N Side	1630251.1	722505.1	63.7	Down	0 (D)
3	2	1	B	Center	Rack 1	4.4 ft below top; 11 ft S of N Side	1630260.5	722527.6	63.7	Down	0 (D)
3	3	1	C	Center	Rack 1	4.4 ft below top; 11 ft S of N Side	1630271.0	722551.7	63.7	Down	0 (D)
3	4	2	A	South	Rack 1	4.4 ft below top; 13.2 ft S of N Side	1630281.7	722576.6	63.7	Down	0 (D)
3	5	2	B	North	Rack 1	4.4 ft below top; 8.8 ft S of N Side	1630293.9	722604.8	63.7	Down	0 (D)
3	6	2	C	South	Rack 1	4.4 ft below top; 13.2 ft S of N Side	1630302.6	722625.0	63.7	Down	0 (D)
4	9	3	A	North	Rack 1	4.4 ft below top; 8.8 ft S of N Side	1630316.0	722655.9	63.7	Down	0 (D)
4	10	3	B	Center	Rack 1	4.4 ft below top; 11 ft S of N Side	1630325.6	722678.1	63.7	Down	0 (D)
4	11	3	C	North	Rack 1	4.4 ft below top; 8.8 ft S of N Side	1630336.9	722704.4	63.7	Down	0 (D)
4	12	4	A	South	Rack 1	4.4 ft below top; 13.2 ft S of N Side	1630346.8	722727.1	63.7	Down	0 (D)
4	13	4	B	South	Rack 1	4.4 ft below top; 13.2 ft S of N Side	1630357.2	722751.4	63.7	Down	0 (D)
4	17	4	C	Center	Rack 1	4.4 ft below top; 11 ft S of N Side	1630368.6	722777.6	63.7	Down	0 (D)
5	20	5	A	Center	Rack 1	4.4 ft below top; 11 ft S of N Side	1630380.1	722804.3	63.7	Down	0 (D)
5	21	5	B	North	Rack 1	4.4 ft below top; 8.8 ft S of N Side	1630391.5	722830.6	63.7	Down	0 (D)
5	22	5	C	Center	Rack 1	4.4 ft below top; 11 ft S of N Side	1630401.1	722852.9	63.7	Down	0 (D)
5	23	6	A	North	Rack 1	4.4 ft below top; 8.8 ft S of N Side	1630413.6	755881.7	63.7	Down	0 (D)
5	26	6	B	South	Rack 1	4.4 ft below top; 13.2 ft S of N Side	1630422.3	722901.9	63.7	Down	0 (D)
5	27	6	C	South	Rack 1	4.4 ft below top; 13.2 ft S of N Side	1630432.7	722926.1	63.7	Down	0 (D)
6	31	7	A	Center	Rack 5	4.4 ft below top; 8.8 ft S of N Side	1630454.0	722951.1	11.0	Up	29 (D)
6	32	7	A	Center	Rack 1	4.4 ft below top; 11 ft S of N Side	1630446.2	722957.0	63.7	Down	20 (D)
24	413	8	B	Center	Rack 5	4.4 ft below top; 11 ft S of N Side	1630497.1	723050.6	14.0	Up	28 (D)
24	412	8	B	Center	ESBS	2 ft below pivot; 13 ft S of N Side	1630482.6	723057.7	39.18	Down	15 (U)
6	30	9	C	South	Rack 1	4.4 ft below top; 13.2 ft S of N Side	1630530.2	723151.9	63.7	Down	9 (D)
6	33	9	C	North	Rack 5	4.4 ft below top; 8.8 ft S of N Side	1630540.9	723152.0	11.0	Up	29 (D)
1	53	10	B	North	Rack 1	4.4 ft below top; 8.8 ft S of N Side	1630554.0	723207.1	63.7	Down	9 (D)
1	105	10	B	North	Rack 5	4.4 ft below top; 8.8 ft S of N Side	1630563.0	723203.2	11.0	Up	29 (D)
21	400	1	B	North	Frame[5]	3.5 ft S of N side of slot at EL 25'	1630301.5	722517.8	25.0	Up	5 (D)
21	401	1	B	North	Frame	3.5 ft S of N side of slot at EL 70'	1630293.1	722521.4	70.0	Down	17 (U)
21	402	2	B	Center	Frame	10 ft S of N side of slot at EL 25'	1630331.4	722587.1	25.0	Up	5 (D)
21	403	2	B	Center	Frame	10 ft S of N side of slot at EL 70'	1630323.1	722590.8	70.0	Down	17 (U)
22	405	4	B	Center	Frame	10 ft S of N side of slot at EL 25'	1630396.5	722737.7	25.0	Up	5 (D)
22	404	4	B	Center	Frame	10 ft S of N side of slot at EL 70'	1630388.1	722741.3	70.0	Down	17 (U)
23	408	5	B	North	Frame	3.5 ft S of N side of slot at EL 25'	1630431.6	722818.9	25.0	Up	5 (D)
23	409	5	B	North	Frame	3.5 ft S of N side of slot at EL 70'	1630423.2	722822.6	70.0	Down	17 (U)
23	411	6	B	South	Frame	3.5 ft S of N side of slot at EL 25'	1630464.1	722894.2	25.0	Up	5 (D)
23	410	6	B	South	Frame	3.5 ft S of N side of slot at EL 70'	1630455.7	722897.8	70.0	Down	17 (U)

[1] Measured in degrees off of a vertical plane separating upstream and downstream directions
[2] Geographical Coordinates were provided by Marshall Richmond's team at PNNL
[3] Rack refers to a trash rack, six of which are stacked in an intake slot. Racks are number from top to bottom.
[4] ESBS refers to an extended length submerged bar screen
[5] All transducers on frames at PSC slot entrances were located 3.5 ft upstream of the slot entrance

Table 7
Transducer Locations at Bonneville Dam Spillway and Powerhouse 2

Sys-tem	Trans-ducer	Spill Bay	Turbine Intake	Struc-ture	Lateral Position	Location Description	E-coord [2]	N-coord	Vertical Position	Aim	Aiming Angle [1] (Deg.)
15	112	17		Gate	Center	25.5 ft S of N & upstream side	1631851.1	724790.1	28.5 ft below top [3]	Down	8 (U)
16	48	8		Gate	North	17.1 ft S of N & upstream side	1631839.5	724267.8	28 ft below top	Down	8 (U)
16	49	10		Gate	South	40.0 ft S of N & upstream side	1631841.6	724363.0	28 ft below top	Down	8 (U)
16	50	12		Gate	Center	25.6 ft S of N & upstream side	1631844.5	724492.2	28 ft below top	Down	8 (U)
16	56	14		Gate	South	36.8 ft S of N & upstream side	1631846.5	724602.4	28 ft below top	Down	8 (U)
16	54	15		Gate	Center	28.5 ft S of N & upstream side	1631848.7	724669.6	28 ft below top	Down	8 (U)
17	42	2		Gate	Center	28.5 ft S of N & upstream side	1631831.1	723901.9	28 ft below top	Down	8 (U)
17	43	4		Gate	North	17.1 ft S of N & upstream side	1631834.1	724031.3	28 ft below top	Down	8 (U)
17	44	5		Gate	South	37.0 ft S of N & upstream side	1631835.0	724070.4	28 ft below top	Down	8 (U)
17	45	6		Gate	Center	28.5 ft S of N & upstream side	1631836.7	724138.6	28 ft below top	Down	8 (U)
17	46	7		Gate	South	37.1 ft S of N & upstream side	1631837.4	724188.5	28 ft below top	Down	8 (U)
7	41		11c	Rack 1 [4]	South	19.8 ft S of N & downstream side	1632521.1	725450.2	EL 36.5 ft	Down	5 (D)
7	35		11c	Rack 4	South	19.8 ft S of N & downstream side	1632520.9	725445.8	EL 1.0 ft	Up	29 (D)
7	34		12a	Rack 1	North	7.3 ft S of N & downstream side	1632551.8	725483.2	EL 36.5 ft	Down	5 (D)
7	37		12a	Rack 4	North	7.3 ft S of N & downstream side	1632548.2	725475.2	EL 1.0 ft	Up	29 (D)
7	36		13b	Rack 1	Center	13.0 ft S of N & downstream side	1632631.8	725569.1	EL 36.5 ft	Down	5 (D)
7	40		13b	Rack 4	Center	13.0 ft S of N & downstream side	1632633.7	725567.3	EL 1.0 ft	Up	29 (D)
7	38		14c	Rack 1	Center	13.0 ft S of N & downstream side	1632715.3	725659.2	EL 36.5 ft	Down	5 (D)
7	42		14c	Rack 4	Center	13.0 ft S of N & downstream side	1632717.4	725657.4	EL 1.0 ft	Up	29 (D)
8	60		15c	Rack 1	South	19.8 ft S of N & downstream side	1632776.9	725725.7	EL 36.5 ft	Down	5 (D)
8	59		15c	Rack 4	South	19.8 ft S of N & downstream side	1632776.7	725721.3	EL 1.0 ft	Up	29 (D)
8	63		16c	Rack 1	North	7.3 ft S of N & downstream side	1632847.1	725801.3	EL 36.5 ft	Down	5 (D)
8	61		16c	Rack 4	North	7.3 ft S of N & downstream side	1632849.2	725799.4	EL 1.0 ft	Up	29 (D)
8	69		17b	Rack 1	Center	13.0 ft S of N & downstream side	1632887.4	725844.7	EL 36.5 ft	Down	5 (D)
8	64		17b	Rack 4	Center	13.0 ft S of N & downstream side	1632889.4	725842.8	EL 1.0 ft	Up	29 (D)
8	55		14c	Clump	Center	about 100 ft upstream of TIE			Elev. ~20 ft	Up	0
8	56		17b	Clump	Center	about 100 ft upstream of TIE			Elev. ~20 ft	Up	0
9	51		18b	Rack 1	South	19.8 ft S of N Side	1632946.7	725908.7	EL 36.5 ft	Down	5 (D)
9	52		18b	Rack 4	South	19.8 ft S of N Side	1632948.8	725906.8	EL 1.0 ft	Up	29 (D)
18	414		14c	Pier	North	Upstream of trash rack			EL 20.7 ft	Up	5 (U)
18	415		14c	Pier	North	Upstream of trash rack			EL 70.0 ft	Down	19 (U)
18	416		17b	Pier	South	Upstream of trash rack			EL 20.7 ft	Up	5 (U)
18	417		17b	Pier	South	Upstream of trash rack			EL 70.0 ft	Down	19 (U)

[1] Measured in degrees off of a vertical plane separating upstream (U) and downstream (D) directions

[2] Geographical Coordinates were provided by Marshall Richmond's team at PNNL

[3] Top refer to the top of a 60 ft tall spill gate, so transducers were 32 ft above the bottom of the gate

[4] Rack refers to a trash rack, six of which are stacked in an intake slot. Racks are number from top to bottom.

Sampling the Prototype Surface Collector

Two different approaches were used to sample smolt passage at the PSC units (1 - 6). The first was based upon in-turbine deployments and sampling with single-beam transducers and the second relied on split-beam deployments and sampling in the forebay immediately upstream of the PSC slot entrances.

In each of 18 intakes downstream of the PSC, one 7 deg single-beam transducer was mounted at the top of trash rack 1 and aimed straight down 11 deg off the plane of the trash racks (Figure 2). Fish passing through the beam above an elevation located 0.5 m below the top of the PSC floor were classified as collected by the PSC. This elevation was selected based upon flow trajectories from the PSC floor to the center of the hydroacoustic beam. The down-looking beams had a blanking distance of 1 m and limited detectability in the first 3 m and they also could not sample the shallow sluice opening (mean depth = 2 ft) inside the center slot of every PSC unit. The loss of the uppermost 1 m may not have been significant as it accounted for only 1.4 percent of the fish passage sampled with six up-looking beams in 1999. The in-turbine transducer in the B slot of every PSC unit also could not count fish passing into the sluice opening at those locations. Sluice gates at A and C intakes were always closed. Fish passing through a down-looking beam > 0.5 m below the PSC floor were classified as passing under the PSC.
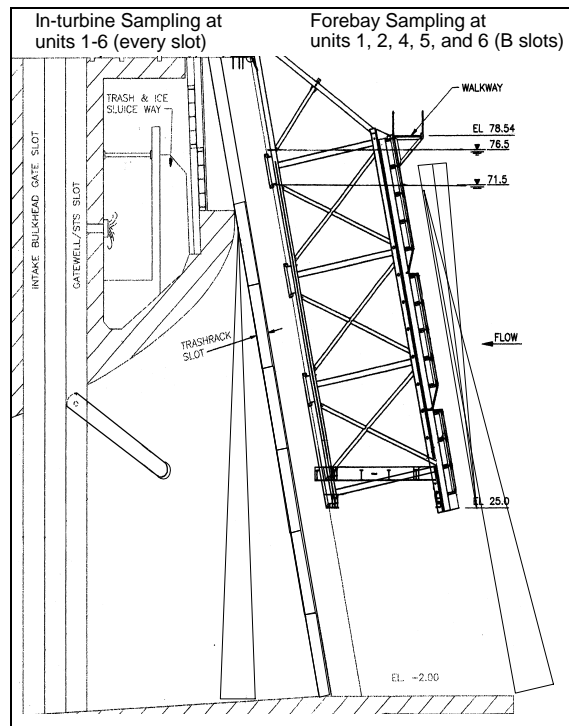
Figure 2.   Cross sectional view through the center slot of a Powerhouse 1 turbine unit with the PSC attached to the upstream side. Numbers of guided fish were estimated from counts in shaded areas of hydroacoustic beams downstream or upstream of the PSC. The deep portion of the in-turbine beam was used to estimate unguided fish numbers

Chapter 2   Materials and Methods

The upper portion of a down-looking beam covered 10 percent of the cross sectional area in the upper one-half of the intake, and the lower portion covered 30.5 percent of the bottom half of the intake. Therefore, the down-looking in-turbine transducers provided excellent spatial coverage for estimating numbers of fish passing under the PSC and adequate coverage for fish passing through the PSC. All in-turbine transducers had a pulse-repetition rate of 14 pings per second and sampled 20 1-minute periods per hour.

Slot entrances at center intakes of PSC Units 1, 2, 4, 5, and 6 were sampled with 6 deg split-beam transducers (Figure 2). A team of PNNL researchers sampled the slot entrance at Unit 3. Opposing split-beam transducers were mounted at the top and bottom of 45-ft tall frame (Figure 3). The lateral position of the transducer pair on the frame was chosen at random so that the pair would sample the north, center, or south third of the 20-ft slot entrance. The frames were deployed by crane and rested on horizontal crossbeams that tied the front of the A and C modules of the PSC together at several elevations. At each slot entrance, the deep transducer was aimed upward 6 deg upstream of the plane of slot entrance to count fish near the upper half of the slot. The shallow transducer was aimed downward 6 deg upstream of the plane of the entrance to count fish entering the bottom half of the slot. Fish passage estimates through every slot were based on counts of fish traces with trajectories into the PSC and average displacements ≥ 1 cm/ping.

Figure 3. Installation of a 45-ft tall frame with split-beam transducers at the top and bottom center

Fish passage estimates through every slot were based on counts of traces with trajectories into the PSC, each with an average displacement ≥ 1 cm/ping. Counts from the PSC slots were considered as guided fish as an alternative to the guided counts derived from the upper portion of the single-beam transducers within each turbine slot. Thus, there were two competing estimators of collection efficiency depending on the source of the estimate of guided numbers. Unguided numbers were always obtained from counts of fish passing through the deep portion of the in-turbine beams. Vertical distribution estimates in the forebay were obtained by counting fish within 1-m strata in the upper portion of the up-looking split-beam > 6.5 m from that transducer and in 1-m strata in the down-looking split-beam from 6.5 to 25 m from the down-looking transducer. All split-beam transducers had a pulse repetition rate of 10 pings per second and sampled 20 1-minute intervals per hour.

Sampling Units 7, 9, and 10

At turbine Units 7, 9, and 10, hydroacoustic sampling was performed within one of three randomly selected intake slots per turbine. In Units 7 and 9, one upward- and one downward-angled, 7 deg single-beam transducers were placed in the selected slots to monitor guided and unguided passage, respectively (Figure 4). An identical deployment was made in Unit 10, except that the transducers were 6 deg split-beams. Sampling was for 20 1-minute intervals per hour per transducer location, and the pulse repetition rate was 14 pings per second for each transducer.

Sampling Unit 8

At Unit 8, the center slot with an ESBS was sampled with an upward- and a downward-angled, 6 deg split-beam transducer to estimate guided and unguided numbers, respectively (Figure 5). Sampling was continuous, 60 minutes per hour, and the pulse repetition rate was 16.7 pings per second for each transducer.

Figure 4. Cross sectional view through an intake like those sampled at Units 7, 9, and 10 showing up- and down-looking hydroacoustic beams
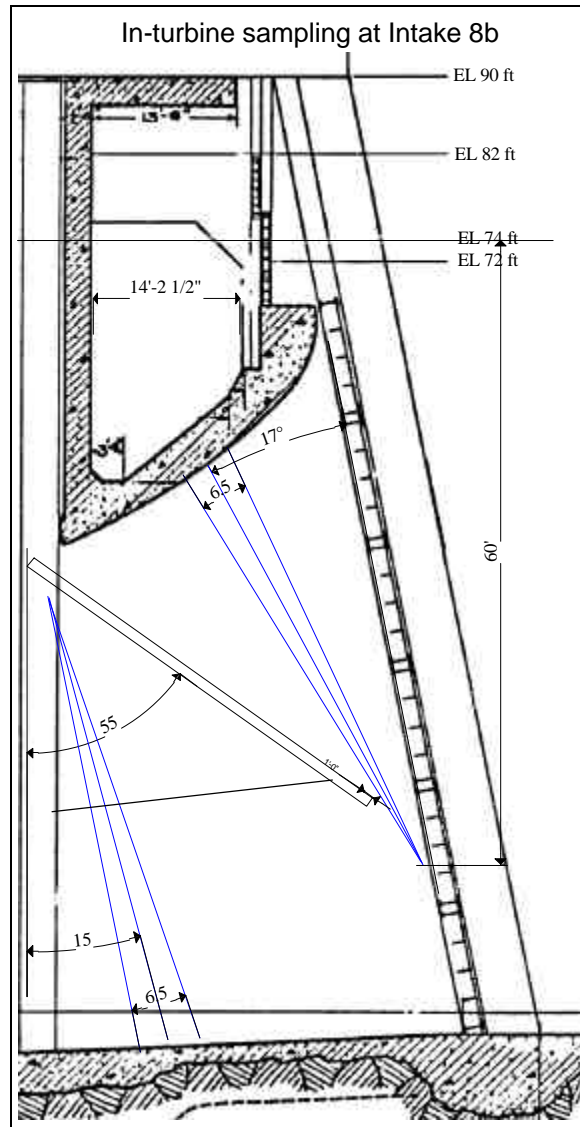
Figure 5.   Cross sectional view through Intake 8b where up- and down-looking split-beam transducers were used to sample guided and unguided fish, respectively

Sampling the Spillway

Spillway bays 2, 4, 6, 8, 10, 12, 14, and 16 were each sampled with one down-looking, 10 deg single-beam transducer, and Spill Bay 17 was sampled with one down-looking, 12 deg split-beam transducer. Bays were selected to allow interpolation of fish passage to bays that were not sampled and to emphasize sampling at gates that would pass the most water according to the 1999 Fish Passage Plan. Transducers were mounted 28 ft below the tops of spill gates and aimed 8 deg upstream (Figure 6; Table 7). Transducers were at el 56.5 ft when the gate was closed and at el 69 ft when the gate was opened 12.5 ft (7 dogs). Maximum ranges from the transducer to the ogee were about 44.7 ft when a gate
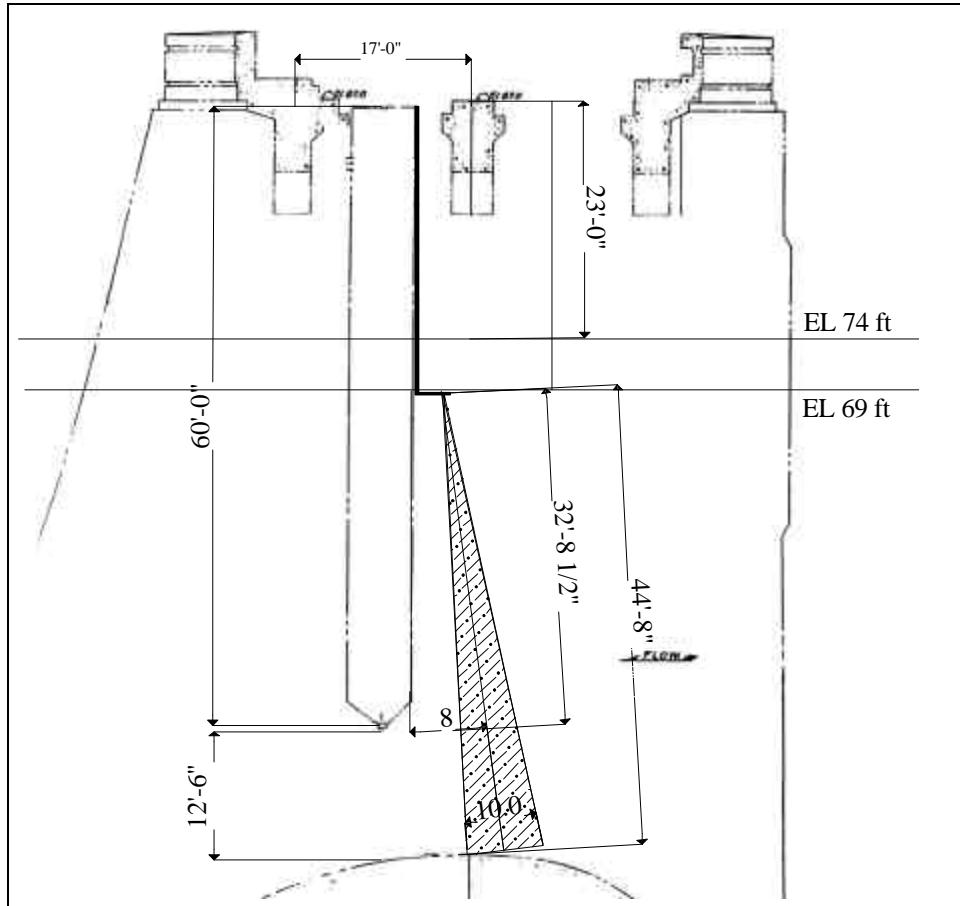
Figure 6.   Cross sectional view through a spill bay at Bonneville Dam. The diagram shows a transducer mount on the upstream side of a spill gate and the orientation of the hydroacoustic beam. Flow was from right to left through the beam

was opened 12.5 ft above the ogee and 32.5 ft when a gate was closed. Dam operations data were used to determine spill gate positions and to estimate range to the ogee for automated processing of data. Based upon fish trajectories and speeds through the split beam deployed at Spill Bay 17, most fish 8-25 ft from transducers passed down through the beam at speeds of 6-12 ft per second and would have been committed to passing by the time they were detected. Fish approaching at the elevation of the ogee were traveling 13-15 fps as they passed through the beam. Transducers transmitted at 30 pings per second for 12 1-minute periods per hour.

Sampling at Powerhouse 2

At Powerhouse 2, one of three intakes at every turbine unit was randomly selected for sampling. A pair of transducers was mounted on the downstream side of trash racks 1 and 4 (Table 7; Figure 7) at each sampled intake. One transducer of each pair was mounted near the top of the uppermost trash rack and aimed downward to sample unguided fish passing below the tip of the traveling screen.

The second transducer of each pair was mounted near the bottom of the fourth trash rack from the top and aimed upward to sample fish passing above the tip of the screen. Each transducer transmitted sound pulses at 14 pings per second, and pairs of transducers were fast multiplexed so that each pair sampled 15 1-minute periods per hour, 23 hours per day. The two transducers deployed in Unit 18 were split beams. Three transceivers and computers were used to control the 16 transducers. The locations of transducers within intakes also were randomized among north, center, and south locations (Table 7).
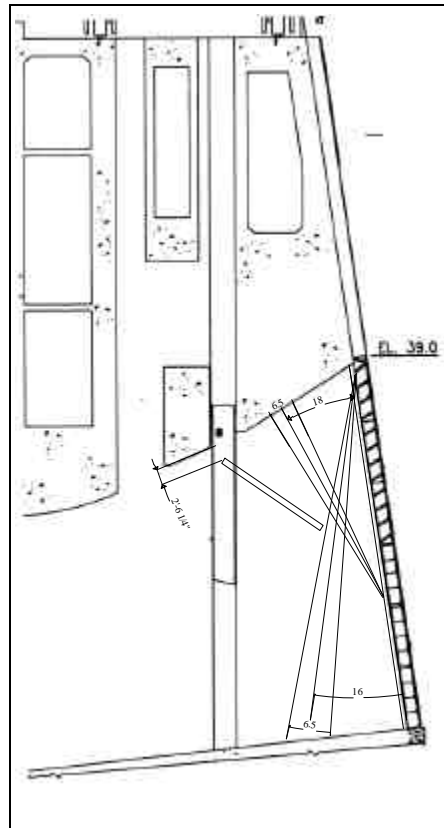
Figure 7.   Cross sectional view through a Powerhouse 2 turbine showing up- and down-looking transducer beams for sampling guided and unguided fish respectively

Vertical distributions of fish were also sampled upstream of Units 14 and 17 at Powerhouse 2. At each unit, an up-looking 6 deg single-beam transducer was deployed on a clump anchor 100 ft upstream of the TIEs and a pair of up- and down-looking 6 deg split-beam transducers were used on a pier adjacent to the upstream side of intake trash racks (Figure 8).
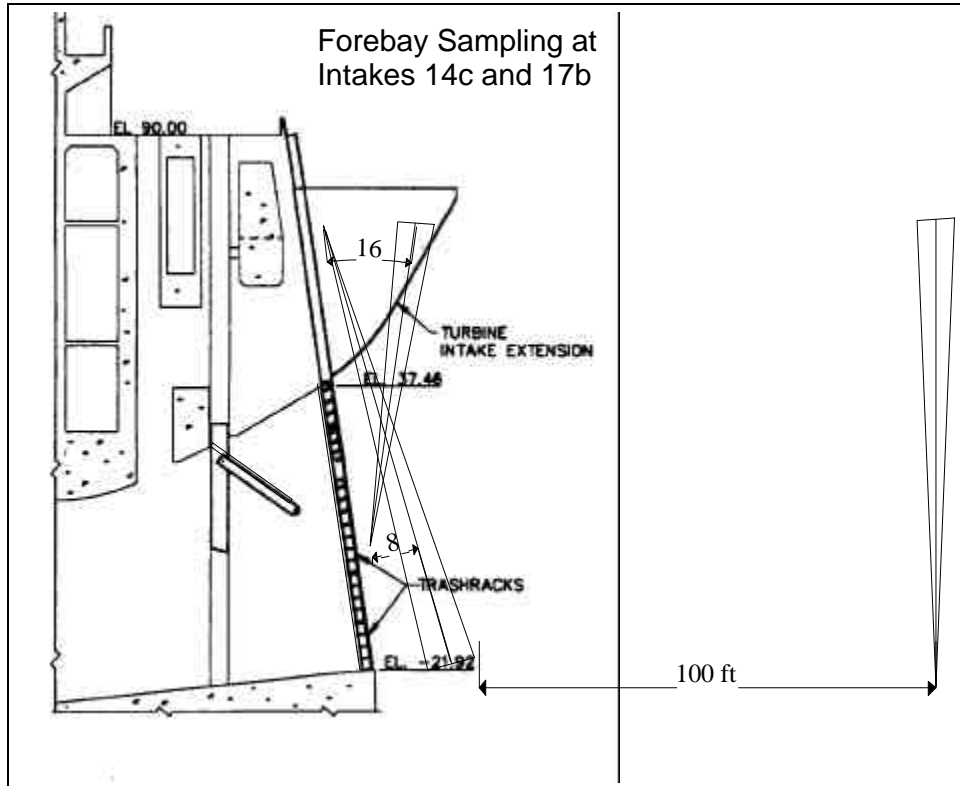
Figure 8. Cross sectional view through intake 14c or 17b at Bonneville Dam
Powerhouse 2 in spring 2000 showing an up-looking hydroacoustic
beam 100 ft upstream of the turbine intake extension and up- and
down-looking beams immediately upstream of intake trashracks

Fish Tracking and Filtering Criteria

The criteria used to accept or reject echo patterns as fish and to filter tracked
fish observations are presented in Tables 8 and 9. The greatest differences in
criteria were between sampling in forebay areas and inside turbine units because
fish were not entrained through beams in the forebay, except at the spillway.
Criteria for sampling turbine units were consistent or, if different (e.g., range),
were corrected for in spatial expansions by results of detectability modeling,
which is described below.

Since the hydroacoustic sampling effort on Bonneville Dam was so extensive
and generated such a large volume of data (156 Gigabytes) in 2000, it was
impossible to manually track enough data to make reliable fish-passage estimates
with available staff. Therefore, we relied on autotracking software developed over

Table 8
List of Fish-tracking Criteria for Deployments at the PSC, Unit 8, and Units 7, 9, and 10

Tracking Criterion Or Filters	PSC Units 1-6	PSC Slot Entrances	Unit 8	Units 7, 9, and 10
Minimum number of echoes with core of at least 4 echoes in 5 pings	4	4	4	4
Maximum ping gap for track segments	6	6	6	6
Maximum number of echoes	30	60	30	30
Structural filters = drop traces where the first ping and last ping are within a designated range bin	Yes	Yes	Yes	Yes
Trace slope	-9 to 9 cm / ping	-9 to 9 cm / ping	-9 to 9 cm / ping	-9 to 9 cm / ping and not between -0.05 and 0.05 cm / ping on down-looking beams
Fit to line or parabola (Route Mean Square Error in cm) was used to accept only very linear or parabolic traces in noisy areas on some beams	Line < 3 cm Parabola < 2 cm	Line < 3 cm Parabola < 2 cm	Line < 3 cm Parabola < 2 cm	Line < 3 cm Parabola < 2 cm
Range	3.0-10.5 m = guided 10.5-max = unguided	Upper slot = 6.75 m to the surface Lower slot = 6.75 to 13.5 m Under slot = 13.5 m to bottom	Up-looking = 3 m to ceiling Down-looking = 3 m to bottom	Up-looking = 9.0 m to ceiling Down-looking = 8.5 m to bottom
Direction of movement	None	Yes[1]	None	None
Target or echo strength				
-Spring and summer until 15 June	-56 to -37 dB	-56 to -37 dB	-56 to -37 dB	-56 to -37 dB
-Summer from 15 June to 30 June	-56 to -45 dB	-56 to -45 dB	-56 to -45 dB	-56 to -45 dB
-Summer after 30 June	-56 to -47 dB	-56 to -47 dB	-56 to -47 dB	-56 to -47 dB

[1] Azimuth angle from first to last echo had to indicate movement between the edges of the 20-ft PSC slot entrances.

Table 9
List of Fish-tracking Criteria for Deployments at the Spillway, Inside Units 11-18, and Upstream of Units 14 and 17

Tracking Criterion Or Filters	Spillway	Inside Units 11-18 at Powerhouse 2	On Upstream Side of Trash Racks at Units 14 and 17 at Powerhouse 2	Forebay 100 ft Upstream of Units 14 and 17 at Powerhouse 2
Minimum number of echoes with core of at least 4 echoes in 5 pings	4	4	4	4
Maximum ping gap for track segments	6	6	6	6
Maximum number of echoes	60	30	60	60
Structural filters = drop traces where the first ping and last ping are within a designated range bin	No	Yes	Yes	No
Trace slope	-9 to 9 cm / ping	-9 to 9 cm / ping	-9 to 9 cm / ping	-9 to 9 cm / ping and not between -0.05 and 0.05 cm / ping on down-looking beams
Fit to line or parabola (Route Mean Square Error in cm) was used to accept only very linear or parabolic traces in noisy areas in some beams	Line <3 cm Parabola <2 cm	Line <3 cm Parabola <2 cm	Line <3 cm Parabola <2 cm	None
Range	>2.3 m	Up-looking $=4.3$ m to ceiling Down-looking $=7.8$ m to bottom	Up-looking $=10.0$ m to surface Down-looking $=18.3$ m to bottom	Up-looking $=3$ m to surface
Direction of movement	None	None	Yes	None

[1] Azimuth angle from first to last echo had to indicate movement between the pier on either side of the intake

the last 3 years by the Fisheries Field Unit and the EL to process raw data into tracked fish observations. The autotracker software tells the computer to:

    a. Identify and remove echoes at constant range from structure.

    b. Identify and remove echoes at constant range from structure.

    c. Find seed echoes for candidate tracks.

        (1) Go to every echo.

        (2) Define a 10 ping by 1-m window centered on that echo.

        (3) Place all echoes in the window into 5-degree angle bins.

        (4) If any bin-count >3, flag the center echo as a candidate seed.

    d. Re-examine candidate seed echoes.

        (1) Go to every seed-echo window.

        (2) Count echoes in all possible line features (Hough transform).

        (3) If no echoes in the window are part of a strong line feature, then drop the seed echo (to distinguish between dense noise and dense fish tracks).

    e. Initiate alpha-beta tracking.

        (1) Track forward starting at each seed echo.

        (2) Track backward from the same seed echo after forward tracking has ended.

        (3) Check the track segment against criteria (core criterion; minimum and maximum gap). Link track segments that are collinear into single tracks, (i.e., project track segments forward and backward and link them if the ping gap < 6 pings and forward and backward projections of two track segments line up).

    f. Write out track statistics (echo statistics optional).

For several months in spring, samples of the autotracker's performance for every deployment were reviewed on a fish-by-fish basis to evaluate and fine-tune the autotracker. Researchers released the autotracker to process data for a given deployment only after they determined that it was tracking the same echo patterns that the researchers would track most of the time.

Although the autotracker was a very efficient analysis tool, its performance had to be continually verified with respect to trained human trackers. Five human

trackers were employed who received extensive training on raw hydroacoustic data from previous years before the 2000 tracking season began. The autotracker was evaluated by comparing its counts to those of several human trackers who all processed the same sample data sets. This approach was used because fish counts, even for the same files, can vary widely among human trackers (Ploskey et al. 2001). The hope was that the autotracker would perform like an average human tracker rather than like trackers at either extreme.

In order to evaluate inter-tracker differences, all of the human trackers tracked the same daily samples of all systems from five different days. These "calibration days" were scattered throughout the passage seasons, three in spring and two in summer. For each "calibration day" a single file was selected for each of the hydroacoustic systems from every hour between downloads on consecutive days. The "calibration days" were: Early spring, Julian Day 111-112; Middle spring, Julian Day 152-153; Late spring, Julian Day 157-158; Early summer, Julian Day 176-177, and Late summer, Julian Day 196-197. This arrangement was devised to evaluate inter-tracker differences under seasonally changing conditions of fish passage and fish size. The autotracker also processed the same samples from all 5 days.

Human and autotracked counts for each transducer (channel) were compared because there are important differences in passage characteristics, ranges of interest, trace slopes and lengths, and noise conditions for each deployment site and aiming. Although tracker performance has previously been compared by system (including several transducer channels), it was decided that comparing transducer channels gives the best measure of human and autotracker differences because it removes site and aiming differences within comparisons and evaluates performance across the greatest possible range of different tracking conditions among comparisons. For each of the 5 days, the fish count output files from each human or automatic tracker were post processed identically. Post processing included deployment-specific "filtering" for trace length, trace slope, echo or target strength, structure and other regular noise, and other characteristics described in Table 3. The resulting filtered fish counts for each tracker (human or automatic) on each day were then summed separately for each transducer channel.

Counts from five human trackers on all of the "calibration days" were compared by examining scatter plots and correlation statistics and by plotting the cumulative count of the human trackers and the autotracker over time to examine cumulative temporal deviations.

Dam Operations and Fish Passage

Project operations data, including discharge by spill bay and turbine unit were entered into a data set and integrated with fish passage data. Fish passage was set to zero when passage routes were closed. Turbine discharge at Powerhouse 1 was estimated from megawatts (MW) and head (the difference between the forebay and tailwater elevations) using multiple regression equations.

Standard units with STSs (Units 1-3, 5, and 7-10):

$$CFS = 9396.49 + 257.43(MW) - 173.27(HEAD)$$

(1)

Minimum gap runner with STSs (Units 4 and 6):

$$CFS = 9396.49 + 257.43(MW) - 173.27(HEAD)$$

(2)

The data used to derive these equations were obtained from the Hydroelectric Design Center (HDC), Portland District, through Karen Kuhn, a District Hydraulic Engineer. The first equation had an r^2 of 0.96 (N = 3,269) and the second had an r^2 of 0.94 (N = 2,502). Data files were obtained that listed MW, head, and other operations data by 5-minute intervals throughout the season from Rod Hurst at HDC. Daryl Hunt, Chief of Operations at Bonneville Dam and his staff of operators supplied data that were missing from the electronic files. Another equation was used to estimate discharge through the PSC slot from PSC unit discharge and forebay elevation, as follows:

$$CFS = -4405.429 + 45.667(el) + 0.445(Q)$$

(3)

where CFS was discharge through the PSC slot in cubic feet per second, el is forebay elevation in feet, and Q was the discharge in cubic feet per second through the same turbine. This equation had an r^2 of 0.75; N=12.

Missing Data

A special effort was made to make certain that missing samples were accounted for in the spring and summer data sets. First, a data set was created consisting of all possible sample locations and times each season and an expanded fish variable was set to missing in every observation. Second, the missing data set was merged with the acquired data set and counts of expanded fish, if present in the acquired data, overwrote missing counts. When a sample had not been collected, there was nothing in the acquired data set to overwrite the missing value for expanded fish; therefore, that observation was appropriately designated as missing and could be addressed as follows before data analysis:

All hydroacoustic systems were operated continuously (> 23 hours/day), except for a 15-45 minute period every morning when data were copied from the acquisition computer onto removable Jaz disks, or when equipment failed and data from the affected routes were not collected. Short equipment failures lasting up to 45 minutes were not a problem because fish counts and associated variances could still be estimated from the remaining within-hour samples. Computer lock ups usually were fixed within an hour because staff were on duty from 0800 to 1700 hours and contractors monitored systems from 1700 to 0800 hours.

Transducer cables that failed once at Unit 6, twice at Unit 8, and once at Unit 10 were repaired within a few days as soon as project support or divers became available.

Missing hourly data that resulted from equipment outages > 45 minutes were estimated by temporal linear interpolation for periods < 6 hours and by spatial interpolation or linear regression for periods > 6 hours. When an up-looking beam for counting fish guided by an STS failed, the upper portion of the paired down-looking beam was sometimes used to estimate those numbers. Occasionally the ratio of guided to unguided numbers at adjacent turbines with similar screens was useful for interpolating estimates of guided or unguided numbers. Regression equations relating hourly variances with hourly sums were sometimes used to estimate missing variance estimates.

Detectability Modeling and Spatial Expansions

The count of every fish was expanded based upon the ratio of the opening width to beam diameter at the range of detection:

$$EXP\_NUM = \frac{OW}{\left[MID\_R \times TAN\left(\frac{EBA}{2} \right) \times 2 \right]} \tag{4}$$

where

OW = opening width in meters

MID_R = mid-point range of a trace in meters

TAN = tangent

EBA = effective beam angle in degrees

Effective beam angle depends upon the detectability of fish of different sizes in the acoustic beam and is a function of nominal beam width, ping rate, trace criteria, and fish size, aspect, trajectory, velocity, and range. Detectability was modeled for every transducer deployment to determine effective beam angle as a function of range from a transducer. Target-strength estimates were obtained from the average backscattering cross section of fish detected by split-beam transducers and flow-velocity data by 1-m depth strata from a physical or computational fluid design (CFD) model. These data and other hydroacoustic-acquisition data (e.g., beam tilt, ping rate, target-strength threshold, number of echoes, and maximum ping gaps) were entered into a stochastic detectability model. Model inputs are described in Tables 10 and 11. Model output consisted of effective beam angle as a function of range from a transducer. Polynomials fitted to those data were substituted for EBA in Equation 4 to correct for differences in detectability by range among transducers and locations.

Table 10
Values of Variable Inputs to the Detectability Model for Every Type of Deployment Used in 2000

Deployment	-3dB Beam Angle	Transducer Tilt from Vertical	Blanking Range	Pings / Second	Mean TS	Standard Deviation	TS Threshold	Min Echoes	Ping Gap	Maximum Range
Spring										
Units 1-6; forebay; down-looking	6	0	1	13	-45.0	4.2	-56	4	4	17
Units 1-6; forebay; up-looking	6	4	1	13	-45.0	4.2	-56	4	4	17
Units 1-6; in-turbine; down-looking	6	0	1	14	-45.0	4.2	-56	4	4	21
Units 7 and 9; in-turbine; down-looking	6	20	1	14	-45.0	4.2	-56	4	4	22
Units 7 and 9; in-turbine; up-looking	6	29	1	14	-45.7	4.0	-56	4	4	15
Unit 10; in-turbine; down-looking	6	20	1	14	-45.0	4.2	-56	4	4	22
Unit 10; in-turbine; up-looking	6	29	1	14	-45.7	4.0	-56	4	4	15
Unit 8; in-turbine; down-looking	6	-15	1	17	-45.0	4.0	-56	4	4	15
Unit 8; in-turbine; up-looking	6	28	1	17	-44.9	4.3	-56	4	4	15
Spill bays except 17; down-looking	10	-8	0	30	-43.5	4.9	-56	4	4	13
Spill bay 17; down-looking	10	-15	0	30	-43.5	4.9	-56	4	4	13
Units 11-17; in-turbine; down-looking	6	16	1	14	-47.6	3.3	-56	4	4	20
Units 11-17; in-turbine; up-looking	6	0	1	10	-46.4	2.8	-56	4	4	25
Unit 18; in-turbine; down-looking	6	16	1	14	-47.6	3.3	-56	4	4	20
Unit 18; in-turbine; up-looking	6	20	1	14	-46.4	2.8	-56	4	4	13
Units 14&17; 100 ft upstream of TIE; up-looking	6	0	1	10	-46.4	2.8	-56	4	4	25
Summer										
Units 1-6; forebay; down-looking	6	0	1	13	-49.3	1.9	-56	4	4	17
Units 1-6; forebay; up-looking	6	4	1	13	-49.3	1.9	-56	4	4	17
Units 1-6; in-turbine; down-looking	6	0	1	14	-49.3	1.9	-56	4	4	21
Units 7 and 9; in-turbine; down-looking	6	20	1	14	-49.3	1.9	-56	4	4	22
Units 7 and 9; in-turbine; up-looking	6	29	1	14	-50.1	2.3	-56	4	4	15
Unit 10; in-turbine; down-looking	6	20	1	14	-49.3	1.9	-56	4	4	22
Unit 10; in-turbine; up-looking	6	29	1	14	-50.1	2.3	-56	4	4	15
Unit 8; in-turbine; down-looking	6	-15	1	17	-47.8	1.9	-56	4	4	15
Unit 8; in-turbine; up-looking	6	28	1	17	-49.0	2.2	-56	4	4	15
Spill bays except 17; down-looking	10	-8	0	30	-49.0	1.9	-56	4	4	13
Spill bay 17; down-looking	10	-15	0	30	-49.0	1.9	-56	4	4	13
Units 11-17; in-turbine; down-looking	6	16	1	14	-52.2	2.3	-56	4	4	20
Units 11-17; in-turbine; up-looking	6	0	1	10	-49.5	1.6	-56	4	4	25
Unit 18; in-turbine; down-looking	6	16	1	14	-52.2	2.3	-56	4	4	20
Unit 18; in-turbine; up-looking	6	20	1	14	-49.5	1.6	-56	4	4	13
Units 14 & 17; forebay trash racks; down-looking	6	16	1	10	-52.2	2.3	-56	4	4	28
Units 14 & 17; forebay trash racks; up-looking	6	16	1	10	-49.5	1.6	-56	4	4	21
Units 14&17; 100 ft upstream of TIE; up-looking	6	0	1	10	-49.5	1.6	-56	4	4	25

Table 11
Polynomials Used to Describe Transducer Beam Shapes and Flow Trajectory and Speed as a Function of Range From Transducers. The variable X in polynomials is half-beam angle (degrees) for beam shape and midrange for trajectory and speed. B is the beam-pattern factor; plunge is degrees below horizontal and mps is m/second

Deployment	Input Variable	Polynomial or Constants
Units 1-6; forebay; down-looking	Beam Shape	B = .011170692053X⁴ - .158786483125X³ + .231914384635X² - .5101118323179999X + .056466461582
	Trajectory	plunge = 11
	Speed	mps = 1.07
Units 1-6; forebay; up-looking	Beam Shape	B = .011170692053X⁴ - .158786483125X³ + .231914384635X² - .5101118323179999X + .056466461582
	Trajectory	plunge = 11
	Speed	mps = 1.07
Units 1-6; in-turbine; down-looking	Beam Shape	B = -.003330226586X⁴ + .017471453954X³ - .310142606627X² + .035753868397X - .004849601465
	Trajectory	plunge = -.001281603844X⁴ + .049052933499X³ - .515811823786X² + 1.518635260846X - 16.59383269705
	Speed	mps = -.000106500555X⁴ + .00478133785X³ - .077676690819X² + .559559789228X - .17997330301
Units 7 and 9; in-turbine; down-looking	Beam Shape	B = -.003330226586X⁴ + .017471453954X³ - .310142505527X² + .035753868397X - .004849602465
	Trajectory	plunge = .002373764589X⁴ - .112735778158X³ + 1.56076075983X² - 6.603395811676X + 36.885504201695
	Speed	mps = .000018623951X⁴ - .001270343248X³ + .025384265243X² - .103042996658X + .677731764708
Units 7 and 9; in-turbine; up-looking	Beam Shape	B = -.003330226586X⁴ + .017471453954X³ - .310142505527X² + .035753868397X - .004849602465
	Trajectory	plunge = -.000308771027X⁴ + .001553540498X³ + .275668020657X² - 5.22697691328X - 4.1964285714
	Speed	mps = .000000000001X⁴ + .000291396396X³ - .003501776837X² - .051568234978X + 1.362891428571
Unit 10; in-turbine; down-looking	Beam Shape	B = -.00738221648X⁴ + .040217634582X³ - .404438802016X² + .036170817387X - .00152995463
	Trajectory	plunge = .002373764589X⁴ - .112735778158X³ + 1.56076075983X² - 6.603395811676X + 36.885504201695
	Speed	mps = .000018623951X⁴ - .001270343248X³ + .025384265243X² - .103042996658X + .677731764708
Unit 10; in-turbine; up-looking	Beam Shape	B = -.00738221648X⁴ + .040217634582X³ - .404438802016X² + .036170817387X - .00152995463
	Trajectory	plunge = -.000308771027X⁴ + .001553540498X³ + .275668020657X² - 5.22697691328X - 4.1964285714
	Speed	mps = .000000000001X⁴ + .000291396396X³ - .003501776837X² - .051568234978X + 1.362891428571
Unit 8; in-turbine; down-looking	Beam Shape	B = .011170692053X⁴ - .158786483125X³ + .231914384635X² - .5101118323179999X + .056466461582
	Trajectory	plunge = -.000086076347X⁴ + .016096619208X³ - .667377525502X² + 10.273234879192X - 56.813249624336
	Speed	mps = -.000607X³ + .0388228X² - .201837X + .8758629
Unit 8; in-turbine; up-looking	Beam Shape	B = .011170692053X⁴ - .158786483125X³ + .231914384635X² - .5101118323179999X + .056466461582
	Trajectory	plunge = -26
	Speed	mps = .000018340049X⁴ - .001702427407X³ + .04529765004X² - .435040205779X + 2.2606
Spill bays except 17; down-looking	Beam Shape	B = -.000479254381X⁴ + .005816071612X³ - .17653166225X² + .108057677967X - .001573760223
	Trajectory	plunge = -.08224067599X⁴ + 2.06132672882X³ - 17.20578942702X² + 60.665036907455X - 110.10999999990
	Speed	mps = -.000528205128X⁴ + .010511771562X³ - .06068467366X² + .517001107226X + .5129833333279999
Spill bay 17; down-looking	Beam Shape	B = -.000530808092X⁴ + .0063859799826X³ - 0.09439529188199999X² + .028290262437X - .004820576609
	Trajectory	plunge = -.08224067599X⁴ + 2.06132672882X³ - 17.20578942702X² + 60.665036907455X - 110.10999999990
	Speed	mps = -.000528205128X⁴ + .010511771562X³ - .06068467366X² + .517001107226X + .5129833333279999
Units 11-17; in-turbine; down-looking	Beam Shape	B = -.003330226586X⁴ + .017471453954X³ - .310142505527X² + .035753868397X - .004849601465
	Trajectory	plunge = -.003360361183X⁴ + .145723292012X³ - 2.010411084854X² + 7.381654309909X + 26.672858617129
	Speed	mps = .000049630032X⁴ - .001581448873X³ + .012092068792X² + .071453243301X + .81122724458
Units 11-17; in-turbine; up-looking	Beam Shape	B = -.003330226586X⁴ + .017471453954X³ - .310142505527X² + .035753868397X - .004849601465
	Trajectory	plunge = -26
	Speed	mps = -.000499129625X⁴ + .010107508945X³ - .072403499059X² + .194463002585X + 1.254298181816
Unit 18; in-turbine; down-looking	Beam Shape	B = -0.008221677889000001X⁴ + .043194835636X³ - .381788997264X² + .051218444314X - .005343461204
	Trajectory	plunge = -.003360361183X⁴ + .145723292012X³ - 2.010411084854X² + 7.381654309909X + 26.672858617129
	Speed	mps = .000049630032 X y⁴ - .001581448873 X y³ + .012092068792 X y² + .071453243301 X y + .81122724458
Unit 18; in-turbine; up-looking	Beam Shape	B = -0.008221677889000001X⁴ + .043194835636X³ - .381788997264X² + .051218444314X - .005343461204
	Trajectory	plunge = -26
	Speed	mps = -.000499129625X⁴ + .010107508945X³ - .072403499059X² + .194463002585X + 1.254298181816
Units 14&17; 100 ft upstream of TIE; up-looking	Beam Shape	B = -.003330226586X⁴ + .017471453954X³ - .310142505527X² + .035753868397X - .004849601465
	Trajectory	plunge = 0
	Speed	mps = -.000499129625X⁴ + .010107508945X³ - .072403499059X² + .194463002585X + 1.254298181816
Units 14 & 17; forebay trash racks; down-looking	Beam Shape	B = 0.011170692053X⁴ - 0.158786483125X³ + 0.231914384635X² - 0.510111832318X + 0.056466461582
	Trajectory	plunge = -.003360361183X⁴ + .145723292012X³ - 2.010411084854X² + 7.381654309909X + 26.672858617129
	Speed	mps = .000049630032X⁴ - .001581448873X³ + .012092068792X² + .071453243301X + .81122724458
Units 14 & 17; forebay trash racks; up-looking	Beam Shape	B = 0.011170692053X⁴ - 0.158786483125X³ + 0.231914384635X² - 0.510111832318X + 0.056466461582
	Trajectory	plunge = -26
	Speed	mps = -.000499129625X⁴ + .010107508945y³ - .072403499059X² + .194463002585X + 1.254298181816

Statistical Estimators and Comparisons

The following sections describe how the estimate of smolt passage was calculated at the various locations at Powerhouse 1.

Estimating In-Turbine PSC Unguided Passage

The estimate of unguided numbers at the PSC was calculated according to the formula

$$\hat{P}U = \sum_{i=1}^{d} \sum_{j=1}^{23} \sum_{k=1}^{18} \frac{N_{ijk}}{n_{ijk}} \sum_{l=1}^{n_{ijk}} u_{ijkl} \tag{5}$$

where $u_{ijkl} = $ expanded unguided fish count in the lth sampling unit ($l = 1, \ldots n_{ijk}$) of the kth intake slot ($k = 1, \ldots, 18$) of the jth hour ($j = 1, \ldots, 23$) of the ith day ($i = 1, \ldots, d$).

Based on simple random sampling (SRS) of minutes within the hour, the variance of $\hat{P}U$ can be estimated by

$$V\hat{a}r\left(\hat{P}U\right) = \sum_{i=1}^{d} \sum_{j=1}^{23} \sum_{k=1}^{18} \left[N_{ijk}^2 \left(1 - \frac{n_{ijk}}{N_{ijk}} \right) \frac{s_{u_{ijk}}^2}{n_{ijk}} \right] \tag{6}$$

where $s_{u_{ijk}}^2 = \dfrac{\sum_{l=1}^{n_{ijk}} \left(u_{ijkl} - \overline{u_{ijk}} \right)^2}{\left(n_{ijk} - 1 \right)}$,

$$\overline{u_{ijk}} = \frac{\sum_{l=1}^{n_{ijk}} u_{ijkl}}{n_{ijk}} \ ,$$

and where $N_{ijk} = $ possible number of sample units within an hour (i.e., nominally $N_{ijk} = 60$)

$n_{ijk} = $ actual number of samples drawn within the jth hour $\left(j = 1, \ldots, 23 \right)$ of the kth intake $\left(k = 1, \ldots, 8 \right)$ of the ith day $\left(i = 1, \ldots, d \right)$ (i.e., nominally $n_{ijk} = 20$).

Estimating In-Turbine PSC Guided Passage

The estimates of guided passage within the single-beam transducer beams are analogous to the estimates of unguided passage within the single-beam transducer beam. The estimate of guided numbers was calculated according to the formula

$$\hat{P}G_1 = \sum_{i=1}^{d} \sum_{j=1}^{23} \sum_{k=1}^{18} \frac{N_{ijk}}{n_{ijk}} \sum_{l=1}^{n_{ijk}} v_{ijkl}$$

(7)

where V_{ijkl} = expanded number of guided fish count in the lth sampling unit $\left(l = 1, \ldots, n_{ijk}\right)$ of the kth intake slot $\left(k = 1, \ldots, 18\right)$ of the jth hour $\left(j = 1, \ldots, 23\right)$ of the ith day $\left(i = 1, \ldots, d\right)$.

Again, based on an SRS of minutes within the hour, the variance of $\hat{P}G_1$ can be estimated by

$$V\hat{a}r\left(\hat{P}G_1\right) = \sum_{i=1}^{d} \sum_{j=1}^{23} \sum_{k=1}^{18} \left[N_{ijk}^2 \left(1 - \frac{n_{ijk}}{N_{ijk}}\right) \frac{s_{v_{ijk}}^2}{n_{ijk}} \right]$$

(8)

where $s_{v_{ijk}}^2 = \dfrac{\sum_{l=1}^{n_{ijk}} \left(v_{ijkl} - \overline{v_{jk}}\right)^2}{\left(n_{ijk} - 1\right)}$,

and where $\overline{v_{ijk}} = \dfrac{\sum_{l=1}^{n_{ijk}} v_{ijkl}}{n_{ijk}}$.

Estimating PSC-Guided Passage From Forebay Sampling

The sampling within the PSC slots can be envisioned as stratified sampling of two distinct strata composed of top and bottom positions of each of the five surface collector slots sampled. In which case, PSC-guided passage can also be estimated as

$$\hat{P}G_2 = \sum_{h=1}^{d} \sum_{i=1}^{23} \sum_{j=1}^{6} \sum_{k=1}^{2} \frac{M_{hijk}}{m_{hijkl}} \sum_{l=1}^{m_{hijk}} y_{hijkl}$$

(9)

where y_{hijkl} = expanded number of guided fish in the lth sampling unit $(l = 1, \ldots, m_{hijk})$ of the kth vertical stratum $(k = 1,2)$ of the jth PSC slot $(j = 1, \ldots, 6)$ in the ith hour $(i = 1, \ldots, 23)$ of the hth day $(h = 1, \ldots, d)$;

M_{hijk} = possible number of sampling units within an hour (i.e., nominally $M_{hijk} = 60$);

m_{hijk} = actual number of samples drawn within the ith hour $(i = 1, \ldots, 23)$ at the jth intake slot $(j = 1, \ldots, 6)$ and kth vertical stratum $(k = 1,2)$ of the hth day $(h = 1, \ldots, d)$ (i.e., nominally $m_{ijkl} = 20$).

The variance of $\hat{P}G_2$ can be estimated by the formula

$$Var\left(\hat{P}G_2\right) = \sum_{h=1}^{d} \sum_{i=1}^{23} \sum_{j=1}^{6} \sum_{k=1}^{2} M_{hijk}^2 \left(1 - \frac{m_{hijk}}{M_{hijk}}\right) \frac{s_{y_{hijk}}^2}{m_{hijk}} \qquad (10)$$

where $s_{y_{hijk}}^2 = \dfrac{\displaystyle\sum_{l=1}^{m_{hijk}} \left(y_{hijkl} - \overline{y_{hijk}}\right)^2}{\left(m_{hijk} - 1\right)}$

and where $\overline{y_{hijk}} = \dfrac{\displaystyle\sum_{l=1}^{m_{hijk}} y_{hijkl}}{m_{hijk}}$

Estimating Unit 8 Fish Guidance Efficiency

Background. At turbine intake slot 8b at Powerhouse 1, an ESBS was deployed. The goal of the statistical analysis was to estimate FGE at intake 8B using hydroacoustic data and to compare those estimates with FGE estimates collected using netting. The following describes estimators for FGE and associated variance estimates and statistical tests of FGE comparison.

Estimating unguided numbers. Using the single continuously sampled split-beam transducer, total unguided smolts numbers $\left(\hat{N}\right)$ were estimated using the formula

$$\hat{U} = \sum_{i=1}^{d} \sum_{j=1}^{23} \sum_{k=1}^{60} \hat{w}_{ijk}$$

where w_{ijk} = expanded number of unguided smolts entering the turbine intake
slot during the kth minute $(k = 1, \ldots, 60)$ of the jth hour
$(j = 1, \ldots, 23)$ of the ith day $(i = 1, \ldots, d)$.

The value of $\hat{w}_{ijk}$ was the expanded number of smolt detections across the
intake slot during a 1-minute time interval. The above estimate was compared
directly to fyke-net estimates by the NMFS but was expanded by a factor of three
to estimate unguided passage for all intakes at Unit 8 in comparisons with PSC
estimates.

Unlike many previous hydroacoustic investigations, sampling was continuous
over time, precluding the use of finite sampling methods to estimate the variance
of $\hat{U}$. Nevertheless, there was measurement error associated with the
interpretation of acoustic signals and the spatial expansion of the counts to the
entire intake. For convenience and to extract estimates of hydroacoustic sampling
error empirically, estimates of error variance were calculated on an hourly basis
during the duration of estimation. Hence, the variance of $\hat{U}$ was expressed as

$$V\hat{a}r\left(\hat{U}\right) = \sum_{i=1}^{d} \sum_{j=1}^{23} V\hat{a}r\left(\hat{w}_{ij}\right)$$

where $\hat{w}_{ij} = \sum_{k=1}^{60} \hat{w}_{ijk}$.

Methods for estimating the hourly measurement error associated with $\hat{w}_{ij}$ will
be discussed below. The variance estimate was expanded by a factor of nine to
estimate the variance of all three intakes at Unit 8 for comparison with PSC
estimates.

Estimating guided numbers. Using the single continuously sampled split-
beam transducer, an estimate of total guided smolts $\left(\hat{G}\right)$ can be estimated
according to the formula

$$\hat{G} = \sum_{i=1}^{d} \sum_{j=1}^{23} \sum_{k=1}^{60} \hat{x}_{ijk}$$

where $\hat{x}_{ijk}$ = expanded number of guided smolts bypassed during the kth minute
$(k = 1, \ldots, 60)$ of the jth hour $(j = 1, \ldots, 23)$ of the ith day
$(i = 1, \ldots, d)$.

The value of $\hat{x}_{ijk}$ was the expanded number of smolts detected across the intake slot during a 1-minute time interval. The above estimate was compared directly to gatewell dipping estimates but was expanded by a factor of three to estimate guided passage for all intakes at Unit 8 in comparisons with the PSC estimates.

The variance of $\hat{G}$ was expressed on an hourly basis as

$$Var\left(\hat{G}\right) = \sum_{i=1}^{d} \sum_{j=1}^{23} Var\left(\hat{x}_{ij}\right)$$

where $\hat{x}_{ij} = \sum_{k=1}^{60} \hat{x}_{ijk}$.

Methods for estimating the hourly measurement error associated with $\hat{x}_{ij}$ will be discussed in a subsequent section. This variance estimate was expanded by a factor of nine to estimate the variance of all three intakes at Unit 8 for comparisons with PSC estimates.

Fish guidance efficiency estimate. Using the independent estimates of guided $\left(\hat{G}\right)$ and unguided $\left(\hat{U}\right)$ fish numbers for a time interval of interest, FGE was estimated according to the formula

$$F\hat{G}E = \frac{\hat{G}}{\hat{G} + \hat{U}}$$

with associated variance estimator

$$Var\left(F\hat{G}E\right) = F\hat{G}E^2 \left(1 - F\hat{G}E\right)^2 \left[\frac{Var\left(\hat{G}\right)}{\hat{G}^2} + \frac{Var\left(\hat{U}\right)}{\hat{U}^2}\right].$$

Asymptotic $\left(1 - a\right)$ 100% confidence intervals for FGE were calculated as

$$F\hat{G}E \pm Z_{1-\frac{\alpha}{2}} \sqrt{Var\left(F\hat{G}E\right)} \quad .$$

Comparing methods. The National Marine Fisheries Service (NMFS) sampled the center slot of Unit 8 to calculate FGE using netting and gatewell data concurrent with this study. Paired hydroacoustic and fyke-net estimates of FGE were calculated for each NMFS trial and compared using a paired t-test. The paired t-test tested the null hypothesis of equal mean FGE estimates for the two estimation techniques at a significance level of a = 0.05 two-tailed. When numbers of fish detected by hydroacoustics during concurrent sampling with

netting were low, hydroacoustic FGE was calculated from estimates of guided and unguided fish for a 4-hour sampling period instead of the concurrent sampling period. The extended hydroacoustic sampling period was used to collect additional smolt counts and to dampen the binomial sampling variance associated with the hydroacoustic FGE estimates.

Estimating hydroacoustic measurement error. Because of the continuous within-hour sampling, sampling error was eliminated from the estimates of guided and unguided numbers. Nevertheless, measurement error persisted and needed to be estimated. The approach to estimating measurement error was an extension of a compound-Poisson process Skalski and Robson (1992) used to model abundance in continuous intervals.

The estimate of measurement error was based on the assumptions:

a. Per-minute measurement error $\left(\boldsymbol{s}^2_{ME}\right)$ was constant within an hour.

b. Within an hour, smolt passage has a constant mean and variance.

c. Within a minute, smolt counts were Poisson-distributed with mean and variance $\boldsymbol{l}_k$ $(k = 1, \ldots, 60)$.

d. Within an hour, the Poisson parameters $\boldsymbol{l}_k$ were distributed with mean $\boldsymbol{m}$ and variance $\boldsymbol{s}^2$.

e. The $\boldsymbol{l}_k$ were auto-correlated with a function of distance between the 1-minute intervals.

Based on the above assumptions, the variance for the estimated smolt count in a 1-minute interval $\left(\hat{x}_k\right)$ can be calculated to be

$$\hat{Var}\left(\hat{x}_k\right) = Var_3\left\{E_2\left[Var_1\left(\hat{x}_k\,|2,3\right)\right]\right\} + E_3\left\{Var_2\left[E_1\left(\hat{x}_k\,|2,3\right)\right]\right\}$$
$$+ E_3\left\{E_2\left[Var_1\left(\hat{x}_k\,|2,3\right)\right]\right\}$$

where 1, 2, and 3 denote

1 = stage 1 of hydroacoustic measurement error of $\hat{x}_k$ about x_k with variance $\boldsymbol{s}^2_{ME}$,

2 = stage 2 of x_k Poisson-distributed with mean $\boldsymbol{l}_k$,

3 = stage 3 of $\boldsymbol{l}_k$ distributed with mean $\boldsymbol{m}$ and variance $\boldsymbol{s}^2$ within the hour.

Then

$$Var\left(\hat{x}_k\right) = Var_3\left[E_2\left(x_k\,|3\right)\right] + E_3\left[Var_2\left(x_k\,|3\right)\right] + E_3\left[E_2\left(\sigma_{ME}^2\,|3\right)\right]$$

$$= Var_3\left(\lambda_k\right) + E_3\left(\lambda_k\right) + E_3\left(\sigma_{ME}^2\right) \qquad (11)$$

$$Var\left(\hat{x}_k\right) = \boldsymbol{s}^2 + \boldsymbol{m} + \boldsymbol{s}_{ME}^2$$

If an additional assumption was that the variance $\boldsymbol{s}^2$ is insignificantly small between consecutive 1-minute intervals (i.e., $\boldsymbol{s}^2 = 0$), then Equation (1) reduces to

$$Var\left(\hat{x}_k\right) = \mu + \sigma_{ME}^2 \qquad (12)$$

Equation (2) suggested the method of moment estimator

$$\sigma_{ME}^2 = V\hat{a}r\left(\hat{x}_k\right) - \hat{\mu}_k \qquad (13)$$

where $V\hat{a}r\left(\hat{x}_k\right) = \dfrac{\left(\hat{x}_k - \hat{x}_{k+1}\right)^2}{2}$,

$$\hat{\mu}_k = \dfrac{\left(x_k + x_{k+1}\right)}{2}.$$

If $\boldsymbol{s}^2$ is not zero, then $\hat{\boldsymbol{s}}_{ME}^2$ overestimates the size of $\boldsymbol{s}_{ME}^2$.

The within-hour measurement error associated with $\hat{x}_{ij}$ was expressed as

$$V\hat{a}r\left(\hat{x}_{ij}\right) = \frac{60}{59}\sum_{k=1}^{59}\left[\frac{\left(\hat{x}_{ijk} - \hat{x}_{ijk+1}\right)^2}{2} - \frac{\left(\hat{x}_{ijk} + \hat{x}_{ijk+1}\right)}{2}\right] \qquad (14)$$

If $V\hat{a}r\left(\hat{x}_{ij}\right) < 0$, it was set equal to zero for the ijth hour. The variance of $\hat{G}$ was then a sum of the within-hour measurement errors where

$$V\hat{a}r\left(\hat{G}\right) = \sum_{i=1}^{d}\sum_{j=1}^{23} V\hat{a}r\left(\hat{x}_{ij}\right) \qquad (15)$$

An analogous procedure for estimating the variance of $\hat{U}$ was used. Variance estimator (Equation 14) was used whenever the complete hour was acoustically monitored. It was applied when unintentional losses of data occurred such as an

equipment outage or data downloading. In these events, the variance was calculated according to the formula

$$Var\left(\hat{x}_{ij}\right) = \frac{60}{a}\sum_{k=1}^{a}\left[\frac{\left(\hat{x}_{ijk} - \hat{x}_{ijk+1}\right)^2}{2} - \frac{\left(\hat{x}_{ijk} + \hat{x}_{ijk+1}\right)}{2}\right] \tag{16}$$

where a is the number of intervals with two successive 1-minute samples intact.

It should be noted that if s^2 in Equation 11 was zero, then Equation 14 could be alternatively estimated by the formula

$$60 \cdot s^2_{x_{ijk}}$$

where

$$s^2_{x_{ijk}} = \frac{\sum_{k=1}^{60}\left(\hat{x}_{ijk} - \hat{x}_{ij}\right)^2}{\left(60 - 1\right)}$$

because in this case,

$$E\left(60\, s^2_{x_{ijk}}\right) = 60\sigma^2_{ME}$$

the same expected value as that of Equation 14. Any difference in magnitude between Equation 14 and Equation 16 is an estimate of the within-hour value of s^2. Equations 14 and 16 provide similar results for a situation with little temporal variability in smolt counts.

Estimating Unguided Passage at Units 7, 9, and 10

The unguided passage into Units 7, 9, and 10 can be estimated by the formula

$$\hat{TU} = 3\sum_{i=1}^{d}\sum_{j=1}^{23}\sum_{k=1}^{3}\frac{H_{ijk}}{h_{ijk}}\sum_{l=1}^{h_{ijk}} z_{ijkl} \tag{17}$$

where z_{ijkl} = expanded unguided fish counts in the lth sampling unit

$\left(l = 1, \ldots, h_{ijk}\right)$ at the kth turbine intake $\left(k = 1, 2, 3\right)$ in the jth hour $\left(j = 1, \ldots, 23\right)$ of the ith day $\left(i = 1, \ldots, d\right)$;

H_{ijk} = possible number of sampling units within an hour (i.e., nominally $H_{ijk} = 60$);

h_{ijk} = actual number of samples drawn within the *j*th hour $(j = 1, ..., 23)$ at the *k*th turbine unit $(k = 1, 2, 3)$ on the *i*th day $(i = 1, ..., d)$ (i.e., nominally $h_{ijk} = 20$).

Here, the z_{ijkl} are counts in only the single intake slots that were actually monitored. The estimator (Equation 17) expands these counts by a factor of three to estimate total unguided passage through Units 7, 9, and 10.

To account for the slot-to-slot variance within turbine units, the sampling scheme for Units 7, 9, and 10 was viewed as sampling of three of nine intakes with STSs. The second stage of sampling was the sampling of time intervals within the slot-hour. So, instead of using a variance estimator based upon simple random sampling, the following formula was used:

$$Vâr\left(\hat{H}U\right) = \sum_{g=1}^{5} \frac{L_g^2\left(1 - \frac{l_g}{L_g}\right)s_{\hat{U}_g}^2}{l_g} + \sum_{g=1}^{5}\left[\frac{L_g \sum_{k=1}^{l_g} Vâr\left(\hat{U}_{gk}\right)}{l_g}\right] \tag{18}$$

where

L_g = number of turbine intake slots in the *g*th stratum $(g = 1)$ (here, $l_g = 9$);

l_g = number of turbine intake slots sampled in the *g*th stratum $(g = 1)$ (here, $l_g = 3$);

$$s_{\hat{U}_g}^2 = \frac{\sum_{k=1}^{l_g}\left(\hat{U}_{gk} - \hat{\bar{U}}_g\right)^2}{\left(l_g - 1\right)}$$

$$\hat{\bar{U}}_g = \frac{\sum_{k=1}^{l_g}\hat{U}_{gk}}{l_g}$$

$$\hat{U}_{gk} = \sum_{i=1}^{d} \sum_{j=1}^{23} \frac{R_{ijgk}}{r_{ijgk}} \sum_{l=1}^{r_{ijgk}} b_{ijkl}$$

$$V\hat{a}r\left(\hat{U}_{gk}\right) = \sum_{i=1}^{d} \sum_{j=1}^{23} \left[\frac{R_{ijgk}^2 \left(1 - \frac{r_{ijgk}}{R_{ijgk}}\right) s_{b_{ijgk}}^2}{r_{ijgk}} \right]$$

and where

r_{ijgk} = actual number of time intervals sampled in the jth hour $(j = 1, \ldots, 23)$ of the ith day $(i = 1, \ldots, d)$ at the kth intake slot $(k = 1, \ldots, l_g)$ in the gth stratum $(g = 1)$ (i.e., nominally 15 1-minute samples);

R_{ijgk} = number of possible time intervals that could be sampled in the jth hour $(j = 1, \ldots, 23)$ of the ith day $(i = 1, \ldots, d)$ at the kth intake slot $(k = 1, \ldots, l_g)$ in the gth stratum $(g = 1)$ (i.e., nominally 60 1-minute samples);

b_{ijgkl} = estimated unguided fish passage in the lth sample $(l = 1, \ldots, r_{ijgk})$ in jth hour $(j = 1, \ldots, 23)$ of the ith day $(i = 1, \ldots, d)$ at the kth intake slot $(k = 1, \ldots, l_g)$ in the gth stratum $(g = 1)$;

$$s_{b_{ijgk}}^2 = \frac{\sum_{l=1}^{r_{ijgk}} \left(b_{ijgkl} - \overline{b_{ijgk}}\right)^2}{\left(r_{ijgk} - 1\right)};$$

$$\overline{b_{ijgk}} = \frac{\sum_{l=1}^{r_{jgk}} b_{ijgkl}}{r_{ijgk}}.$$

Estimating Guided Passage at Units 7, 9, and 10

The estimation scheme for the guided passage at sampled intake slots at Units 7, 9, and 10 is analogous to the estimation of unguided numbers at Units 7, 9, and 10. An estimate of guided numbers at these turbine units is then

$$\hat{T}G = 3\sum_{i=1}^{d}\sum_{j=1}^{23}\sum_{k=1}^{3}\frac{H_{ijk}}{h_{ijk}}\sum_{l=1}^{h_{ijk}}a_{ijkl}$$

(19)

where a_{ijkl} = expanded guided fish counts in the lth sampling unit $\left(l=1,\ldots,h_{ijk}\right)$ at the kth turbine intake $\left(k=1,2,3\right)$ in the jth hour $\left(j=1,\ldots,23\right)$ of the ith day $\left(i=1,\ldots,d\right)$.

The same two-stage sampling scheme that was used for estimating unguided passage also was used in analyzing the guided fish passage in order to calculate a conservative variance estimator, as follows:

$$V\hat{a}r\left(\hat{H}G\right)=\sum_{g=1}^{5}\frac{L_g^2\left(1-\dfrac{l_g}{L_g}\right)s_{\hat{G}_g}^2}{l_g}+\sum_{g=1}^{5}\left[\frac{L_g\displaystyle\sum_{k=1}^{l_g}V\hat{a}r\left(\hat{G}_{gk}\right)}{l_g}\right]$$

(20)

$$s_{\hat{G}_g}^2=\frac{\displaystyle\sum_{k=1}^{l_g}\left(\hat{G}_{gk}-\hat{\bar{G}}_g\right)^2}{\left(l_g-1\right)}\ ;$$

$$\hat{\bar{G}}_g=\frac{\displaystyle\sum_{k=1}^{l_g}\hat{G}_{gk}}{l_g}\ ;$$

$$\hat{G}_{gk}=\sum_{i=1}^{d}\sum_{j=1}^{23}\frac{R_{ijgk}}{r_{ijgk}}\sum_{l=1}^{r_{ijgk}}c_{ijgkl}\ ;$$

$$V\hat{a}r\left(\hat{G}_{gk}\right)=\sum_{i=1}^{d}\sum_{j=1}^{23}\left[\frac{R_{ijgk}^2\left(1-\dfrac{R_{ijgk}}{r_{ijgk}}\right)s_{c_{ijgk}}^2}{r_{ijgk}}\right]\ ;$$

$$s_{c_{ijgk}}^2=\frac{\displaystyle\sum_{l=1}^{r_{ijgk}}\left(c_{ijgkl}-\overline{c_{jgk}}\right)^2}{r_{ijgk}}\ ;$$

where

$$\overline{c_{jgk}}=\frac{\displaystyle\sum_{l=1}^{r_{ijgk}}c_{ijgkl}}{r_{ijgk}}\ ;$$

and where

c_{ijgkl} = estimated guided fish passage in the lth sample $\left(l=1,\ldots,r_{ijgk}\right)$ in the jth hour $\left(j=1,\ldots,23\right)$ of the ith day $\left(i=1,\ldots,d\right)$ at the kth intake slot $\left(k=1,\ldots,l_g\right)$ in the gth stratum $\left(g=1,\ldots,5\right)$.

Estimating PSC Performance

The PSC performance was evaluated on a unit-by-unit basis and for the entire structure using two performance measures. The PSC efficiency was estimated by

$$P\hat{S}CE = \frac{\hat{P}G_2}{\hat{P}G_2 + \hat{P}U}$$

(21)

with associated variance estimator

$$V\hat{a}r\left(P\hat{S}CE\right) = P\hat{S}CE^2\left(1 - P\hat{S}CE\right)^2\left[\frac{V\hat{a}r\left(\hat{P}G_2\right)}{\hat{P}G_2^2} + \frac{V\hat{a}r\left(\hat{P}U\right)}{\hat{P}U^2}\right]$$

(22)

using the variances of $\hat{P}U$ and $\hat{P}G_2$ calculated using Equations 6 and 9, respectively.

The PSC performance can also be estimated by the formula

$$P\hat{S}CE = \frac{\hat{P}G_1}{\hat{P}G_1 + \hat{P}U}.$$

(23)

In this case, $\hat{P}G_1$ and $\hat{P}U$ are correlated because the sampling data was coming from the same single-beam downward-angled transducers (Figure 1). The variance of $P\hat{S}CE$ was estimated by

$$V\hat{a}r\left(P\hat{S}CE\right) = \left(PSCE\right)^2\left(1 - PSCE\right)^2\left[\frac{V\hat{a}r\left(\hat{P}G_1\right)}{\hat{P}G_1^2} + \frac{V\hat{a}r\left(\hat{P}U\right)}{\hat{P}U^2} - 2\frac{C\hat{o}v\left(\hat{P}G_1, \hat{P}U\right)}{\hat{P}G_1 \cdot \hat{P}U}\right]$$

(24)

and where

$$Cov\left(\hat{P}G_1, \hat{P}U\right) = \sum_{i=1}^{d} \sum_{j=1}^{23} \sum_{k=1}^{18} N_{ijk}^2 \left(1 - \frac{n_{ijk}}{N_{ijk}}\right) \frac{Cov\left(v_{ijk}, u_{ijk}\right)}{n_{ijk}},$$

$$Cov\left(v_{ijk}, u_{ijk}\right) = \frac{\sum_{l=1}^{n_{ijk}} \left(u_{ijkl} - \overline{u_{ijk}}\right)\left(v_{ijkl} - \overline{v_{ijk}}\right)}{\left(n_{ijk} - 1\right)}.$$

The PSC effectiveness was estimated by the quantity

$$P\hat{S}CF = \frac{\left(\dfrac{\hat{P}G}{V_{SPC}}\right)}{\left(\dfrac{\hat{P}G + \hat{P}U}{V_T}\right)} = P\hat{S}CE \cdot \frac{V_T}{V_{SPC}} \tag{25}$$

where V_{SPC} = water volume entering SPC slots,

V_T = total water volume entering the PSC and turbine slots 1-6

and associated variance estimator

$$Var\left(P\hat{S}CF\right) = \left(\frac{V_T}{V_{SPC}}\right)^2 \cdot Var\left(S\hat{P}CE\right). \tag{26}$$

The general forms of Equations 17 and 19 allow PSC efficiency and effectiveness to be calculated over any temporal and spatial scale of interest. It should also be noted that PSC effectiveness could be estimated using either guided numbers $\hat{P}G_1$ (Equation 7) or $\hat{P}G_2$ (Equation 9).

Asymptotic $(1 - a)$ 100 percent confidence intervals were calculated according to the general formula

$$\hat{q} \pm Z_{1-\frac{a}{2}} \sqrt{Var\left(\hat{q}\right)}$$

for any parameter estimate $\hat{q}$.

Estimating FGE for Units 7-10

The FGE for Units 7-10 was estimated according to the formula

$$F\hat{G}E = \frac{\hat{T}G}{\hat{T}G + \hat{T}U} \qquad (27)$$

with associated variance estimator

$$V\hat{a}r\left(F\hat{G}E\right) = F\hat{G}E^2 \left(1 - F\hat{G}E\right)^2 \left[\frac{V\hat{a}r\left(\hat{T}G\right)}{\hat{T}G^2} + \frac{V\hat{a}r\left(\hat{T}U\right)}{\hat{T}U^2}\right]. \qquad (28)$$

Asymptotic $(1 - a)$ 100 percent confidence intervals were calculated according to the general formula

$$\hat{q} \pm Z_{1-\frac{a}{2}} \sqrt{V\hat{a}r(\hat{q})}$$

for either FGE. It should be noted that variance formula (Equation 28) underestimates the variance of FGE estimates when making inferences to all of Unit 8. However, the variance formula is appropriate when making inferences to the specific intake slots sampled (e.g., slot 8b with the ESBS). The FGE variance estimate for Units 7, 9, and 10 should be conservative because of the conservative variance estimator for those units.

Comparing Fish Passage Performance at Powerhouse 1

Comparison of FPE at the PSC, turbine Units 7, 9, and 10 or turbine Unit 8 was based on inspection of the $(1 - a)$ 100 percent confidence intervals. Overlapping intervals suggested no significant difference; non-overlapping intervals suggested a statistically significant difference at a.

Comparing Guided Fish Passage at the PSC

The two estimates of guided fish passage at the PSC were compared by regressing the single-beam counts on split-beam counts. It was anticipated that the data would fit a regression line with a zero intercept and a slope of one if the sampling approaches were equivalent. This regression analysis was based on daily estimates of guided fish numbers by each method. We also compared the two estimates by examining for overlap between $(1 - a)$ 100 percent confidence

interval estimates of $\hat{P}G_1$ and $\hat{P}G_2$ and by calculating a $(1-a)$ 100 percent confidence interval for the difference:

$$\left(\hat{P}G_1 - \hat{P}G_2\right) \pm Z_{1-\frac{a}{2}} \sqrt{V\hat{a}r\left(\hat{P}G_1\right) + V\hat{a}r\left(\hat{P}G_2\right)}.$$

The above comparisons can be performed on any time intervals of interest such as daily, weekly, or seasonally.

Estimating Spillway Fish Passage

The sampling at the Bonneville spillway was designed as a stratified two-stage sampling regime. The spill bays were assigned to five longitudinal strata corresponding to spillways 2-4, 5-7, 8-10, 11-14, and 15-17 (Table 12). Within strata, spillways were randomly selected with varying levels of within-strata effort. The second stage of sampling was a random sample of time intervals with a spillway-hour.

Table 12
Sampling Strata Established at Bonneville Spillway With Sampled Bays Denoted With an Asterisk (*). The variables H_g and h_g are the maximum number of operational spill bays and sampled spill bays, respectively, in a stratum

								Spillway Strata								
		1				2			3			4			5	
	*		*	*		*		*		*	*	*	*	*		*
~~18~~	17	16	15	14	13	12	11	10	9	8	7	6	5	4	3	2	~~1~~

$H_1 = 3$ $H_2 = 4$ $H_3 = 3$ $H_4 = 3$ $H_5 = 3$

$h_1 = 2$ $h_2 = 2$ $h_3 = 2$ $h_4 = 3$ $h_5 = 2$

Total spillway passage was estimated by the formula

$$\hat{S} = \sum_{g=1}^{5} \left[\frac{H_g}{h_g} \sum_{i=1}^{h_g} \sum_{j=1}^{d} \sum_{k=1}^{23} \frac{T_{gijk}}{t_{gijk}} \sum_{l=1}^{t_{gijk}} p_{gijkl} \right] \tag{29}$$

where p_{gijkl} = expanded fish passage in the *l*th sampling interval
$\left(l = 1, \ldots, t_{gik}\right)$ during the *k*th hour $(k = 1, \ldots, 23)$ in the *j*th day
$(j = 1, \ldots, d)$ at the *i*th spillway $\left(i = 1, \ldots, h_g\right)$ in the *g*th stratum
$(g = 1, \ldots, 5)$;

T_{gijk} = possible number of sampling units within an hour (i.e., nominally $T_{gijk} = 60$);

t_{gijk} = actual number of samples drawn within the kth hour $(k = 1,\ldots,23)$ in the jth day $(j = 1,\ldots,d)$ at the ith spillway $(i = 1,\ldots,h_g)$ in the gth stratum $(g = 1,\ldots,5)$ (i.e., nominally $t_{gijk} = 12$);

H_g = number of operating (open) spill bays within the gth spillway stratum

h_g = number of operating (open) spill bays actually sampled within the gth spillway stratum

Table 12 shows maximum sizes of H_g and h_g by stratum. When a spill bay was closed, fish passage there was set to zero and H_g and h_g was decreased by 1 for that stratum. In choosing spill bays for sampling, the ones selected were most likely to be open according to the spill pattern outlined in the Fish Passage Plan. The variance of $\hat{S}$ was estimated by the quantity

$$\hat{Var}\left(\hat{S}\right) = \sum_{g=1}^{5} \frac{H_g^2 \left(1 - \frac{h_g}{H_g}\right) s_{\hat{S}_g}^2}{h_g} + \sum_{g=1}^{5}\left[\frac{H_g \sum_{j=1}^{h_g} \hat{Var}\left(\hat{S}_{gi}\right)}{h_g}\right] \tag{30}$$

where $s_{\hat{S}_g}^2 = \dfrac{\sum_{j=1}^{h_g}\left(\hat{S}_{g_i} - \hat{\bar{S}}_g\right)^2}{\left(h_g - 1\right)}$,

$\hat{\bar{S}}_g = \dfrac{\sum_{i=1}^{h_g} \hat{S}_{g_i}}{h_g}$,

$\hat{S}_{g_i} = \sum_{j=1}^{d}\sum_{k=1}^{23} \dfrac{T_{gijk}}{t_{gijk}} \sum_{l=1}^{t_{gijk}} p_{gijkl}$,

and where

$$\hat{Var}\left(\hat{S}_{g_i}\right) = \sum_{j=1}^{d}\sum_{k=1}^{23}\left[T_{gijk}^2 \left(1 - \frac{t_{gijk}}{T_{gijk}}\right) \frac{s_{p_{gijk}}^2}{t_{gijk}}\right],$$

$$s_{p_{gijk}}^2 = \frac{\sum_{l=1}^{t_{gijk}} \left(p_{gijkl} - \overline{p_{gijk}} \right)^2}{\left(t_{gijk} - 1 \right)},$$

$$\overline{p_{gijk}} = \frac{\sum_{l=1}^{t_{gijk}} p_{gijkl}}{t_{gijk}}.$$

Note that, in the case of stratum #4, all spill bays were sampled (i.e., $H_5 = h_5$), such that stratum #4 will contribute only to the second term of the variance formula (Equation 30).

Estimating Powerhouse 2 Unguided Passage

Using the fish counts from the down-looking transducers, total unguided fish passage at Powerhouse 2 was estimated by the quantity

$$\hat{HU} = \sum_{i=1}^{d} \sum_{j=1}^{23} \sum_{k=1}^{8} 3 \left[\frac{R_{ijk}}{r_{ijk}} \sum_{l=1}^{r_{ijk}} b_{ijkl} \right] \tag{31}$$

where b_{ijkl} = estimated fish passage in the lth sampling unit $\left(l = 1, \ldots, r_{ijk} \right)$ in the jth hour $\left(j = 1, \ldots, 23 \right)$ at the kth turbine unit $\left(k = 1, \ldots, 8 \right)$ in the ith day $\left(i = 1, \ldots, d \right)$;

R_{ijk} = number of possible sampling units in the jth hour $\left(j = 1, \ldots, 23 \right)$ at the kth turbine unit $\left(k = 1, \ldots, 8 \right)$ in the ith day $\left(i = 1, \ldots, d \right)$ (i.e., nominally 60 1-minute samples);

r_{ijk} = actual number of time intervals sampled in the jth hour $\left(j = 1, \ldots, 23 \right)$ at the kth turbine unit $\left(k = 1, \ldots, 8 \right)$ in the ith day $\left(i = 1, \ldots, d \right)$ (i.e., nominally 15 1-minute samples).

To account for the slot-to-slot variance within turbine units, the sampling scheme at Powerhouse 2 was viewed as a stratified random sampling scheme. Using pairs of consecutive turbine units (11 and 12, 13 and 14, 15 and 16, 17 and 18) as strata, it was assumed that two of six intake slots were randomly selected for monitoring within each stratum. The second stage of sampling was the sampling of time intervals within the slot-hour. This two-stage stratified sampling scheme is analogous to the model used for the analysis of passage data from spillways. The conservative variance estimator (Equation 20) was as follows:

$$Var\left(\hat{H}U\right) = \sum_{g=1}^{5} \frac{L_g^2\left(1-\frac{l_g}{L_g}\right)s_{\hat{U}_g}^2}{l_g} + \sum_{g=1}^{5}\left[\frac{L_g\sum_{k=1}^{l_g}Var\left(\hat{U}_{gk}\right)}{l_g}\right] \tag{32}$$

where

L_g = number of turbine intake slots in the *g*th stratum $\left(g=1,\ldots,5\right)$ (here, $l_g = 6$);

l_g = number of turbine intake slots sampled in the *g*th stratum $\left(g=1,\ldots,5\right)$ (here, $l_g = 2$);

$$s_{\hat{U}_g}^2 = \frac{\sum_{k=1}^{l_g}\left(\hat{U}_{gk}-\bar{\hat{U}}_g\right)^2}{\left(l_g-1\right)} \; ;$$

$$\bar{\hat{U}}_g = \frac{\sum_{k=1}^{l_g}\hat{U}_{gk}}{l_g} \; ;$$

$$\hat{U}_{gk} = \sum_{i=1}^{d}\sum_{j=1}^{23}\frac{R_{ijgk}}{r_{ijgk}}\sum_{l=1}^{r_{ijgk}}b_{ijkl} \; ;$$

$$Var\left(\hat{U}_{gk}\right) = \sum_{i=1}^{d}\sum_{j=1}^{23}\left[\frac{R_{ijgk}^2\left(1-\frac{r_{ijgk}}{R_{ijgk}}\right)s_{b_{ijgk}}^2}{r_{ijgk}}\right] \; ;$$

and where

r_{ijgk} = actual number of time intervals sampled in the *j*th hour $\left(j=1,\ldots,23\right)$ of the *i*th day $\left(i=1,\ldots,d\right)$ at the *k*th intake slot $\left(k=1,\ldots,l_g\right)$ in the *g*th stratum $\left(g=1,\ldots,5\right)$ (i.e., nominally 15 1-minute samples);

R_{ijgk} = number of possible time intervals that could be sampled in the *j*th hour $\left(j=1,\ldots,23\right)$ of the *i*th day $\left(i=1,\ldots,d\right)$ at the *k*th intake slot

$\left(k = 1, \ldots, l_g \right)$ in the gth stratum $\left(g = 1, \ldots, 5 \right)$ (i.e., nominally 60 1-minute samples);

b_{ijgkl} = estimated unguided fish passage in the lth sample $\left(l = 1, \ldots, r_{ijgk} \right)$ in jth hour $\left(j = 1, \ldots, 23 \right)$ of the ith day $\left(i = 1, \ldots, d \right)$ at the kth intake slot $\left(k = 1, \ldots, l_g \right)$ in the gth stratum $\left(g = 1, \ldots, 5 \right)$;

$$s_{b_{ijgk}}^2 = \frac{\sum\limits_{l=1}^{r_{ijgk}} \left(b_{ijgkl} - \overline{b_{ijgk}} \right)^2}{\left(r_{ijgk} - 1 \right)};$$

$$\overline{b_{ijgk}} = \frac{\sum\limits_{l=1}^{r_{jgk}} b_{ijgkl}}{r_{ijgk}}.$$

Estimating Powerhouse 2 Guided Passage

Using the fish counted by the up-looking transducers, the estimate of total guided fish passage at Powerhouse 2 was estimated by the quantity

$$\hat{H}G = \sum_{i=1}^{d} \sum_{j=1}^{23} \sum_{k=1}^{8} 3 \left[\frac{R_{ijk}}{r_{ijk}} \sum_{l=1}^{r_{ijk}} c_{ijkl} \right] \tag{33}$$

where c_{ijkl} = estimated fish passage in the lth sampling unit $\left(l = 1, \ldots, r_{ijk} \right)$ at the kth turbine unit $\left(k = 1, \ldots, 8 \right)$ in the jth hour $\left(j = 1, \ldots, 23 \right)$ in the ith day $\left(i = 1, \ldots, d \right)$.

The same two-stage stratified sampling scheme used in estimating unguided passage was also used in analyzing the guided fish passage in order to calculate a conservative variance estimator. The variance estimator was as follows:

$$Var\left(\hat{H}G \right) = \sum_{g=1}^{5} \frac{L_g^2 \left(1 - \frac{l_g}{L_g} \right) s_{\hat{G}_g}^2}{l_g} + \sum_{g=1}^{5} \left[\frac{L_g \sum\limits_{k=1}^{l_g} Var\left(\hat{G}_{gk} \right)}{l_g} \right] \tag{34}$$

where

$$s_{\hat{G}_g}^2 = \frac{\sum_{k=1}^{l_g}\left(\hat{G}_{gk} - \hat{\bar{G}}_g\right)^2}{\left(l_g - 1\right)};$$

$$\hat{\bar{G}}_g = \frac{\sum_{k=1}^{l_g}\hat{G}_{gk}}{l_g};$$

$$\hat{G}_{gk} = \sum_{i=1}^{d}\sum_{j=1}^{23}\frac{R_{ijgk}}{r_{ijgk}}\sum_{l=1}^{r_{ijgk}}c_{ijgkl};$$

$$V\hat{a}r\left(\hat{G}_{gk}\right) = \sum_{i=1}^{d}\sum_{j=1}^{23}\left[\frac{R_{ijgk}^2\left(1 - \dfrac{R_{ijgk}}{r_{ijgk}}\right)s_{c_{ijgk}}^2}{r_{ijgk}}\right];$$

$$s_{c_{ijgk}}^2 = \frac{\sum_{l=1}^{r_{ijgk}}\left(c_{ijgkl} - \overline{c_{jgk}}\right)^2}{r_{ijgk}};$$

$$\overline{c_{jgk}} = \frac{\sum_{l=1}^{r_{ijgk}}c_{ijgkl}}{r_{ijgk}};$$

and where

c_{ijgkl} = estimated guided fish passage in the lth sample $\left(l = 1,\ldots,r_{ijgk}\right)$ in the jth

hour $\left(j = 1,\ldots,23\right)$ of the ith day $\left(i = 1,\ldots,d\right)$ at the kth intake slot

$\left(k = 1,\ldots,l_g\right)$ in the gth stratum $\left(g = 1,\ldots,5\right)$.

Estimating Spill Efficiency

The spill efficiency at the Bonneville project was estimated by the quotient

$$\hat{SE} = \frac{\hat{S}}{\left[\hat{P}U + \hat{P}G + \hat{T}U + \hat{T}G + \hat{E}U + \hat{E}G + \hat{H}U + \hat{H}G + \hat{S}\right]} = \frac{\hat{S}}{\hat{NS} + \hat{S}} \qquad (35)$$

where the numerator was the estimated fish passage at the spillway and the denominator was total fish passage through the project. The variance of $\hat{SE}$ was be estimated by

$$Var\left(\hat{SE}\right) = \hat{SE}^2\left(1 - \hat{SE}\right)^2\left[\frac{Var\left(\hat{S}\right)}{\hat{S}^2} + \frac{Var\left(\hat{NS}\right)}{\hat{NS}^2}\right] \tag{36}$$

where $\hat{NS} = \hat{P}U + \hat{P}G + \hat{T}U + \hat{T}G + \hat{E}U + \hat{E}G + \hat{H}U + \hat{H}G$,

and where

$$Var\left(\hat{NS}\right) = Var\left(\hat{P}U\right) + Var\left(\hat{P}G\right) + Var\left(\hat{T}U\right) + Var\left(\hat{T}G\right) + Var\left(\hat{E}U\right) + Var\left(\hat{E}G\right)$$
$$+ Var\left(\hat{H}U\right) + Var\left(\hat{H}G\right).$$

Estimating Spill Effectiveness

The spill effectiveness at the Bonneville project was estimated by the quantity

$$\hat{SY} = \frac{\left(\dfrac{\hat{S}}{V_S}\right)}{\dfrac{\left(\hat{NS} + \hat{S}\right)}{V_T}} = \hat{SE} \cdot \frac{V_T}{V_S} \tag{37}$$

where V_S = volume of water spilled,

V_T = total volume of water passing the dam during the period of inference.

The variance of $\hat{SY}$ can be estimated by

$$Var\left(\hat{SY}\right) = \left(\frac{V_T}{V_S}\right)^2 \cdot Var\left(\hat{SE}\right). \tag{38}$$

Estimating Project FPE

The project-wide FPE was estimated by the quotient

$$\hat{FPE} = \frac{\left[\hat{S} + \hat{P}G + \hat{T}G + \hat{E}G + \hat{H}G\right]}{\left[\hat{P}U + \hat{P}G + \hat{T}U + \hat{T}G + \hat{E}U + \hat{E}G + \hat{H}U + \hat{H}G + \hat{S}\right]} \tag{39}$$

where the numerator was the estimated spillway and bypass guided passage and the denominator was total project passage as expressed as

$$F\hat{P}E = \frac{\hat{G}}{\hat{G}+\hat{U}}$$

(40)

where $\hat{G} = \hat{S} + \hat{P}G + \hat{T}G + \hat{E}G + \hat{H}G$

$$\hat{U} = \hat{P}U + \hat{T}U + \hat{E}U + \hat{H}U\,.$$

The variance of FPE was expressed as

$$V\hat{a}r\left(F\hat{P}E\right) = F\hat{P}E^2\left(1 - F\hat{P}E\right)^2\left[\frac{V\hat{a}r\left(\hat{G}\right)}{\hat{G}^2} + \frac{V\hat{a}r\left(\hat{U}\right)}{\hat{U}^2}\right]$$

(41)

where

$$V\hat{a}r\left(\hat{G}\right) = V\hat{a}r\left(\hat{S}\right) + V\hat{a}r\left(\hat{P}G\right) + V\hat{a}r\left(\hat{T}G\right) + V\hat{a}r\left(\hat{E}G\right) + V\hat{a}r\left(\hat{H}G\right)$$

$$V\hat{a}r\left(\hat{U}\right) = V\hat{a}r\left(\hat{P}U\right) + V\hat{a}r\left(\hat{T}U\right) + V\hat{a}r\left(\hat{E}U\right) + V\hat{a}r\left(\hat{H}U\right).$$

Estimating Powerhouse 1 FPE

Considering only the fish that pass through Bonneville Powerhouse 1, the Powerhouse 1 FGE was estimated by

$$F\hat{P}E_1 = \frac{\left[\hat{P}G + \hat{T}U + \hat{E}U\right]}{\left[\hat{P}U + \hat{P}G + \hat{T}U + \hat{T}G + \hat{E}U + \hat{E}G\right]}$$

(42)

where the numerator is the estimated fish passage through the PSC at Units 1-6 and screen-guided fish at Units 7-10. In turn, $F\hat{P}E_1$ can be expressed as

$$FPE_1 = \frac{\hat{G}_1}{\hat{G}_1 + \hat{U}_1}$$

(43)

where $\hat{G}_1 = \hat{P}G + \hat{T}G + \hat{E}G$,

$$U_1 = \hat{P}U + \hat{T}U + \hat{E}U\,.$$

The variance of $F\hat{P}E_1$ was estimated by

$$Var\left(F\hat{P}E_1\right) = F\hat{P}E_1^2\left(1 - F\hat{P}E\right)^2\left[\frac{Var\left(\hat{G}_1\right)}{\hat{G}_1^2} + \frac{Var\left(\hat{U}_1\right)}{\hat{U}_1^2}\right] \tag{44}$$

where $Var\left(\hat{G}_1\right) = Var\left(\hat{P}G\right) + Var\left(\hat{T}G\right) + Var\left(\hat{E}G\right)$

and $Var\left(\hat{U}_1\right) = Var\left(\hat{P}U\right) + Var\left(\hat{T}U\right) + Var\left(\hat{E}U\right)$.

Estimating Powerhouse 2 FPE

The FPE at Powerhouse 2 is essentially the powerhouse-wide FGE where

$$F\hat{P}E_2 = F\hat{G}E_2 = \frac{\hat{H}G}{\hat{H}G + \hat{H}U} \tag{45}$$

with associated variance estimator

$$Var\left(F\hat{P}E_2\right) = F\hat{P}E_2^2\left(1 - F\hat{P}E_2\right)^2\left[\frac{Var\left(\hat{H}G\right)}{\hat{H}G^2} + \frac{Var\left(\hat{H}U\right)}{\hat{H}U^2}\right]. \tag{46}$$

Evaluating Effect of Spill Volume

Two kinds of statistical tests were conducted to evaluate the effect of spill discharge on Project FPE, spill efficiency, and spill effectiveness. Those metrics on spill discharge were also regressed to determine if the slopes of those lines were significantly ($\alpha = 0.05$) different from zero. Each season was divided into "high spill" and "low spill" days, and the null hypothesis that mean values for each metric did not differ between the "high spill" and "low spill" groups was tested ($\alpha = 0.05$; two tailed).

3   Results

Hydroacoustic Detectability

Comparison of counts of guided and unguided fish by netting and hydro-acoustic methods at Unit 8 provided valuable feedback for modeling detectability. After the final round of detectability modeling, the average ratio of net counts to hydroacoustic counts was close to unity for guided fish (0.85) and unguided fish (0.93). Preliminary estimates based upon models using average target strength instead of target strength converted from the average backscattering cross section produced ratios as low as 0.2-0.3 netted fish for every acoustically detected fish.

In spring, most deployments had effective beam angles > 4 deg for the ranges that were sampled (Figure 9). Examples include all transducers in and upstream of PSC units, transducers in Units 7, 9, and 10, and those at spill bays. Exceptions included deployments where sampling had to begin at relatively short ranges < 4 m (e.g., near transducers at Unit 8 and up-looking beams on clump anchors 100 ft upstream of TIEs) or where fish and flow moved rapidly through the relatively narrow portions of hydroacoustic beams (e.g., 4-5 m from up-looking transducers in Units 11-18).

In summer, curves for effective-beam angle by range had similar shapes to those modeled in spring, although angles at all ranges tended to be narrower because the average backscattering cross section of summer-run juvenile fish was lower than that of spring-run fish (compare Figure 9 with Figure 10).

Polynomial regressions were used to describe the relationships between effecttive beam angle and range from a transducer for every type of deployment (Tables 13 and 14). Those equations and passage width data were used to expand the count of each detected fish and to equalize detectability among sample ranges and deployments. The coding solved a deployment-specific polynomial equation for effective beam angle based upon the range of detection of each individual fish, calculated the corresponding beam diameter at the same range, and multiplied the fish's count (i.e., one) by the ratio of the passage width to the beam diameter. The coefficients in Tables 13 and 14 and the general form of the polynomial described in the table titles can be used to generate detectability curves. Sampling ranges that were used to solve for effective beam angle truncated the polynomial curves to what can be seen in Figures 9 and 10.
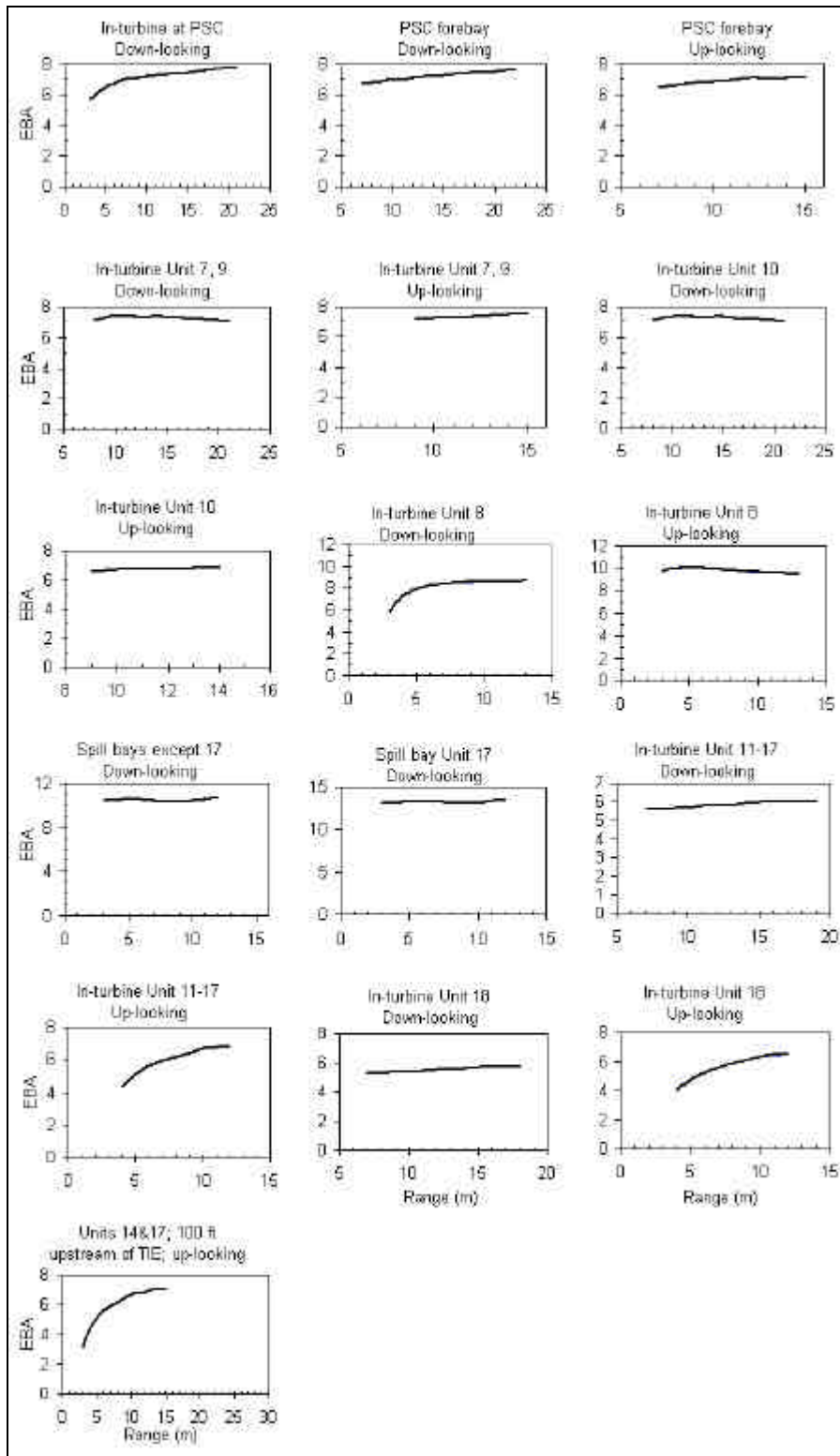
Figure 9.   Effective beam angles (EBA) as a function of range from transducers
            for every type of deployment in spring 2000
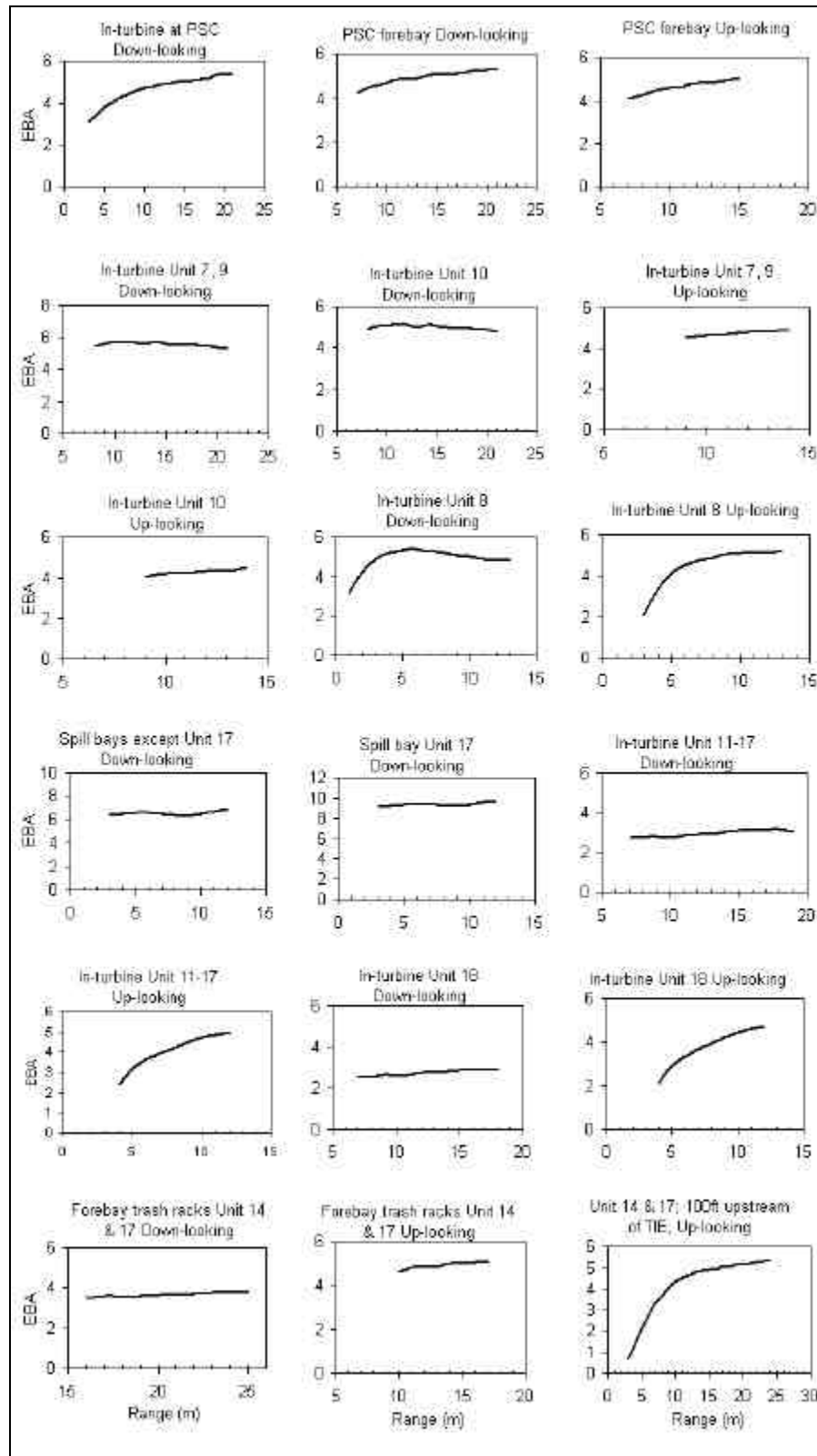
Figure 10. EBA as a function of range from transducers for every type of deployment in summer 2000

Table 13

Coefficients of Polynomials Used to Calculate EBA as a Function of Range From Transducers in Spring. Polynomials had the general form: $C1'MID\_R^6 + C2'MID\_R^5 + C3'MID\_R^4 + C4'MID\_R^3 + C5'MID\_R^2 + C6'MID\_R + Intercept$, where MID_R is the midrange in m and C1-C6 are coefficients tabled below

Deployments	C1	C2	C3	C4	C5	C6	Intercept
Units 1-6; in-turbine; down-looking			-0.00010460	0.00596750	-0.12321500	1.14541490	3.14384480
Units 1-6; forebay; down-looking	-0.00000139	0.00012693	-0.00463897	0.08693833	-0.88115638	4.66015682	-3.41897700
Units 1-6; forebay; up-looking			-0.00058528	0.02686938	-0.44858892	3.29629804	-2.30062783
Units 7 and 9; in-turbine; down-looking			-0.00004197	0.00248778	-0.05594245	0.54575503	6.02326031
Units 7 and 9; in-turbine; up-looking			-0.00074997	0.03215253	-0.51095676	3.65846029	-2.95698551
Unit 10; in-turbine; down-looking			-0.00003746	0.00224213	-0.05136822	0.51389289	5.43770666
Unit 10; in-turbine; up-looking			-0.00056837	0.02536726	-0.42282105	3.19867651	-2.78378372
Unit 8; in-turbine; down-looking		0.00047591	-0.02087290	0.35843872	-3.02830542	12.75503641	-13.35659091
Unit 8; in-turbine; up-looking			-0.00086156	0.03043435	-0.38695604	2.01558838	6.36559538
Spill bays except 17; down-looking			-0.00065967	0.02294640	-0.27063404	1.26439126	8.52500500
Spill bay 17; down-looking			-0.00039674	0.01455617	-0.18133403	0.91941736	11.57919081
Units 11-17; in-turbine; down-looking			-0.00018152	0.00870374	-0.14752616	1.07862469	2.78287926
Units 11-17; in-turbine; up-looking			-0.00048201	0.02140863	-0.36322865	2.91713221	-2.82701798
Unit 18; in-turbine; down-looking			-0.00018466	0.00887122	-0.15064093	1.10116490	2.42932921
Unit 18; in-turbine; up-looking			-0.00012238	0.00967754	-0.22608974	2.24774670	-2.06484848
Units 14&17; 100 ft upstream of TIE; up-looking			-0.00001265	0.00156043	-0.06468929	1.12904748	-0.11028066

Table 14

Coefficients of Polynomials Used to Calculate EBA as a Function of Range From Transducers in Summer. Polynomials had the general form: $C1'MID\_R^6 + C2'MID\_R^5 + C3'MID\_R^4 + C4'MID\_R^3 + C5'MID\_R^2 + C6'MID\_R + Intercept$, where MID_R is the midrange in m and C1-C6 are coefficients tabled below

Deployments	C1	C2	C3	C4	C5	C6	Intercept
Units 1-6; in-turbine; down-looking			-0.00002311	0.00179565	-0.05022499	0.66291092	1.52344757
Units 1-6; forebay; down-looking	-0.00000084	0.00007684	-0.00282981	0.05400850	-0.56855929	3.25169059	-3.53600354
Units 1-6; forebay; up-looking			-0.00015967	0.00917805	-0.19370849	1.84148302	-1.99990339
Units 7 and 9; in-turbine; down-looking			-0.00001918	0.00164578	-0.04850403	0.56513353	3.39818253
Units 7 and 9; in-turbine; up-looking			-0.00026631	0.01265691	-0.23135520	2.01057298	-2.35716284
Unit 10; in-turbine; down-looking			-0.00004427	0.00270207	-0.06250497	0.62710147	2.81344475
Unit 10; in-turbine; up-looking			-0.00011848	0.00698898	-0.15391561	1.56429786	-1.90202298
Unit 8; in-turbine; down-looking			-0.00044235	0.01913834	-0.29089364	1.76470548	1.69683566
Unit 8; in-turbine; up-looking			-0.00059890	0.02668098	-0.44457592	3.32571662	-4.40953047
Spill bays except 17; down-looking			-0.00083016	0.02934492	-0.35254396	1.69108715	3.80524975
Spill bay 17; down-looking			-0.00061652	0.02283748	-0.28611425	1.45669549	6.79296703
Units 11-17; in-turbine; down-looking			-0.00005527	0.00336898	-0.07301651	0.68140569	0.58181818
Units 11-17; in-turbine; up-looking			0.00017483	-0.00108003	-0.08136364	1.40681430	-1.90893939
Unit 18; in-turbine; down-looking			-0.00013707	0.00646929	-0.10806726	0.78675568	0.46986326
Unit 18; in-turbine; up-looking			0.00051719	-0.01219794	0.04794435	0.77555458	-1.12242424
Units 14&17; forebay trash racks; down-looking			-0.00003378	0.00265049	-0.07498884	0.94188402	-1.03711843
Units 14&17; forebay trash racks; up-looking			-0.00006047	0.00458235	-0.12812512	1.59000269	-2.39205051
Units 14&17; 100 ft upstream of TIE; up-looking			-0.00003765	0.00321830	-0.10204666	1.46173652	-2.98680859

Validation of Autotracking Hydroacoustic Data

For the five "tracker calibration days" (early, middle, and late spring; early and late summer), there was good agreement between autotracker mean counts and autotracker counts. For most transducer channels, the variation among human trackers, as indicated by the 80 percent confidence intervals, was a small fraction of the mean count (Figure 11). Exceptions were transducer channels with very low counts so that very small differences (one to a few fish) among individual counts produced relatively large confidence intervals.
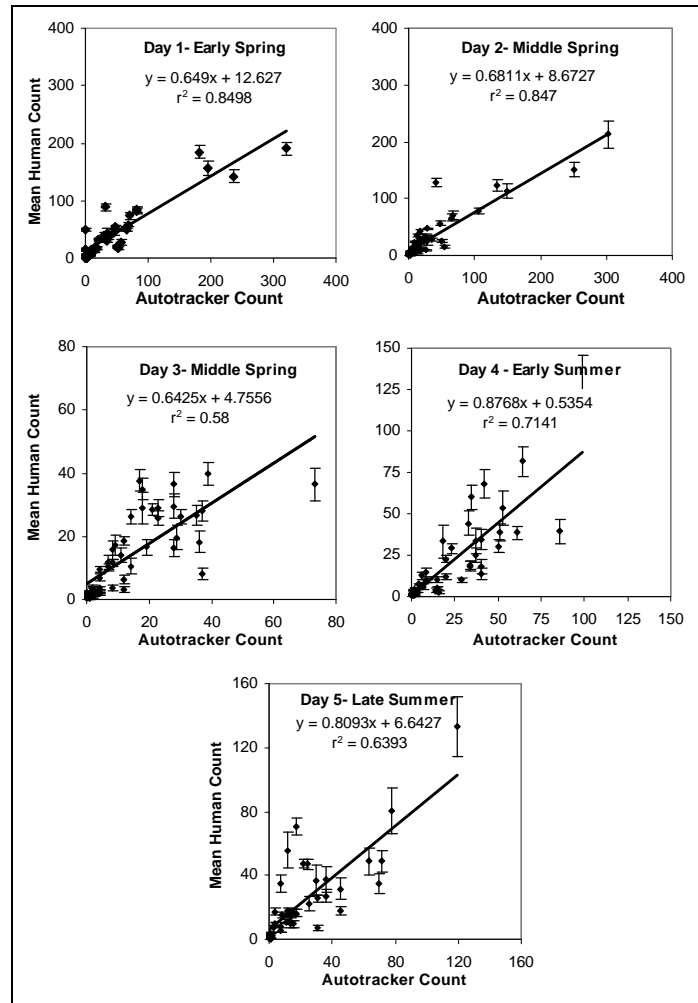
Figure 11. Means of fish counts made by different trained technicians plotted against autotracker counts on the same hydroacoustic data sets taken from five different days in early, middle, and late spring and early and late summer. Vertical error bars indicate 80 percent confidence limits on the human count means

Figures 12 and 13 show the differences in cumulative fish counts among individual humans, the human means, and the autotracker counts for each of the 5 days. These are the same data as in Figure 11, with the addition of the individual counts rather than just their means, but all are expressed as cumulative sums. Figure 12 presents the data for the three spring tracker calibration days and Figure 13 presents the data for the two summer tracker calibration days.
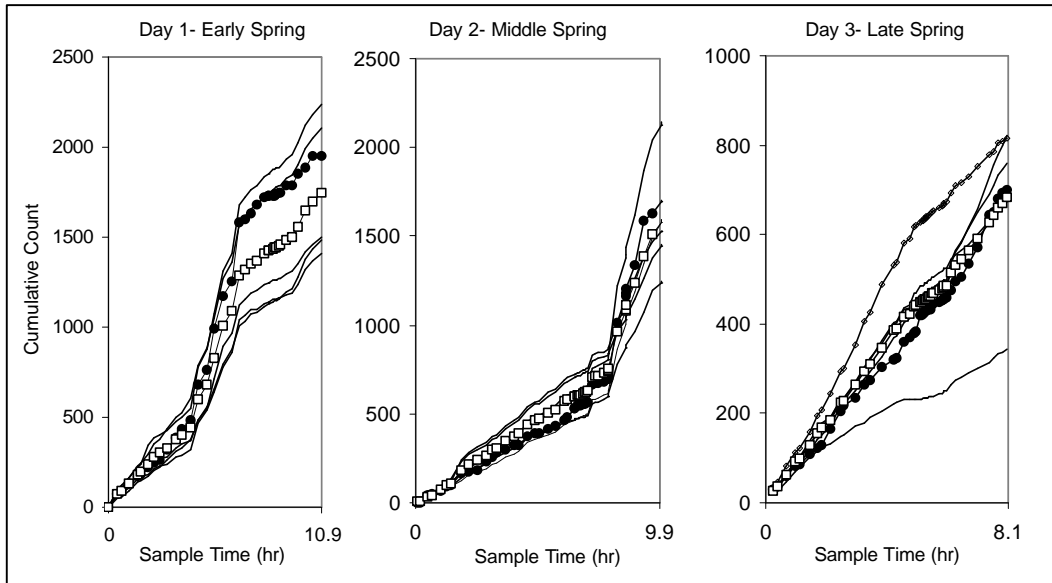
Figure 12. Spring cumulative counts by human trackers (lines are individuals; open squares are the mean) and by the autotracker (dots)
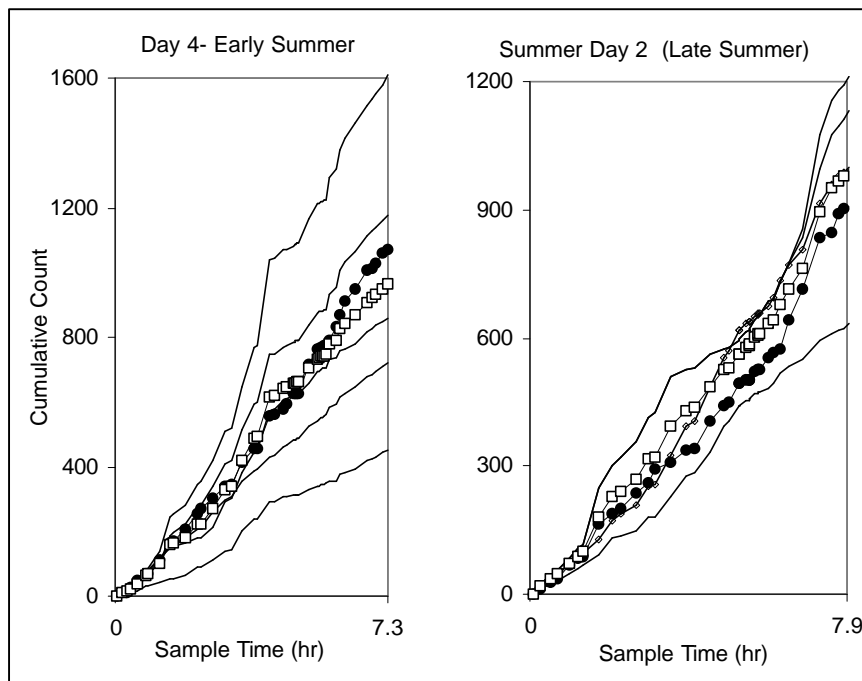
Figure 13. Summer cumulative counts by human trackers (lines are individuals; open squares are the mean) and by the autotracker (dots)

It can be seen that the human error increases from left to right as new transducer channels are added to the sums. It is also clear that the differences among humans are cumulative over the different samples but that the autotracker fairly closely approximates the human mean.

The time sampled for each day ranged from just over 7 hours (Day 4) to nearly 11 hours (Day 1, see Table 15). The cumulative differences between the extreme human (highest or lowest, whichever is more different from the mean human value) and the mean human, and the differences between the autotracker and the mean human value are also presented in Table 15, along with the percent difference in each case.

Table 15
Total Time Sampled (the Summed Time of All Transducer Channel Samples) Contributing to the 5 Calibration Days, the Cumulative Difference and Percent Difference Between the Extreme Human (High or Low, Whichever was Greater) and the Mean Human Tracker, and the Cumulative Difference and Percent Difference Between the Autotracker and the Mean Human Tracker

Calibration Day	Season	Total Hours Represented	Difference between extreme human and mean human	Difference between autotracker and mean human
Day 1	Early Spring	10.87	478.4 (28%)	205.4 (12%)
Day 2	Middle Spring	9.98	547.8 (34%)	108.8 (7%)
Day 3	Late Spring	8.07	388.8 (66%)	17.2 (2%)
Day 4	Early Summer	7.32	645.2 (67%)	107.2 (11%)
Day 5	Late Summer	7.95	331.7 (33%)	85.75 (7%)

Figure 14 presents a regression graph of the same data in Figure 11 except that all 5 days are included in one plot, and the 80 percent confidence bounds on the human means are omitted. The autotracker count for each transducer channel proved to be a reasonably good predictor of the mean human count for that transducer channel sample, the autotracker count explaining about 81 percent of the variation in the mean human tracker count for the 222 transducer channel samples over the 5 days.
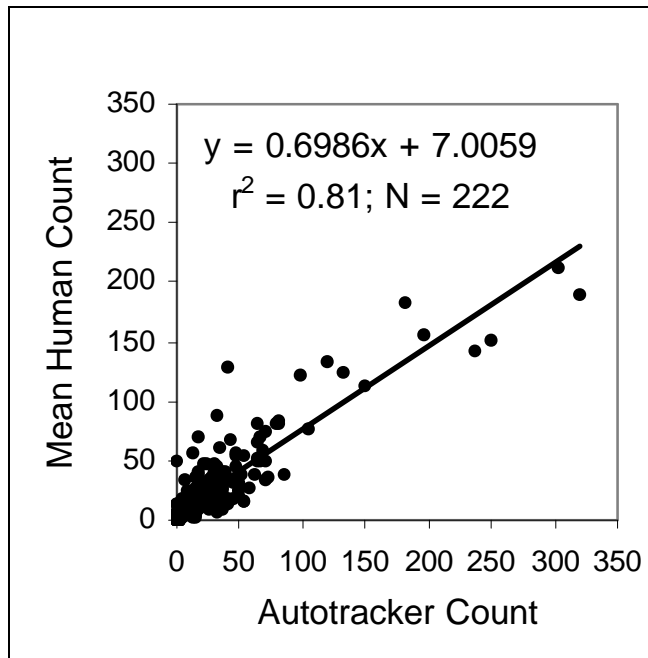
Figure 14. Correlation of mean human tracker counts with autotracker counts based upon five data sets

Major Passage Metrics

Estimates of FPE for the Project and Powerhouses in Spring and Summer

The spring project-wide FPE was estimated to be 0.79 with a confidence interval (CI) of 0.004 in spring. In summer the estimate was also 0.79 (CI = 0.002). The FPE estimate for Powerhouse 1 declined from 0.67 (CI = 0.004) in spring to 0.61 (CI = 0.002) in summer. Powerhouse 2 had FPE estimates of 0.54 in spring (CI = 0.008) and only 0.35 (CI = 0.022) in summer, when most of the turbine units were inactive most of the time.

Estimates of Spill Efficiency and Spill Effectiveness in Spring and Summer

Spill efficiency was estimated to be 0.44 (CI = .004) in spring and 0.49 (CI = 0.004) in summer and spill effectiveness to be 1.36 (CI < 0.005) in spring and 1.03 (CI < 0.005) in summer.

Effects of Spill Level on Project FPE, Spill Efficiency, and Spill Effectiveness in Spring and Summer

In order to evaluate the effects, if any, on project-wide FPE and spill passage, total spill discharge was plotted against FPE, spill efficiency, and spill effectiveness for different days in each season (Figure 15). In general, it was found that the trend lines for project FPE and spill efficiency vs. spill level had very slight positive slopes, suggesting that higher spill level may be associated with slightly higher spill passage (Figure 15, a-d). Those slopes were significantly different from zero for spill level vs. Project FPE in both spring ($P < 0.0001$) and summer ($P = 0.0054$), and for spill efficiency vs. spill level in spring ($P = 0.0007$) but not in summer ($P = 0.0700$). The plots of spill level vs. spill effectiveness produced trend lines with slightly negative slopes in each season (Figure 15, e and f). The spring trend was not significantly different from zero ($P = 0.139$), but the summer trend was significant ($P = 0.012$). The fits of the points to the trend lines are rather loose, the best being that for Project FPE in spring (Figure 15, a), which has an r^2 value of just over 0.5.

To further evaluate the strength of the effects that spill volume may have on Project FPE and spill efficiency and effectiveness, hypothesis tests were conducted on the data. Inspection of Figure 15 reveals that there is a rather clear break between higher and lower spill days. That is, there are no daily total spillway discharge levels (plotted on the horizontal axes) between about 100,000-110,000 ft^3/second in spring and between about 91,000-100,000 ft^3/second in summer. The six data sets were divided into two samples, "high spill" days and "low spill" days using those gaps to define the two groups. Two-tailed t-tests (on unequal sample sizes and assuming unequal variances) were used to test the null hypotheses that there is no difference between the means of project FPE, spill efficiency, and spill effectiveness for "high spill" vs. "low spill" days in each season. Table 16 shows results of those hypothesis tests.

Table 16
Results of Two-tailed t-Tests Performed on Daily Sums of Three Passage Metrics (Project FPE, Spill Efficiency, and Spill Effectiveness). The degrees of freedom (df) and the p-values are given in the right hand column

Effects of Spill Level on Project FPE and Spill Metrics					
Season	Variable Tested	"Low Spill" Mean	"High Spill" Mean	Difference in Means	2-tailed P-value (df)
Spring	Project FPE	0.773	0.823	0.050	0.0001 (11)
Spring	Spill Efficiency	0.431	0.504	0.073	0.002 (9)
Spring	Spill Effectiveness	1.370	1.334	0.036	0.242 (24)
Summer	Project FPE	0.778	0.807	0.029	0.187 (14)
Summer	Spill Efficiency	0.469	0.549	0.080	0.042 (13)
Summer	Spill Effectiveness	1.095	0.934	0.161	0.088 (23)
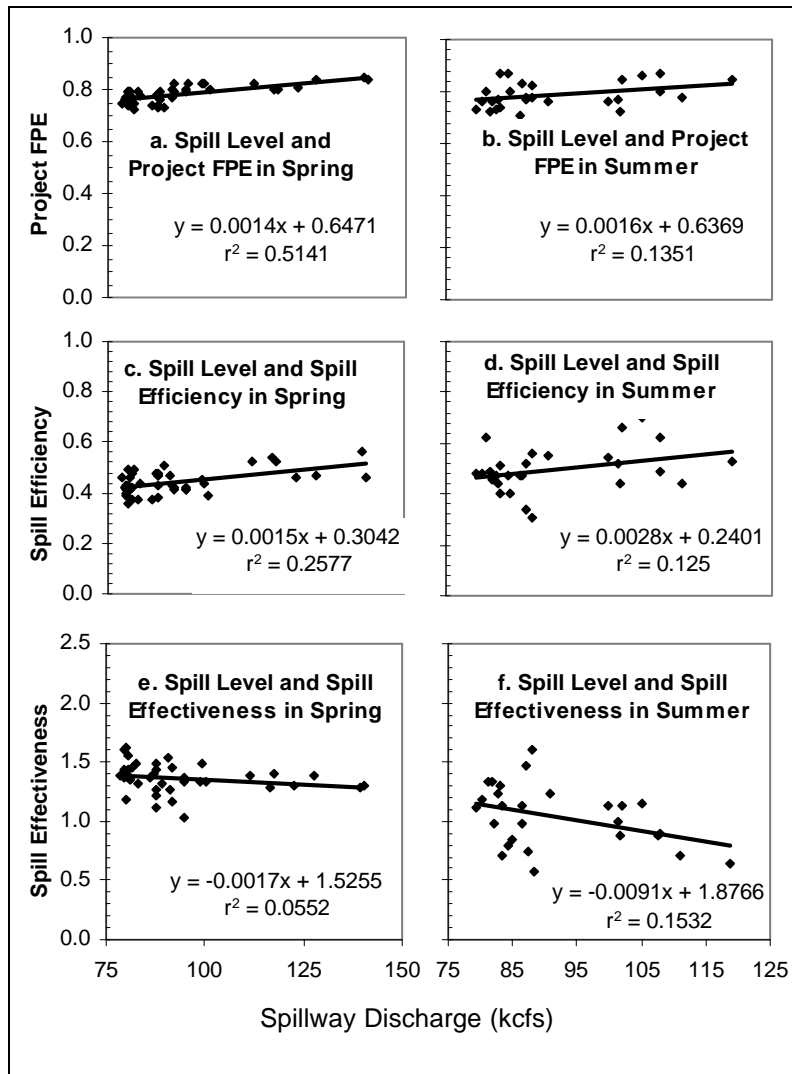
Figure 15. Plots of total daily spill level against project FPE, spill efficiency, and
spill effectiveness in each season

Significant differences were found at $\alpha = 0.05$ in Project FPE and spill efficiency in spring and in spill efficiency in summer. For spill effectiveness in summer the p-value is rather low, although greater than 0.5. As would be expected, the differences were in the direction of increase of Project FPE and spill efficiency and of reduction in spill effectiveness with higher spill level. However, the actual differences between the "High Spill" and "Low Spill" means are small (from 5 to 8 percent for the ratio metrics) considering that the ranges of spill were fairly large (the highest spill was about 1.75 times the lowest in spring and about 1.5 times the lowest in summer).

The highest fish passage by spill bay occurred at intermediate levels of spill although the variation in fish passage was high at all spill levels (Figures 16-19). Therefore, at the individual spill-bay level, higher discharge does not translate into higher fish passage. Since the relationship between spill volume and Project FPE, spill efficiency, and spill effectiveness seemed rather weak, the relationship was
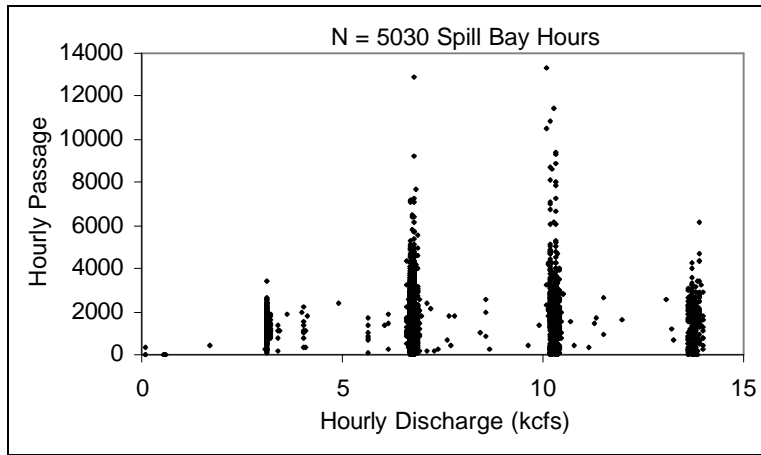
Figure 16. Hourly fish passage as a function of hourly spill bay
            discharge during spring daytime hours (0700-2000)
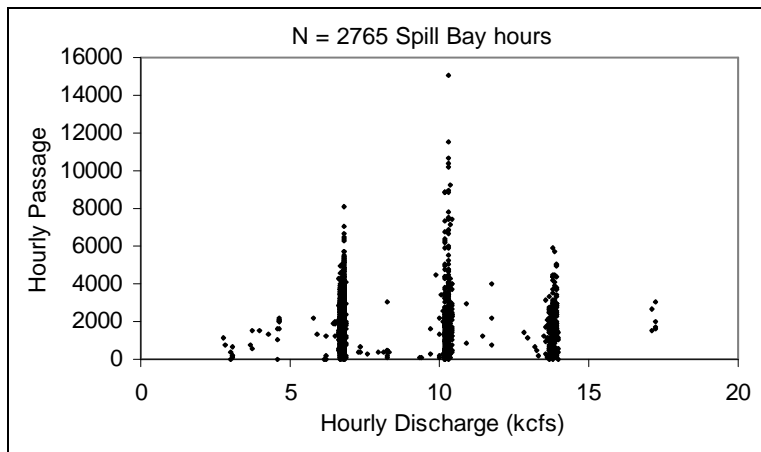
Figure 17. Hourly fish passage as a function of hourly spill bay
            discharge during spring nighttime hours (2200-0400)
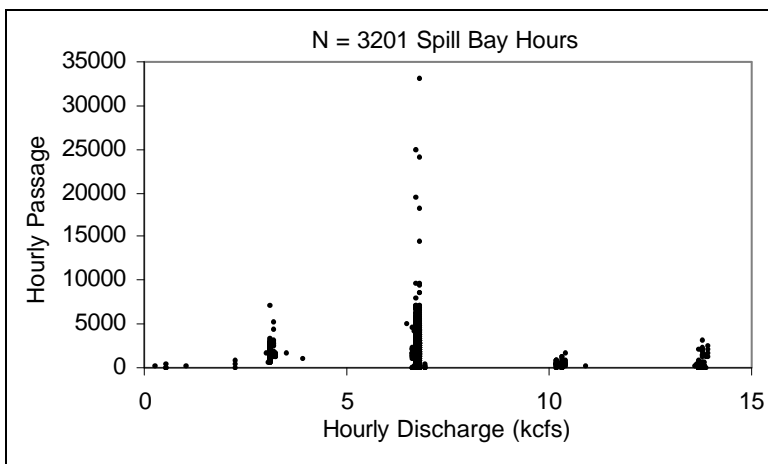
Figure 18. Hourly fish passage as a function of hourly spill bay
            discharge during summer daytime hours (0600-2000)
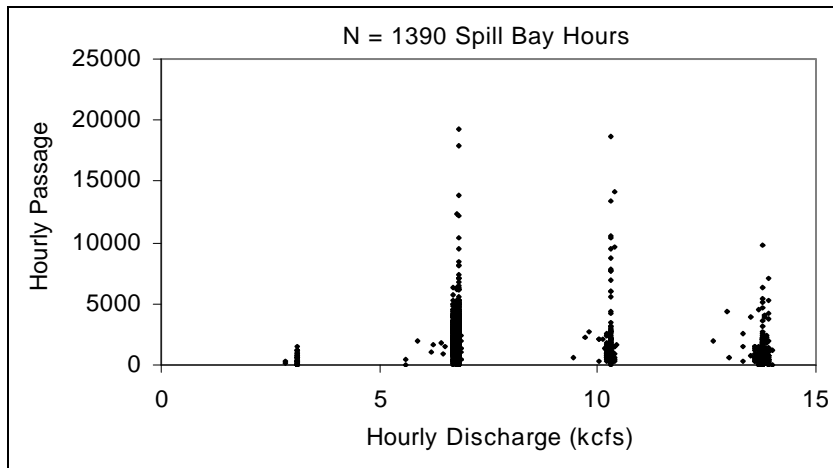
Figure 19. Hourly fish passage as a function of hourly spill bay
           discharge during spring nighttime hours (2100-0600)

investigated between spill discharge at individual spill bays and the estimates of
fish passed at those spill bays. Since there were essentially two different spill
regimes during daytime and nighttime at the dam, and the fish have different
vertical distributions and may have different behavioral patterns as a function of
time of day, the effects of diurnality were removed by doing separate comparisons
for day and night. To remove any ambiguity due to crepuscular differences in the
fish, the 2 hours nearest sunrise and sunset were thrown out.

Weak positive correlations were found between total spillway fish passage
and spill volume during the day and night hour in spring and during night hours in
summer (Figures 20-22). During daylight hours in spring and summer, fish
passage increased significantly with increased spill, but there was a lot of
variation, and spill volume explained only 10 percent or less of the variation in
fish passage. At night in summer, total spill volume explained 21 percent of the
variation in spillway fish passage, but no significant relation was found for
daytime hours in summer (Figure 23).
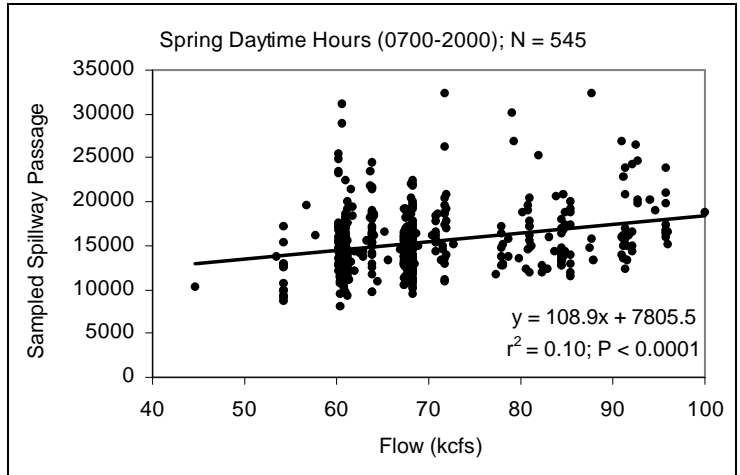
Figure 20. Scatter plot of fish passage through the spillway as
a function of spill discharge during daytime hours
in spring 2000
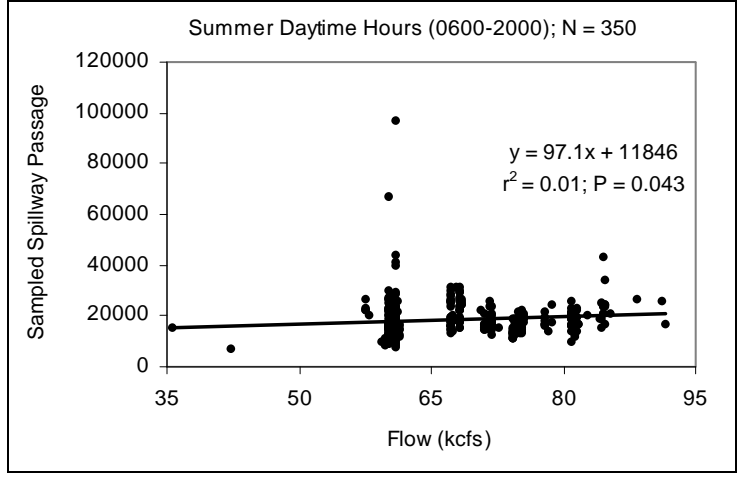
Figure 21. Scatter plot of fish passage through the spillway as
a function of spill discharge during daytime hours
in summer 2000
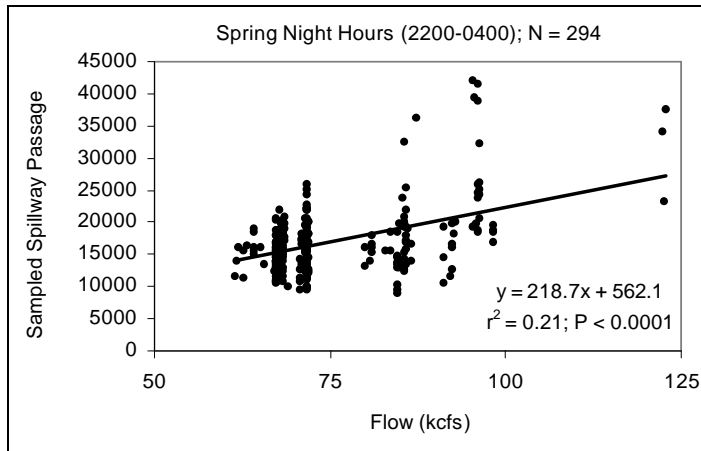
Figure 22. Scatter plot of fish passage through the spillway
as a function of spill discharge during nighttime
hours in spring 2000
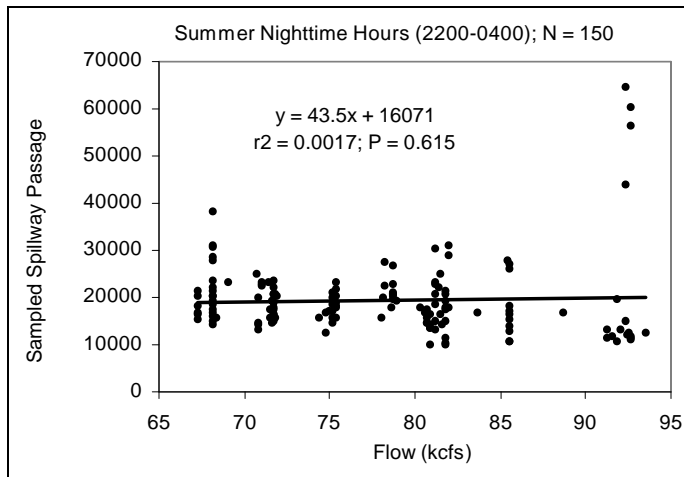
Figure 23. Scatter plot of fish passage through the spillway
as a function of spill discharge during nighttime
hours in summer 2000

Spatial Aspects of Fish Passage

Horizontal Distributions of Fish Passage, Flow, and Fish Density

Horizontal Distribution of Fish Passage. The horizontal distribution of fish passage at each of the main passage routes was examined. Figures 24 and 25 show the total estimated fish passage across the entire project in spring and summer, respectively. The spillway passage estimates, graphed in the center as they occur at the dam, were grouped in sections of either three or four spill bays each and so account for greater horizontal distances across the face of the dam and greater total flows than do the individual turbine units.
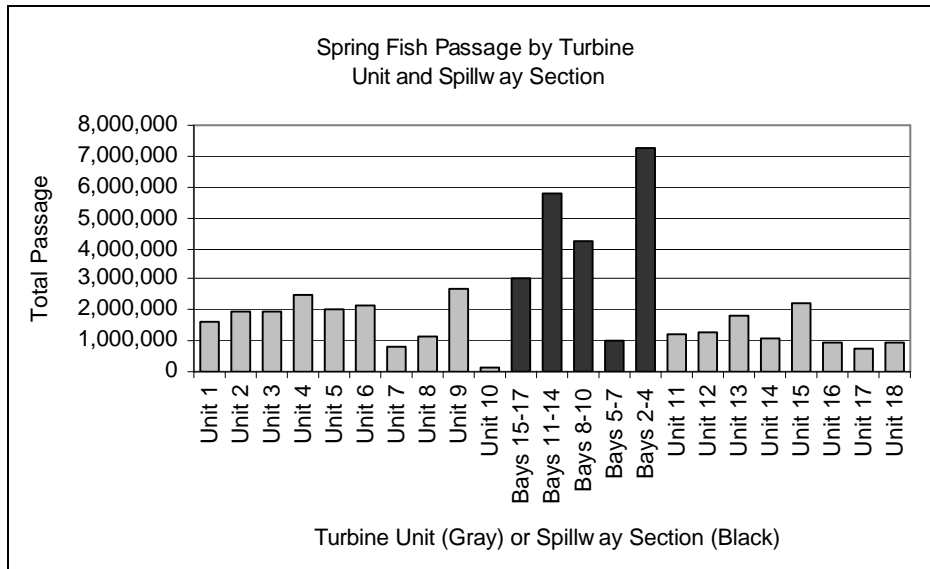
Figure 24. Horizontal distribution of total fish passage at turbines and spillway
sections in spring
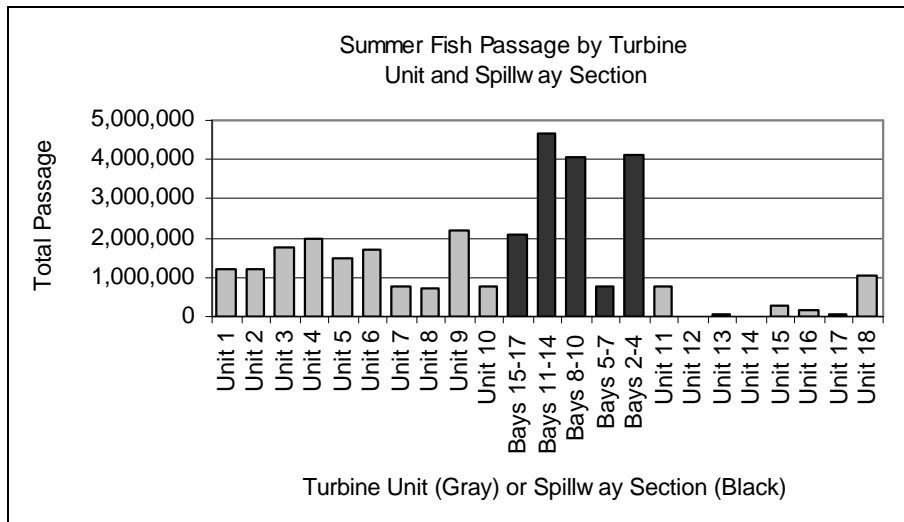
Figure 25. Horizontal distribution of total fish passage at turbines spillway
sections in summer

In spring, it was estimated that just over 48.45 M fish passed the project
during the 43 days that were sampled, with nearly half (44 percent or 21.32 M
fish) passing by spill, over one-third (35 percent or 16.92 M fish) passing
Powerhouse 1, and about one-fifth (21 percent or 10.26 M fish) passing
Powerhouse 2 (Figure 24). Just over 70 percent of the total 16.9 M fish that
passed at Powerhouse 1 passed south of the wing wall through Units 1-6 (the PSC
units). Of the remaining 4.75 M fish passing Units 7-10, over half (2.68 M)

passed Unit 9, which was the turbine unit with the highest estimated total fish passage in spring.

The eight turbine units at Powerhouse 2 passed an estimated 10.26 M fish, about 21 percent of the dam total. Of the eight Powerhouse 2 turbine units the highest passages were at Unit 15 (2.25 M fish) and Unit 13 (1.84 M fish), each very roughly one-fifth of the powerhouse total. The other six units passed around 1 M (760,000 to 1.25 M) fish each, with slightly higher passage at the units towards the southern end of the powerhouse.

Each of the spillway sections, except the one comprising Spill Bays 5-7, passed more fish in spring than did any single turbine unit. Passage was distributed very unevenly across the spillway with Bays 2-4 passing the most fish of all the spill bay sections (estimated passage of over 7.27 M fish). In decreasing order, Bays 11-14 passed an estimated 5.77 M fish, Bays 8-10 passed an estimated 4.25 M fish, Bays 17-15 passed an estimated 2.99 M fish, and Bays 5-7 were by far the lowest with an estimated passage of just over 1 M fish, lower than most of the individual turbine units.

In summer, it was estimated that about 31.80 M fish passed the project during the 26 day period sampled, giving summer a slightly higher daily rate of passage. As in spring, summer spillway passage accounted for about half of the season's total, i.e., 49 percent or 15.71 M fish (Figure 25).

The total passage at Powerhouse 1 was estimated to be about 13.8 M fish, or about 43 percent of the entire dam's summer passage. The horizontal distribution of passage at Powerhouse 1 was very similar to that in spring, with about 68 percent (9.4 M fish) passing south of the wing wall and through Units 1-6. Of the remaining 32 percent (4.4 M fish) that passed to the north of the wing wall, passage was divided almost equally between Unit 9 and the other three units combined (Units 7, 8, and 10). Unit 9 passed about 2.2 M fish and the other three units shared about the same number roughly equally. In summer as in spring, Unit 9 passed more fish than did any other turbine unit at the project.

The primary seasonal difference in dam operations was that Powerhouse 2 was mostly inactive in summer, passing only about 2.29 M fish or 7.2 percent of the project total. The most passage was at the end units (Unit 11 at the south end and Unit 18 at the north end), which are operated in summer to supply attraction flow for adult migrant salmon. Unit 11 passed about 742,000 fish (30 percent of Powerhouse 2 passage) and Unit 18 passed just over 1 M fish (45 percent of Powerhouse 2 passage). The remaining 23 percent (about 520,000 fish) was passed across the rest of the powerhouse, mostly at Units 15 and 16. Unit 12 did not operate at all in summer.

The horizontal distribution of passage across the spillway was slightly less varied than in spring. Spill Bays 11-14 passed the most fish with an estimated 4.69 M, followed by Bays 8-10 and Bays 2-4, which passed about 4.05 and 4.14 M fish, respectively. As in spring, Bays 5-7 passed the fewest fish with just over 7,800 fish.

Horizontal distribution of flow in spring. Figures 26 and 27 show the total estimated flow across the entire project in spring and summer, respectively. As with the fish passage figures, it should be noted that the spillway is graphed in sections of either three or four spill bays each and so account for greater horizontal distances across the face of the dam and greater total flows than do the individual turbine units.
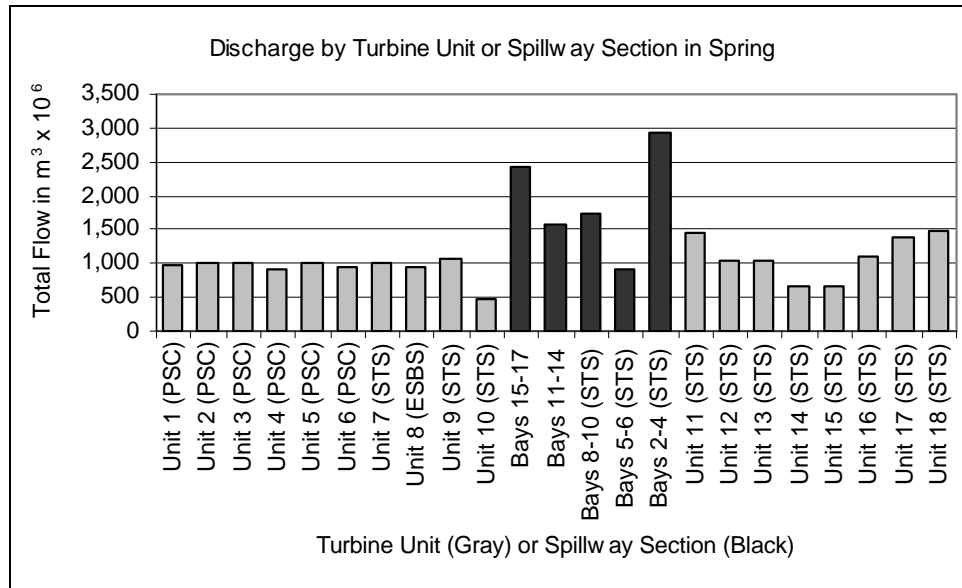

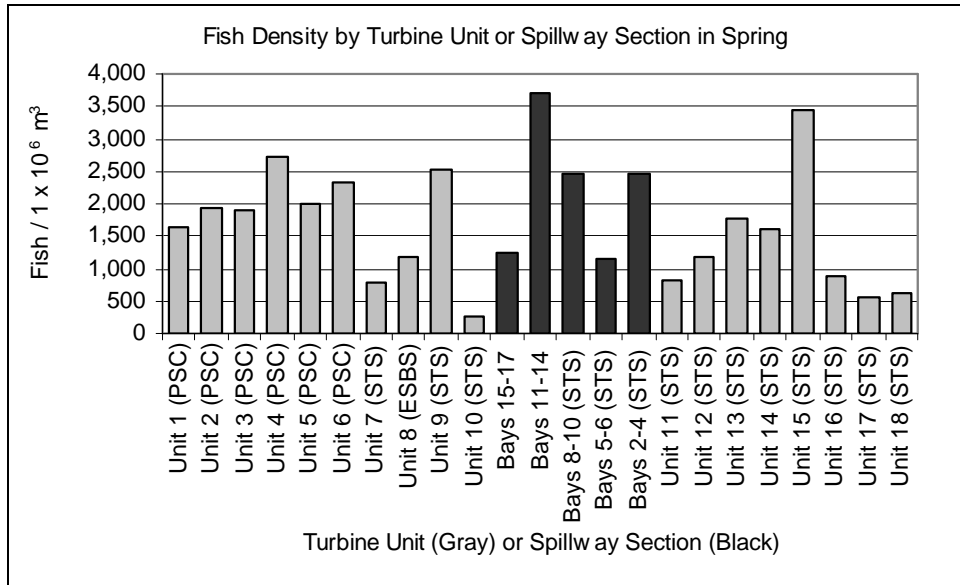
Figure 26. Horizontal distribution of discharge through turbines and five spillway sections in spring
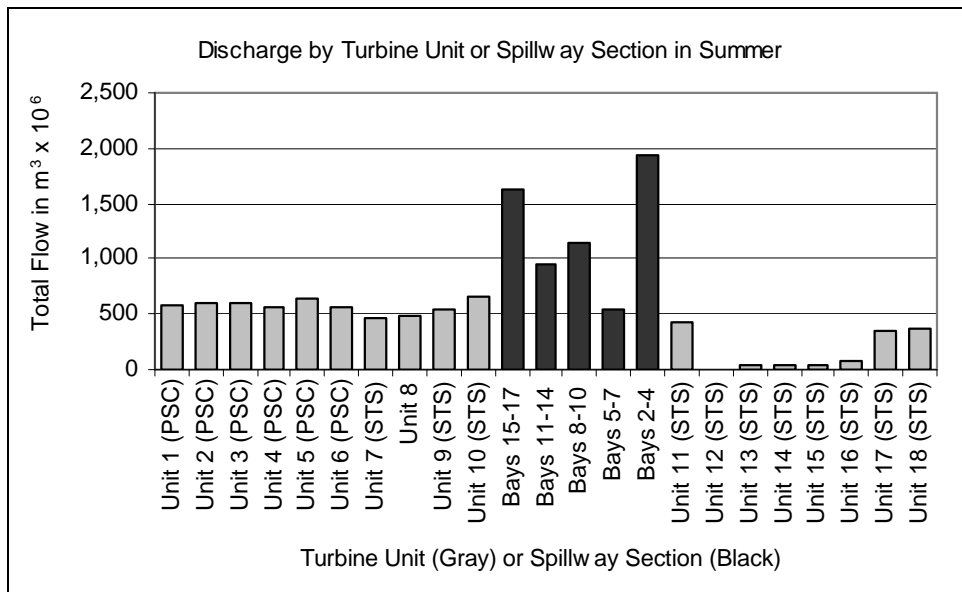
Figure 27. Horizontal distribution of discharge through turbines and five spillway sections in summer

Bonneville Dam passed almost 29,500 x 10^6 m^3 of water in spring and the horizontal distribution of flow, even on the scale of the three major structures (powerhouses and spillway), provided informative contrasts with the distribution of fish passage (Figure 24). It was estimated that Powerhouse 1 passed about 44 percent of the spring fish in about 32 percent of the water. Powerhouse 2 passed its 21 percent of the total spring fish in 36 percent of the total project flow. The spillway passed just under one-third of the water (33 percent) in spring, but passed an estimated 44 percent of the total spring fish run.

On a finer scale, that of specific turbine units and spill bay sections, there is again no clear relationship between the horizontal distribution of flow and that of fish passage. Except for Unit 10, which ran only about half as much as the others, flow through all of the Powerhouse 1 turbine units was approximately equal. But fish passage (Figure 24) was highest at Unit 9 and was also high at Unit 6 and the rest of the units south of the wing wall (the PSC units). Fish passage was notably low at Units 7, 8, and 10.

For the entire spring, the spillway sections that passed the most (Bays 2-4) and least (Bays 5-7) water also passed the most and least fish, respectively (but recall hourly results presented above). The association between flow and fish passage was not as clear for the other three sections. The section with the second highest flow (Bays 15-17) had the second lowest fish passage and the two remaining sections had very similar flows (within 10 percent). Of the sections with similar flows, the one with the greater flow of the two (Bays 8-10) passed 30 percent more fish than did the one with the lesser flow (Bays 11-14).

The dam passed about 12,900 x 10^6 m^3 of water during the 26 days sampled in summer (Figure 27). Powerhouse 2 was largely inactive in summer, contributing only about 11 percent of the dam's total discharge. The spillway passed about half (48 percent) of the water in summer with the remaining 41 percent passing Powerhouse 1.

As in spring, the summer discharge across Powerhouse 1 was fairly uniform, ranging from 463 million m^3 through Unit 7 to 650 million m^3 through Unit 10. A gain flow did not closely mirror fish passage. Unit 9 again passed more fish than any other unit and Units 7, 8, and 10 passed fewer fish than their proportion of flow would predict. At Powerhouse 2, Unit 12 did not pass any water and Units 13-16 operated very little (although Units 15 and 16 had fairly high fish passage those times when they did operate). Unit 17 was especially surprising in that it passed very nearly as much water as did Unit 18 but had only about 5 percent of Unit 18 fish passage (compare Figures 25 and 27).

The same comparisons for flow and fish passage made with regard to the spring figures (Figures 24 and 26), indicating that the turbine units and spill bays that pass the most water do not pass the most fish, also hold for summer (Figures 25 and 27). In fact, except for the inactivity of Powerhouse 2 in summer, the horizontal distributions of flow or fish passage between seasons are much more similar than are the horizontal distributions of water and fish passage within seasons.

Horizontal distribution of fish passage density. Turbine units and spill bay sections are very different structures passing very different flows on very different schedules. There is considerable operational variation among individual turbine units or spill bay sections. To avoid the complexity inherent in different turbine units and spill bay sections having different dimensions and operating schedules, fish passage densities (the ratio of total fish passage to total discharge at each turbine unit or spill bay section) were calculated for both spring and summer. Figures 28 and 29 present those data.

Figure 28. Horizontal distribution of fish density through turbines and five spillway sections in spring
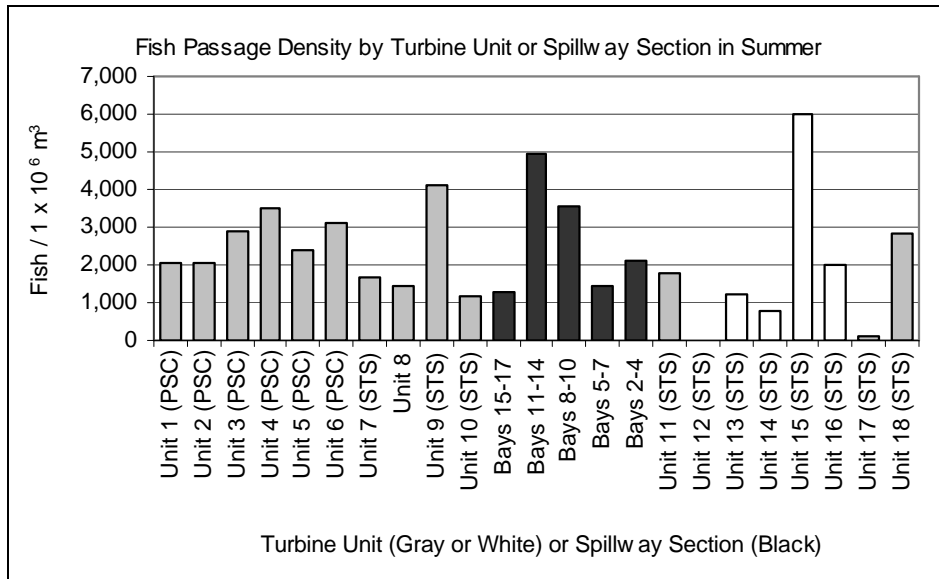
Figure 29. Horizontal distribution of fish density through turbines and five spillway sections in summer

Overall spring fish passage density was 1,643 fish per million m^3 of water passed. The highest fish passage densities were, in descending order, at Bays 8-10, Unit 15 at Powerhouse 2, and Unit 4 at Powerhouse 1 (Figure 28). It should be understood that the values from the turbine units represent both guided and unguided fish. Units 1-6 and 9 at Powerhouse 1, Bays 11-14, 8-10, and 2-4 at the spillway, and Units 12-15 at Powerhouse 2 had generally high fish passage densities in spring.

In summer fish passage density was about 2,465 fish per million m^3, or about 150 percent higher than it was in spring (Figure 29). Except that Unit 9 had a higher fish passage density than did Unit 4, which was the highest on Powerhouse 1 in spring, the general horizontal distribution of fish passage density is very similar between the two seasons. It should be noted, however, that the high values for the interior units on Powerhouse 2 are from very brief samples and, conversely, the very low value for Unit 17 represents an equivalent discharge to the much higher fish passage density at Unit 18.

To better understand spill and passage, the proportions of total fish passage, total volume of water spilled, and fish passage density were compared at the five different spill bay sections in spring (Figure 30) and summer (Figure 31).

In spring the spillway section that spilled the most water (Bays 2-4) passed the most fish but did so with relatively low fish passage density as compared with a spillway section (Bays 11-14), which spilled slightly over half (53 percent) as much water and passed over 79 percent as many fish (Figure 30). Directly south of the relatively effective (in terms of water) Bays 11-14, Bays 15-17 used over 154 percent as much water to pass half (52 percent) as many fish.
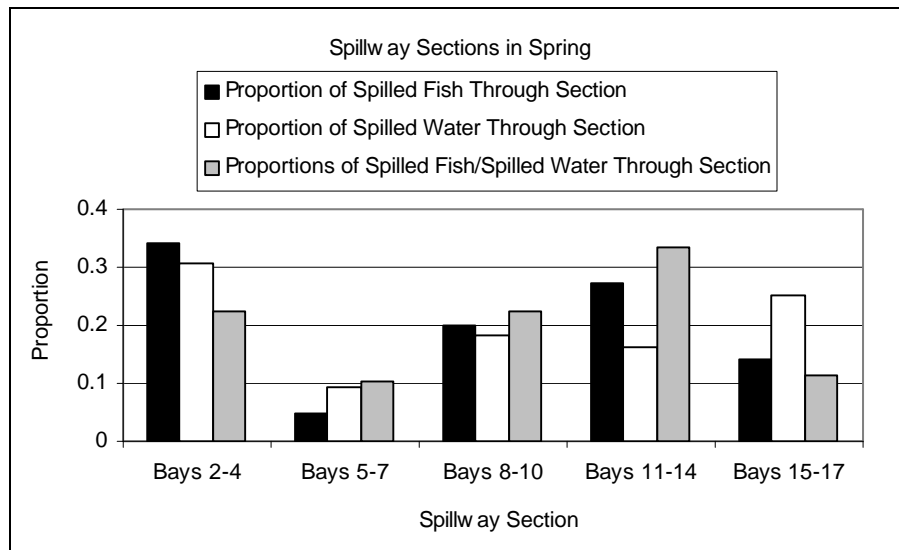

Figure 30. Horizontal distribution of total fish passed, total water spilled, and total fish density spilled through five spillway sections in spring
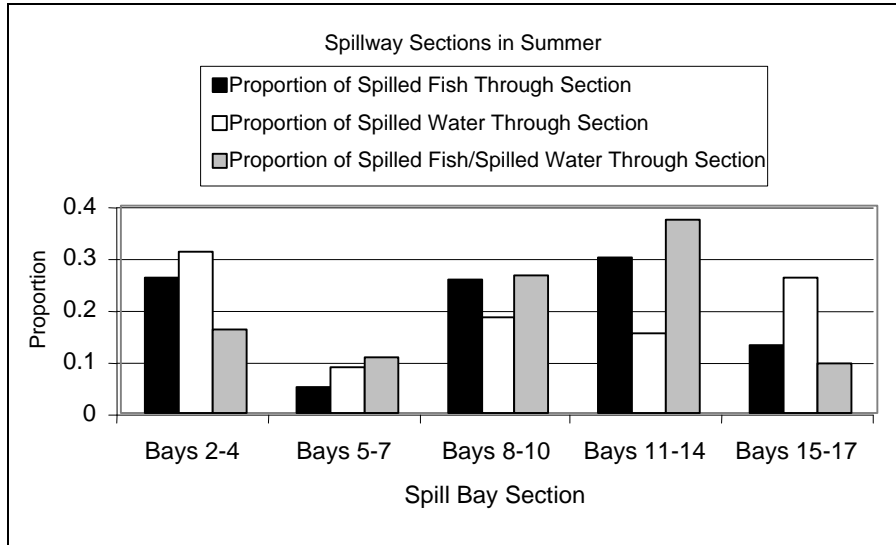
Figure 31. Horizontal distribution of total fish passed, total water spilled, and
total fish density spilled through five spillway sections in summer

In summer the highest spilling spillway section that passed the most water
(again Bays 2-4) passed only about 88 percent as many fish as did Bays 11-14,
which used just less than half (49 percent) as much water to do so (Figure 31).
Bays 15-17 were again much less effective, in terms of water, than were Bays 11-
14 in that they used 72 percent more water to pass 44 percent fewer fish.

Vertical Distribution of Fish Passage

Powerhouse 1. At the first powerhouse, most fish were detected high in the
water column. Upstream of the PSC, from 92 to 99 percent of all fish detected at
each unit during the spring were above the elevation of the floor of the PSC. Fish
were highest in the water column at Unit 6, and were lowest at Units 2 and 5. For
all five PSC slots that were sampled, 95 percent of all detected fish were above
the elevation of the floor of the PSC (Figure 32).
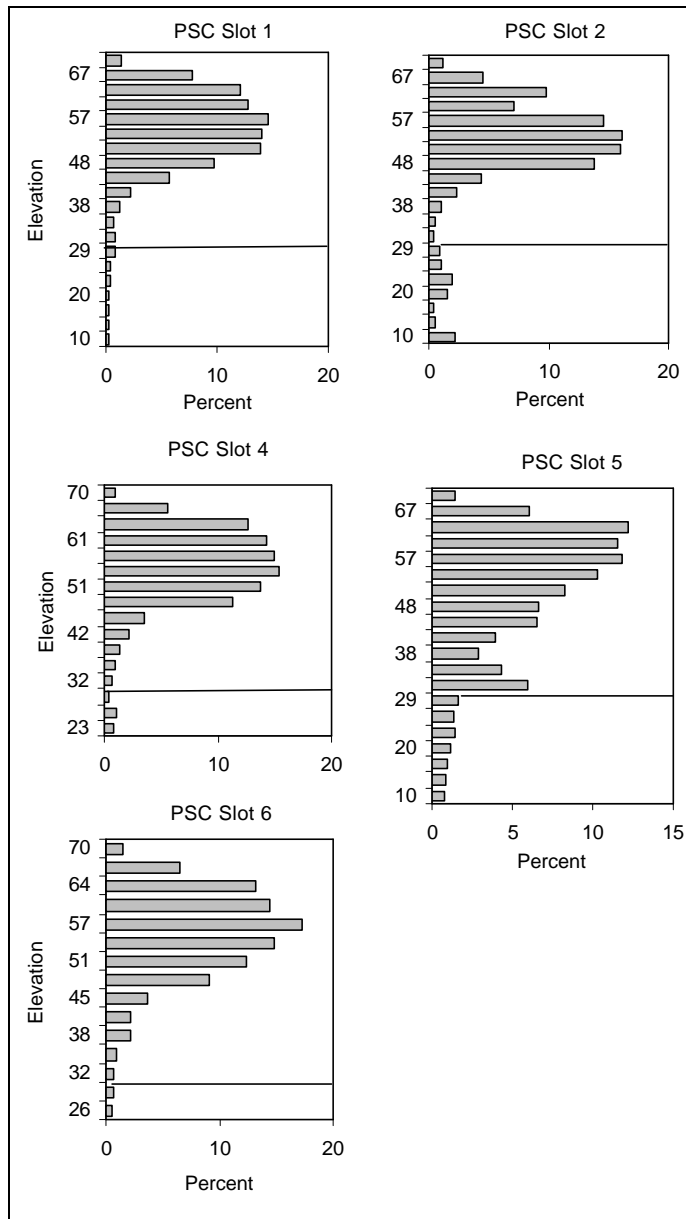
Figure 32. Vertical distribution of fish upstream of PSC slots sampled in this
study in spring 2000

At the first powerhouse, most fish detected during summer also were high in
the water column, and the overall vertical distribution of fish was only slightly
lower than it was during the spring. Upstream of the PSC, from 85 to 96 percent
of all fish detected at each unit during the summer were above the elevation of the
floor of the PSC. For all five sampled PSC slots combined, 93 percent of all
detected fish were above the elevation of the floor of the PSC (Figure 33).
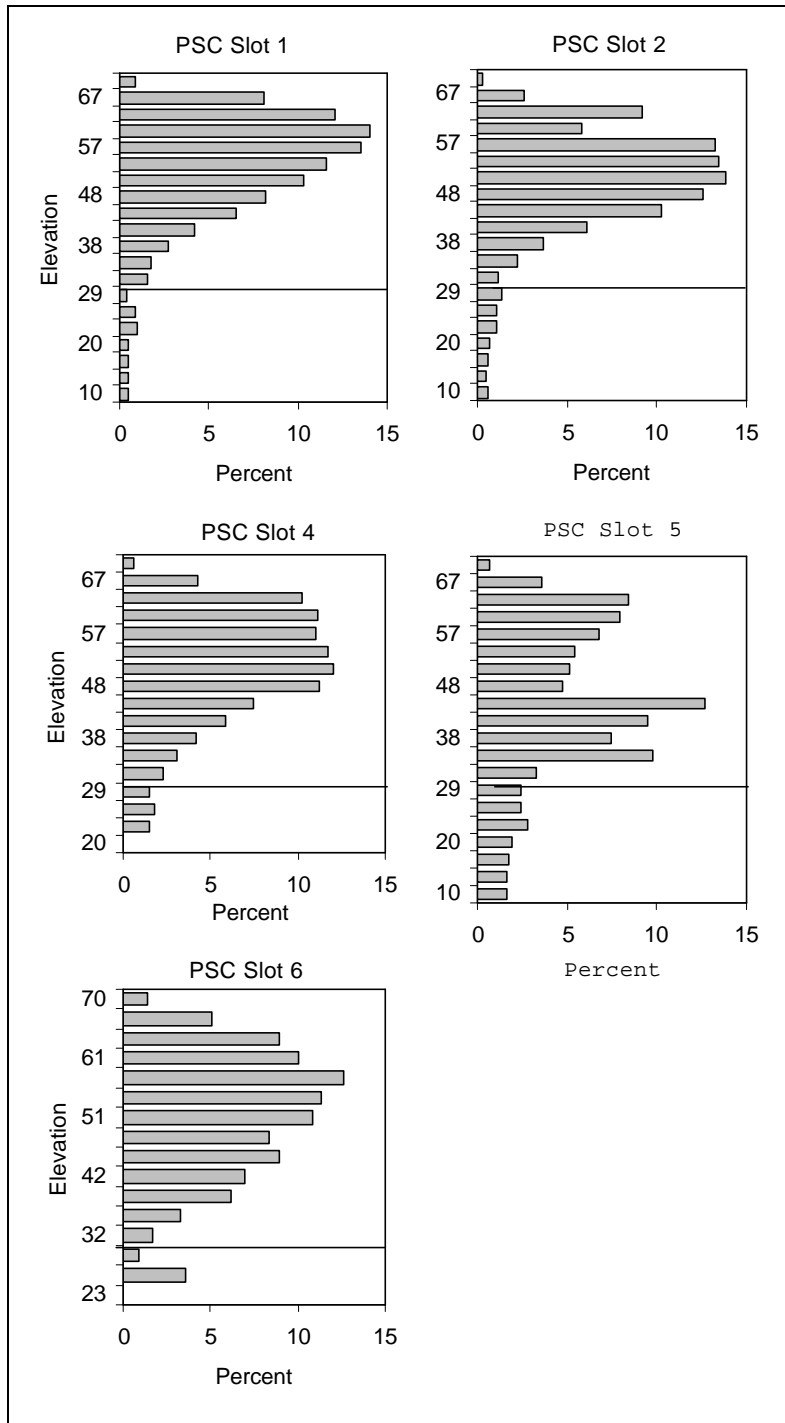
Figure 33. Vertical distribution of fish upstream of PSC slots sampled in this study in summer 2000

In spring and upstream of each of the sampled PSC slots, a higher proportion of fish were detected deeper in the water column at night than during the day. From 93 to 99 percent of fish detected during the day and from 77 to 98 percent of fish at night were detected above the elevation of the floor of the PSC (at

el 30.5 ft). Overall, 97 percent of daytime fish and 88 percent of nighttime fish were detected above the elevation of the floor of the PSC (Figure 34; Table 17).
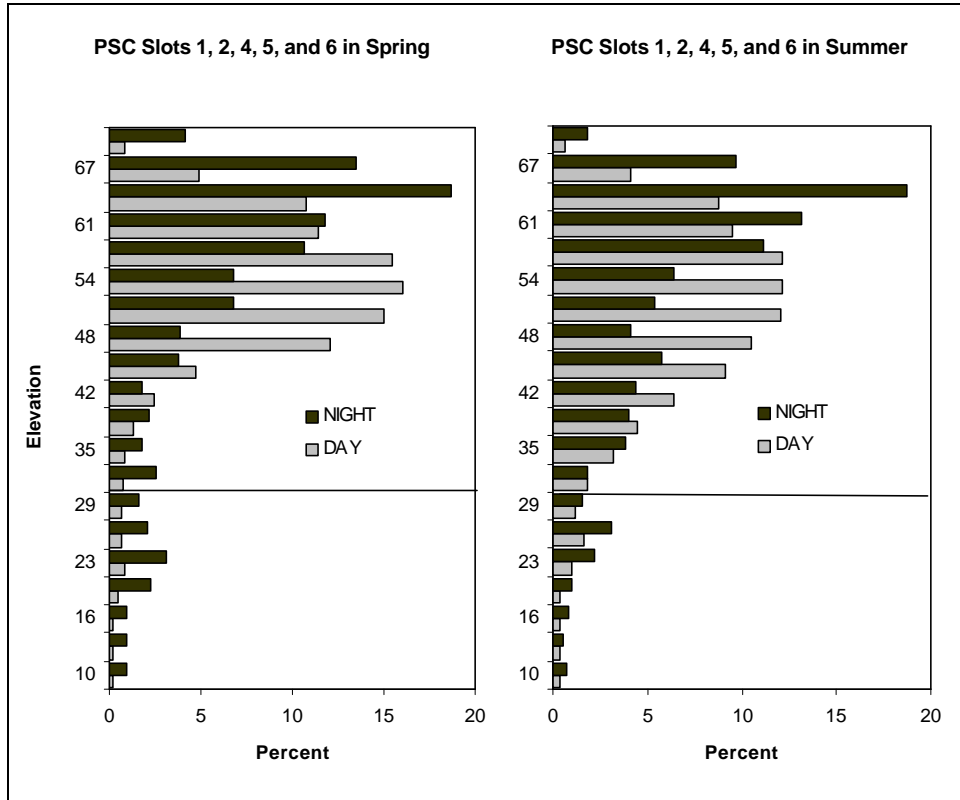
Figure 34. Day and night vertical distributions of fish upstream of sampled PSC slots in spring and summer. The horizontal line indicates the PSC floor elevation

Table 17
Percentage of Fish Detected Above the Floor of the Sampled PSC Slots. The floor was located at elevation 30.5 ft mean sea level

	Spring			Summer		
Location	Day	Night	Overall	Day	Night	Overall
ALL	97	88	95	95	90	93
Slot 1	97	93	97	96	93	96
Slot 2	93	77	92	95	85	94
Slot 4	98	97	98	95	93	95
Slot 5	94	82	92	86	80	85
Slot 6	99	98	99	96	92	95

In summer and upstream of the sampled PSC slots, a higher proportion of fish were detected deeper in the water column at night than during the day. From 86 to 96 percent of fish detected during the day and from 80 to 93 percent of fish at night were detected above the elevation of the floor of the PSC. Overall, 95 percent of daytime fish and 90 percent of nighttime fish were detected above the elevation of the floor of the PSC (Figure 34; Table 17).

Powerhouse 2. In spring the vertical distribution of fish also was surface oriented at Powerhouse 2. Eighty percent of the fish detected 100 ft upstream of Intake 14b and 97 percent of the fish detected upstream of Intake 17c were higher in the water column than the top of the intake openings (Figure 35). In summer the vertical distribution of fish also was surface-oriented at Powerhouse 2. Ninety-seven percent of the fish detected 100 ft upstream of Intake 14b and 96 percent of the fish detected upstream of Intake 17c were higher in the water column than the top of the intake openings (Figure 35).
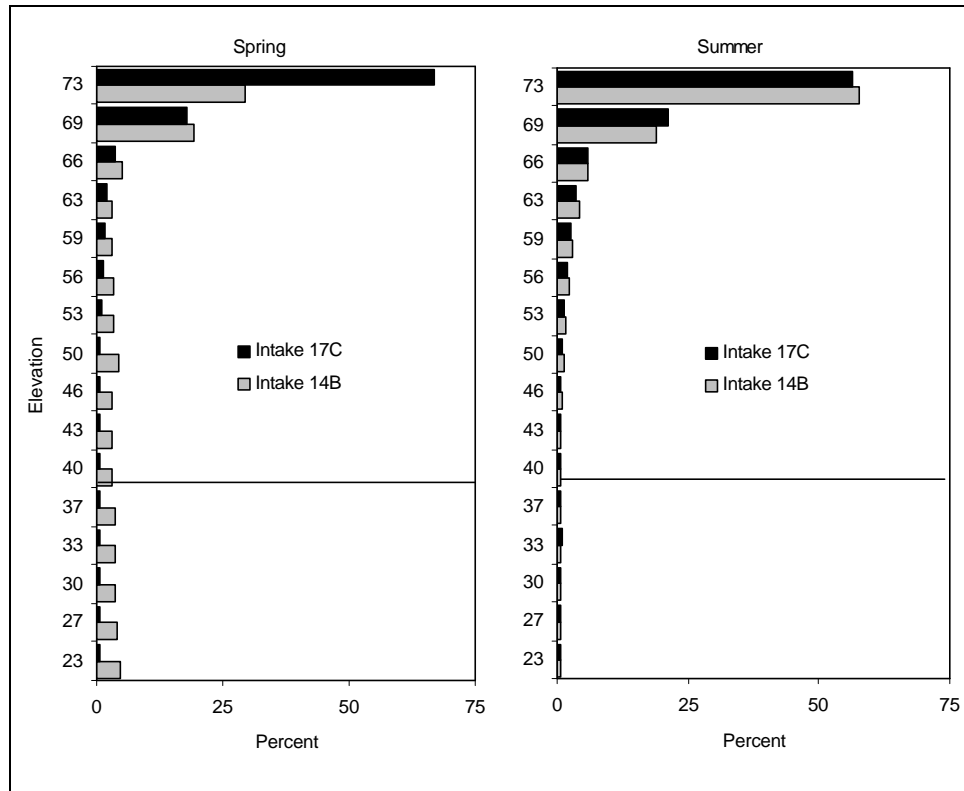
Figure 35. Vertical distribution of fish detected 100 ft upstream of Intakes 14b and 17c at Powerhouse 2 in spring and summer. The elevation of the top of the turbine intake is indicated by a horizontal line

Diel differences were found in the vertical distribution of fish in the forebay of Powerhouse 2 during the spring. At night 80 percent of the fish detected at both clump anchor positions were higher in the water column than the top of the intake openings. During the day, 85 percent of the fish detected 100 ft upstream of Intake 14b and 99 percent of fish detected upstream of Intake 17c were higher in the water column than the top of the intake openings (Figure 36, Table 18).
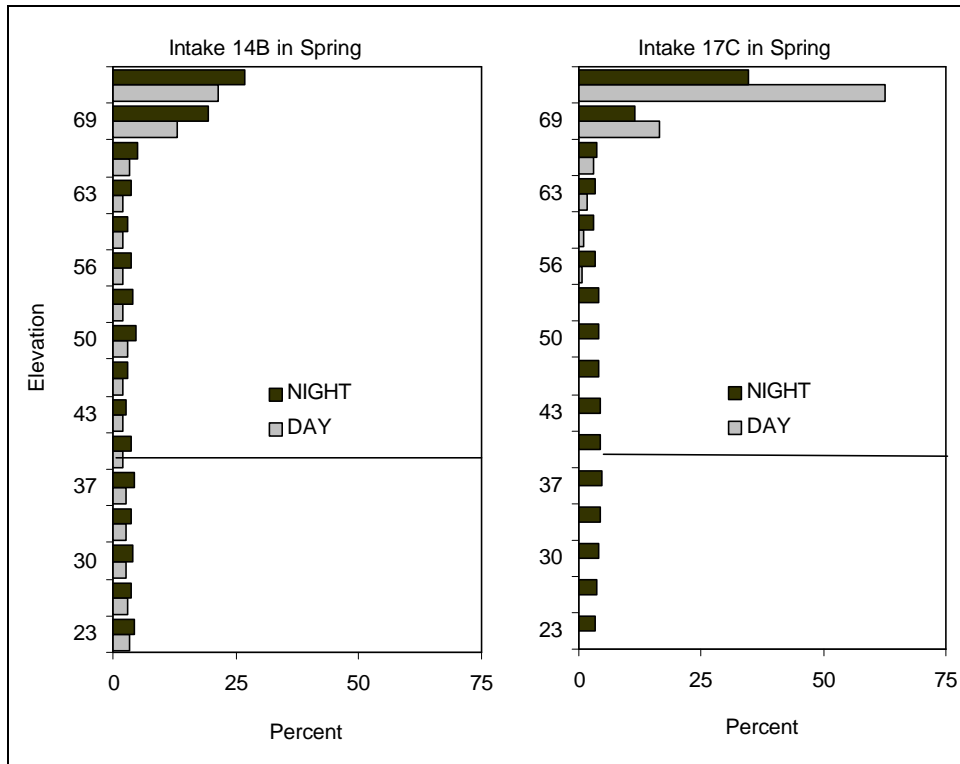
Figure 36. Day and night vertical distribution of fish detected 100 ft upstream of
Intakes 14b and 17c at Powerhouse 2 in spring. The elevation of the
top of the turbine intake is indicated by a horizontal line

Table 18
Percentage of Fish Detected 100 feet Upstream of Powerhouse 2
That Were Above the Elevation of the Top of the Turbine Intake

Season	Location	Day	Night	Overall
Spring	Intake 14b	85	80	80
	Intake 17c	99	80	97
Summer	Intake 14c	98	95	97
	Intake 17c	97	95	96

Only small differences were found in the diel patterns of vertical distribution
of fish in the forebay of Powerhouse 2 during the summer. At night 95 percent of
the fish detected at both clump anchor positions were higher in the water column
than the top of the intake openings. During the day, 98 percent of the fish
detected 100 ft upstream of Intake 14b and 97 percent of fish detected upstream of
Intake 17c were higher in the water column than the top of the intake openings
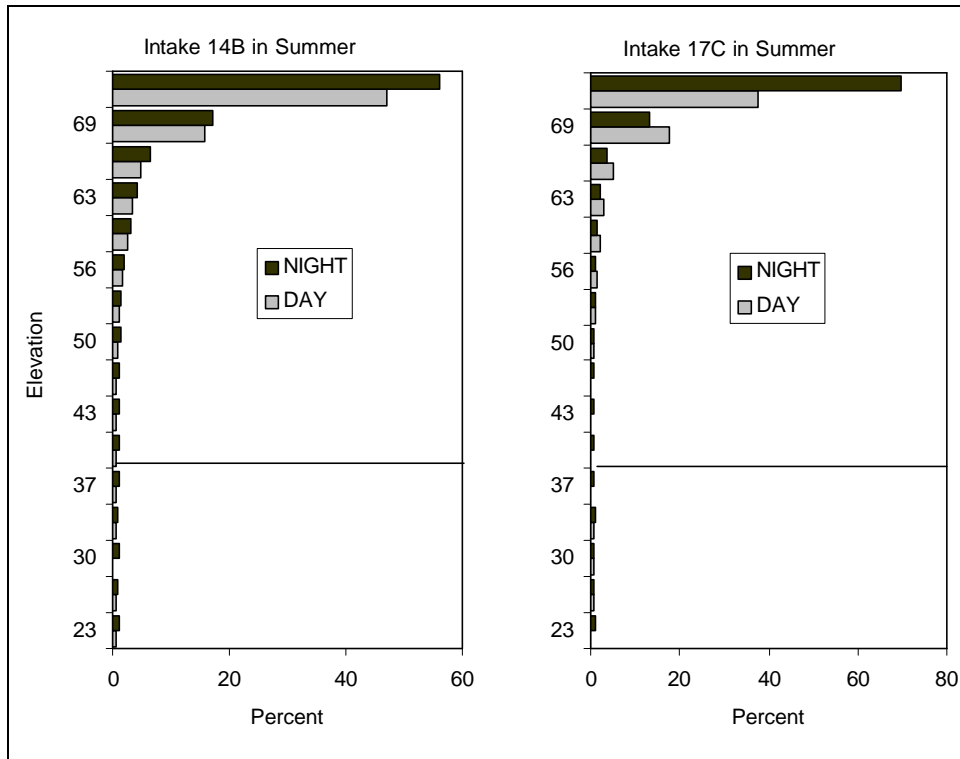(Figure 37, Table 18).

Figure 37. Vertical distribution of fish detected 100 ft upstream of Intakes 14b and 17c at Powerhouse 2 in summer. The elevation of the top of the turbine intake is noted

Also examined were the vertical distributions of fish immediately upstream of the trash racks at Intakes 14b and 17c during the summer. It is estimated that 66 percent of the passing fish detected at Intake 14b and 72 percent of the passing fish detected at Intake 17c were above the elevation of the tops of the intake openings. Additionally, 85 percent of the fish detected at Intake 14b and 93 percent of the fish detected at Intake 17c were above the elevation of the tips of the STSs (Figure 38).

Diel differences in vertical distribution were observed immediately upstream of the trash racks in the summer. At Intake 14b, 74 percent of daytime fish and 59 percent of nighttime fish were detected above the elevation of the top of the intake. At Intake 17c, 78 percent of daytime fish and 68 percent of night fish were detected above the elevation of the top of the intake. At Intake 14b, 89 percent of day fish and 79 percent of night fish were found, and 96 percent of day fish and 88 percent of night fish at Intake 17c were found above the slightly lower elevation of the tip of the screens (Figure 39).
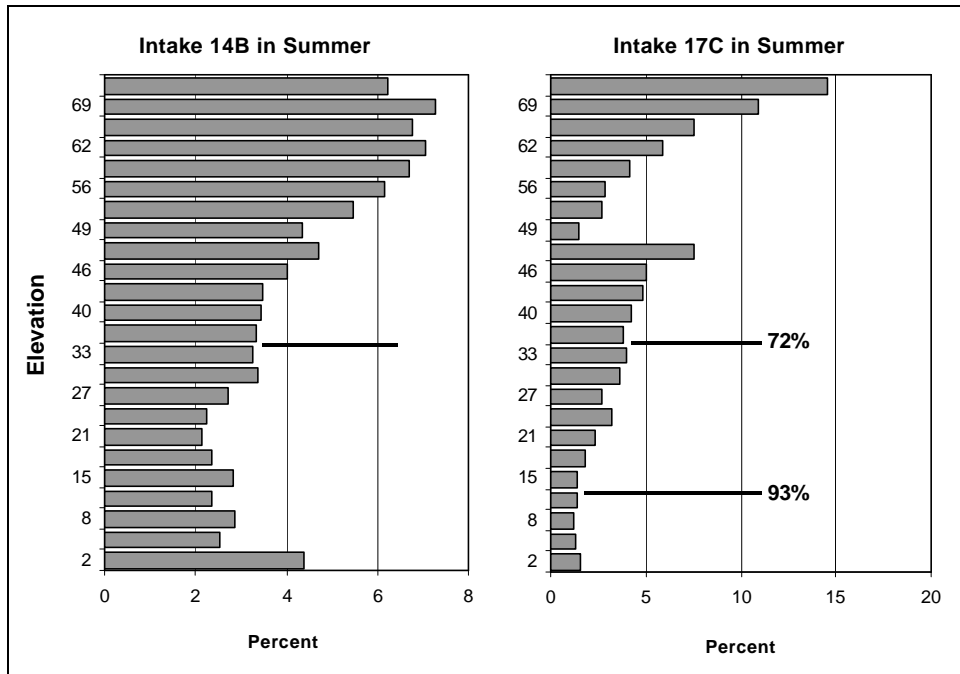
Figure 38. Vertical distribution of all fish detected immediately upstream of trash racks at Intakes 14b and 17c in summer 2000
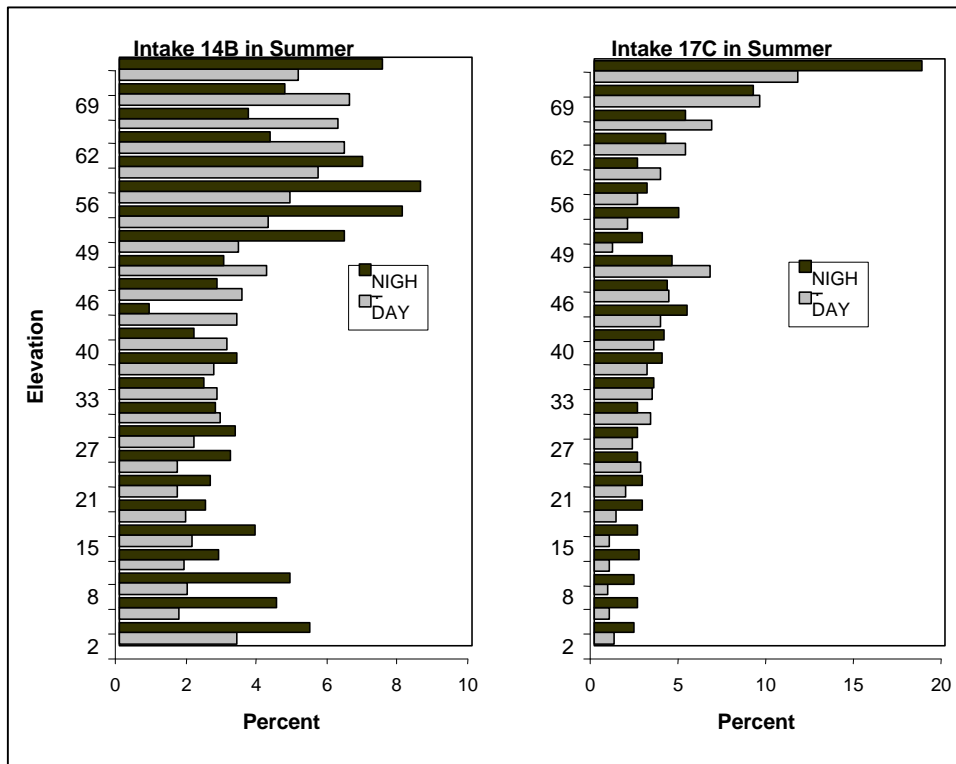

Figure 39. Day and night vertical distribution of all fish detected immediately upstream of trash racks at Intakes 14b and 17c in summer 2000

Temporal Trends in Fish Passage

Seasonal Trends

Spring hydroacoustic sampling at the Bonneville Project and JBS sampling at Powerhouse 2 by the NMFS both indicated that peaks in the spring run occurred near 22 April and sometime during the later part of May (Figure 40).
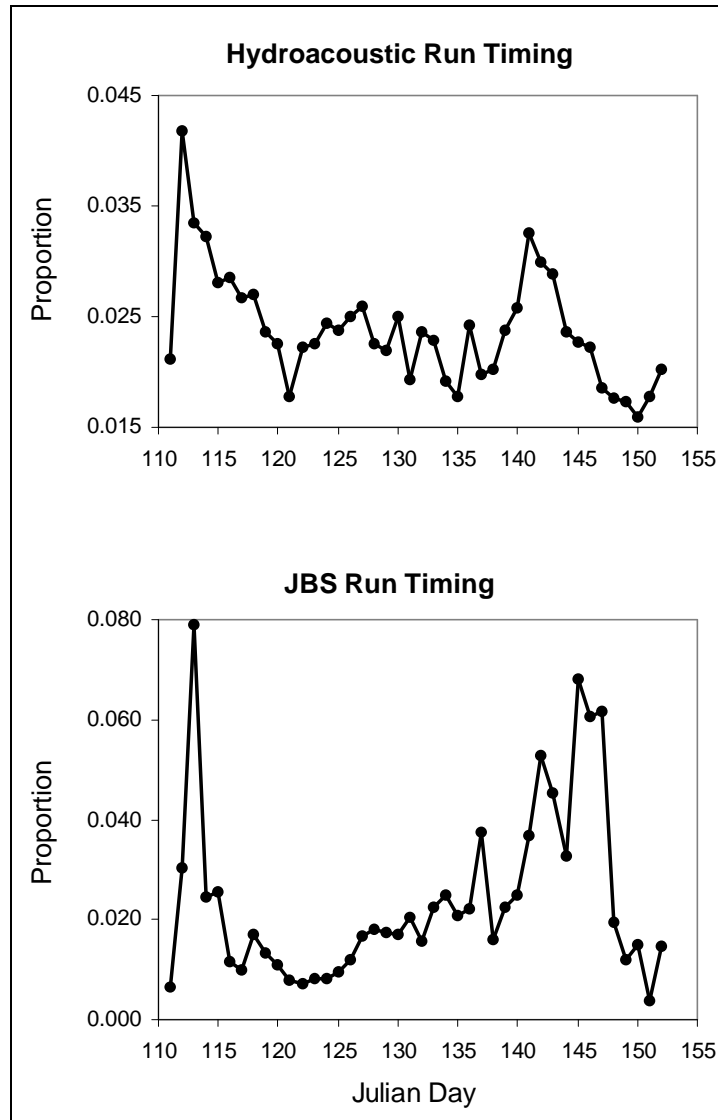
Figure 40. General pattern of spring run timing estimated by hydroacoustics and by sampling with a smolt trap in the Powerhouse 2 JBS

In summer two peaks in fish passage were detected by both sampling methods (Figure 41), with the first occurring around Julian Day 159 (7 June) and another occurring around Julian Day 166 (14 June). A third peak in fish passage detected

by hydroacoustics from Julian Day 178-181 (26-29 June) was not in the JBS sampling.

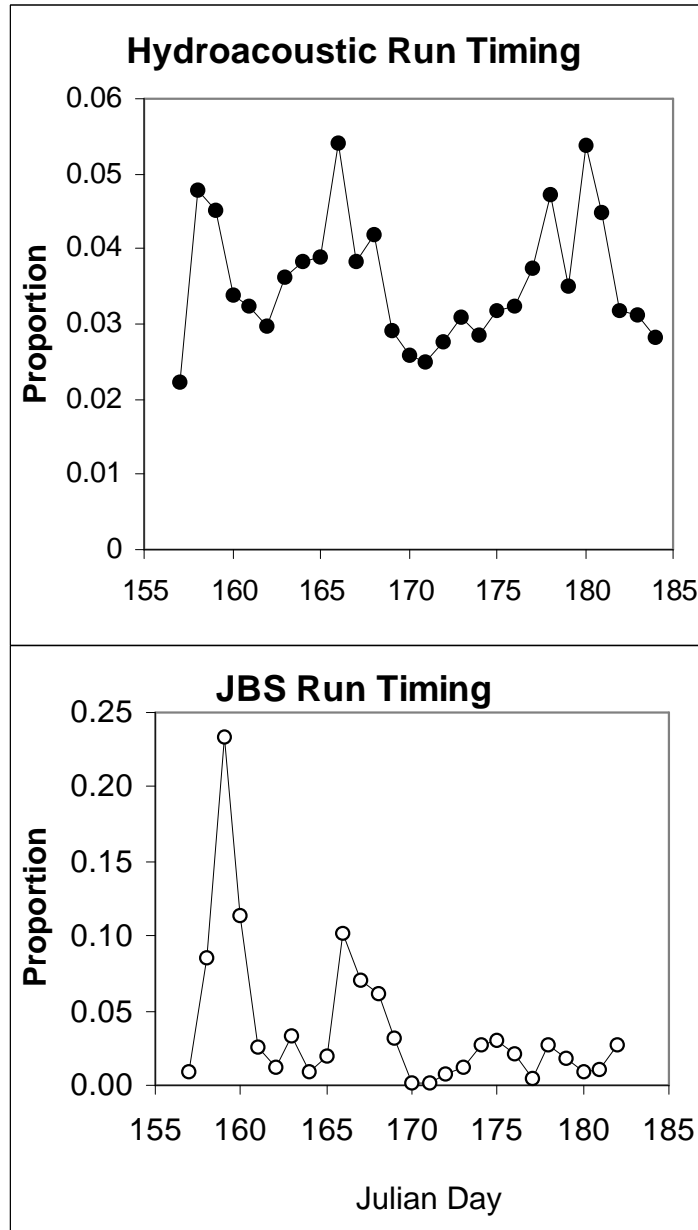**Hydroacoustic Run Timing**

JBS Run Timing

Figure 41. Summer run timing as determined by hydroacoustic sampling and by NMFS sampling of a smolt-trap at Powerhouse 2

Spill efficiency contributed significantly to Project FPE in spring and summer, and the difference between FPE and spill efficiency narrowed in late spring and early summer (Julian days 141-170; Figure 42).

The efficiency of fish passage at Powerhouse 1 declined significantly from early spring through mid-summer, but not as precipitously as the efficiency for Powerhouse 2 (Figure 43). Fish guidance structures at Powerhouse 1 included the

PSC at Units 1-6, an ESBS at Unit 8 and STSs at Units 7, 9, and 10, whereas Powerhouse 2 had only STSs.
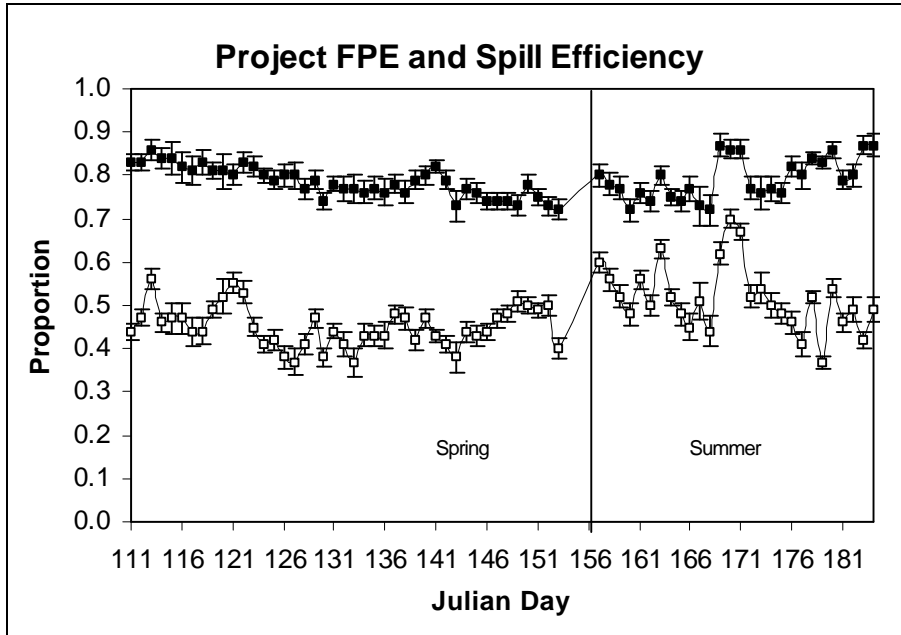

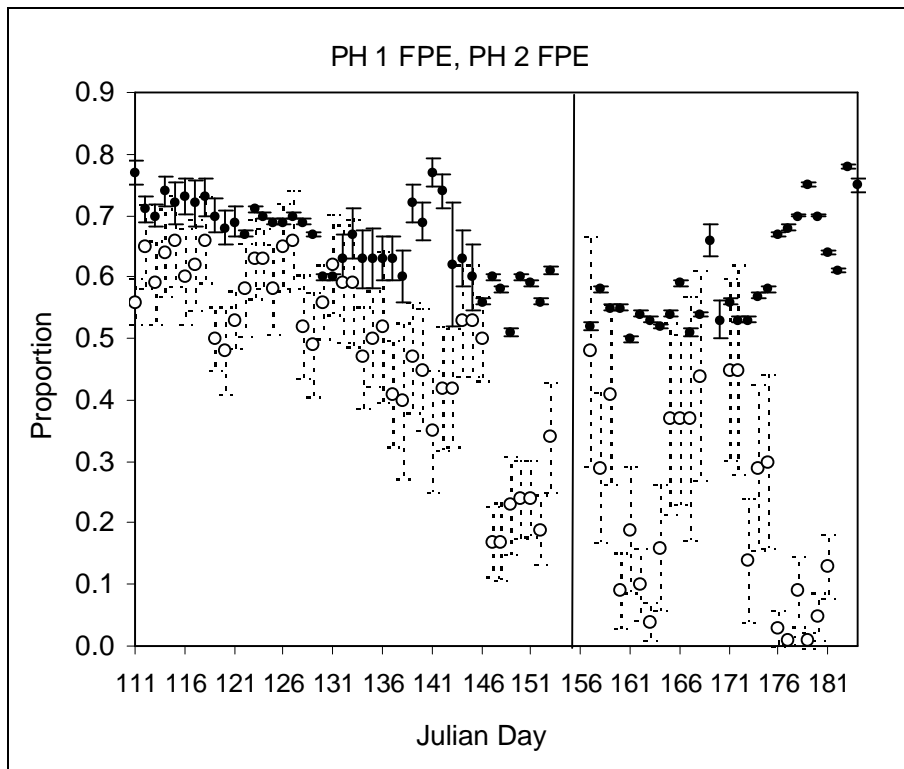Figure 42. Seasonal trends in project FPE and spill efficiency

Figure 43. Plot of the average FPE of Powerhouse 1 and Powerhouse 2 from spring through summer

Unlike the efficiency of the ESBS and STSs, which declined significantly from spring through summer, the efficiency of the PSC remained high in both seasons (Figure 44).
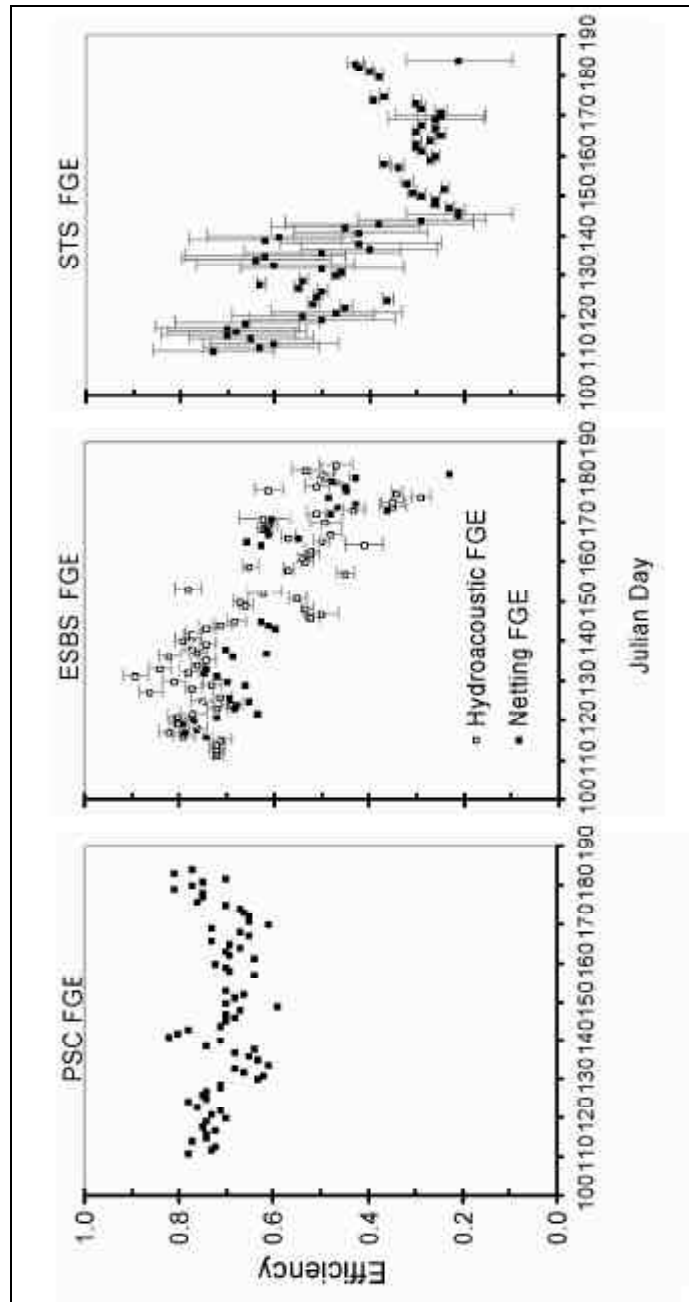

Figure 44. Plot of the FPE of the PSC, the ESBS at Unit 8, and the STS at Units 7, 9, and 10, and spill efficiency by Julian Day in spring and summer

The contribution of our conservative estimate of the PSC efficiency to Project FPE averaged about 6 percent in spring before Julian Day 142 (21 May) and about 12 percent thereafter (Figure 45).

The average effectiveness of the PSC at Powerhouse 1 was significantly higher than that of the project spill effectiveness (Figure 46), where effectiveness is the proportion of fish passed by a route divided by the proportion of water passed.
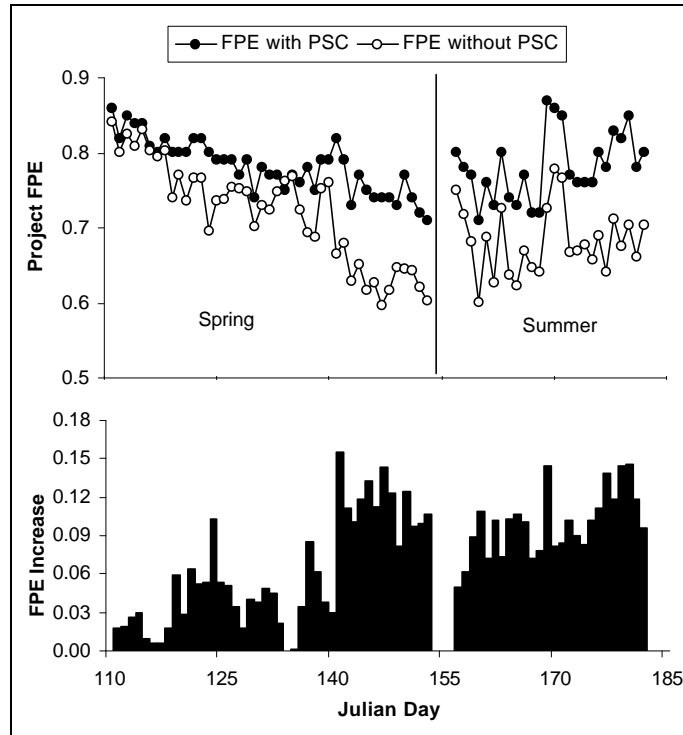

Figure 45. Plot of FPE of the Bonneville Project with and without the PSC (top) and increase in FPE due to the PSC (bottom) over STSs
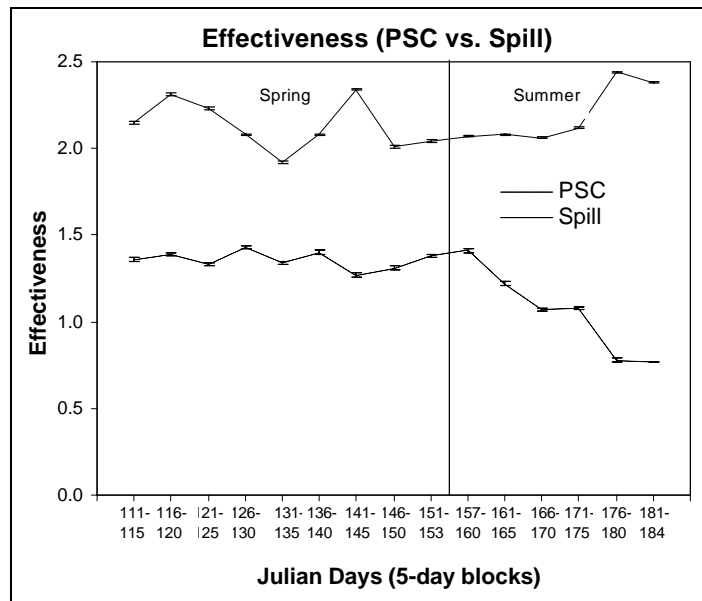

Figure 46. Plot of average PSC and spill effectiveness by Julian Day in spring and summer

Diel Patterns

Some fish passage metrics had diel variation in spring, but Project FPE remained fairly steady over the course of an average day (Figure 47). In contrast, spill efficiency was 5-8 percent lower in spring and about 10 percent lower in summer during the daytime than it was at night (Figure 48). Spill effectiveness did not vary much among hours of the day in spring (Figure 49). In summer spill effectiveness was about 27 percent lower than it was in spring and it was about 8 percent lower from 1100 through 1500 hours than it was during other hours of the day. At Powerhouse 1, the fish passage through turbines tended to be lowest during the day from about 1000 to 1800 hours in spring, whereas it was crepuscular in summer with a peak just after dark and another about sunrise (Figure 50). In contrast to fish passage through turbines, passage through the PSC
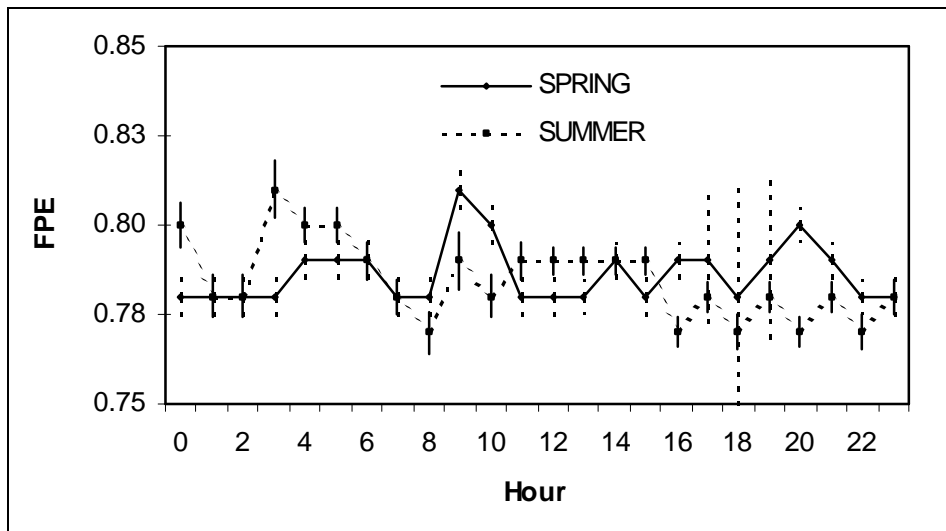

Figure 47. Diel patterns of FPE for Bonneville Dam during spring and summer 2000
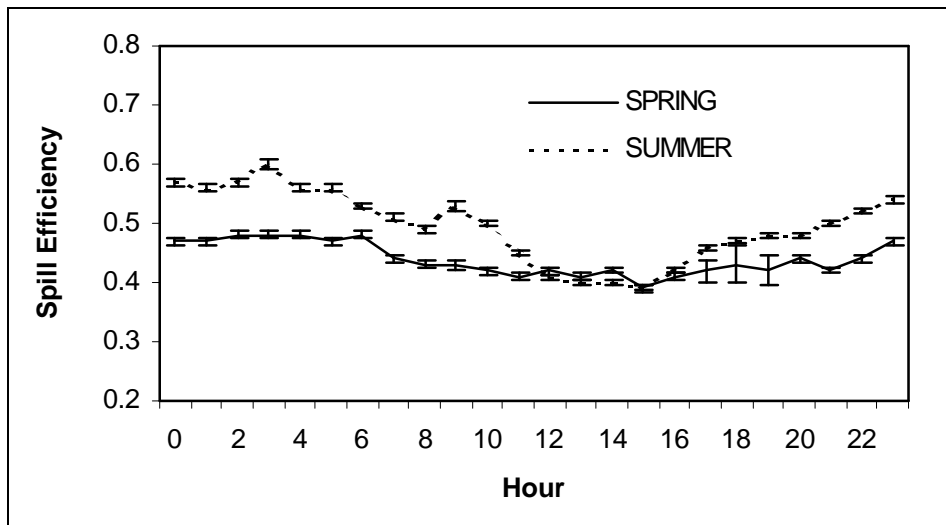

Figure 48. Diel patterns of spill efficiency for Bonneville Dam during spring and summer 2000
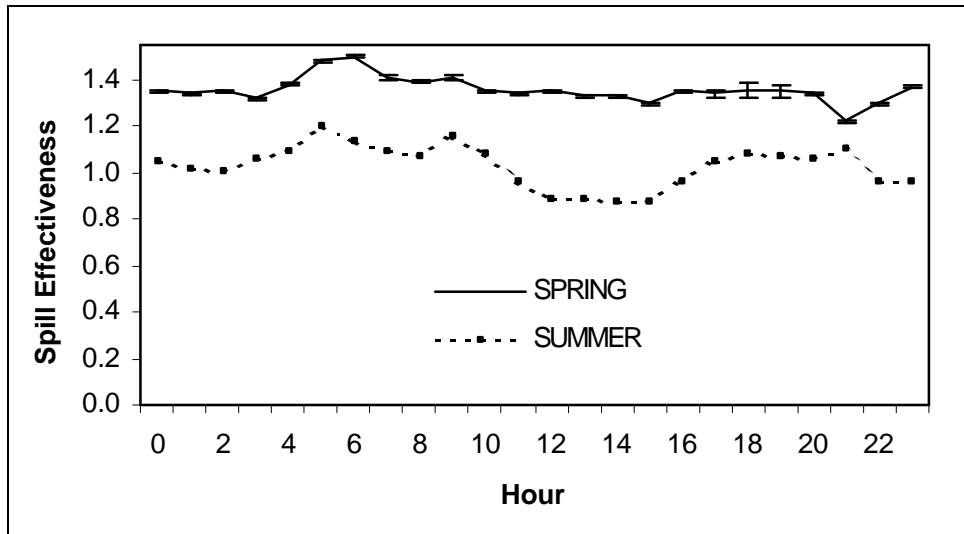
Figure 49. Diel trends in spill effectiveness for spring and summer
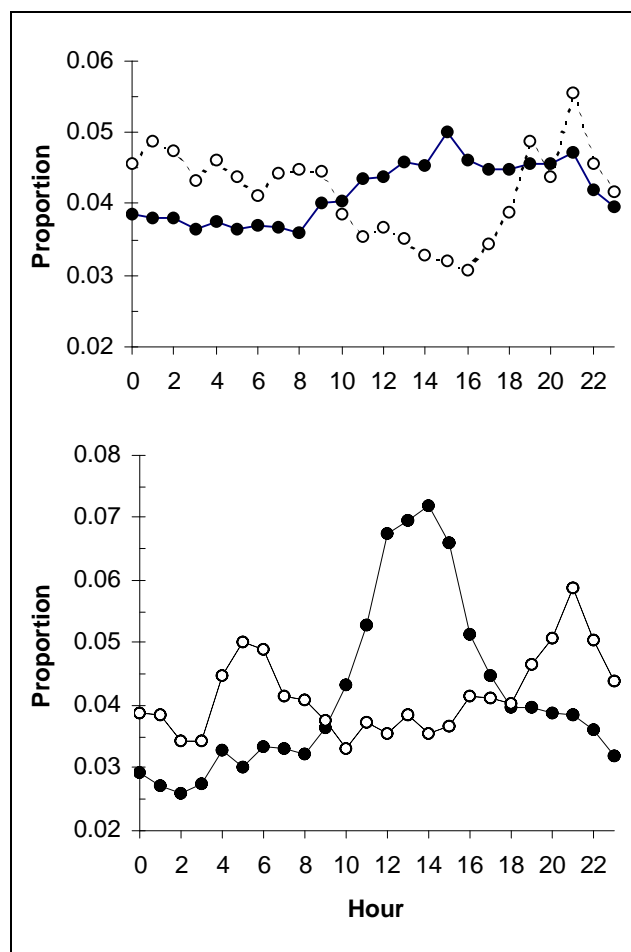

Figure 50. Diel patterns of fish passage through the PSC and turbines at
            Powerhouse 1

was highest during the day from about 0900 to 2100 hours in spring and between 1000 and 1700 hours in summer (Figure 50).

The hourly proportion of fish passing under the PSC varied little among hours of the day in spring, whereas unguided passage under the PSC in summer and under in-turbine screens in spring and summer peaked around the time of sunset (Figure 51).
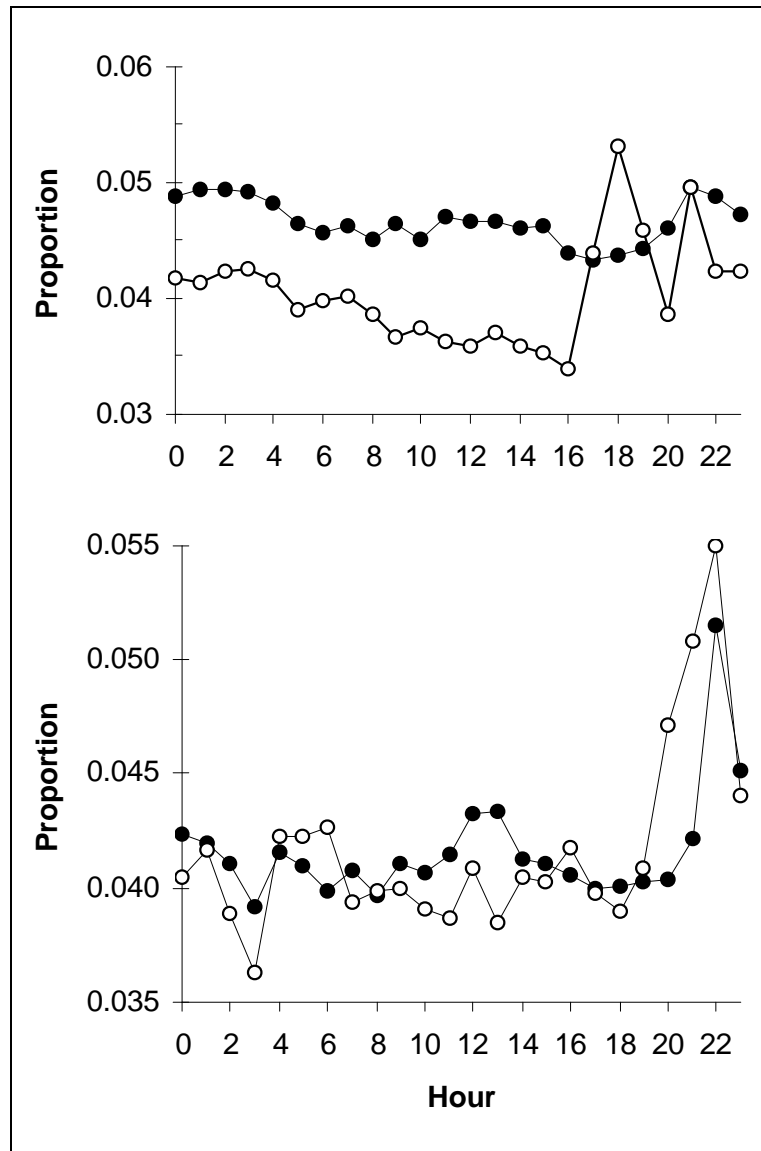
Figure 51. Diel trends in fish passage under the PSC and screens located in Turbines 7-10 at Powerhouse 1 in spring (top) and summer (bottom)

At Powerhouse 2, guided fish passage exhibited a crepuscular pattern in spring with peaks in passage occurring around sunrise and sunset, but in summer, only an evening peak was evident (Figure 52). Little diel pattern was evident for unguided fish at Powerhouse 2 in spring (Figure 53). However, for the few operational turbines in summer, proportionally more fish passed under screens during the day than at night (Figure 53).
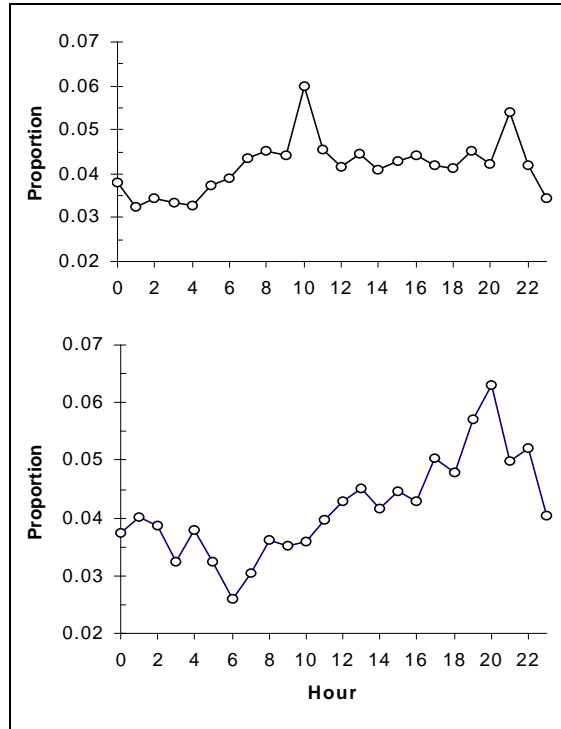
Figure 52. Diel patterns in guided fish passage at Powerhouse 2 in spring (top) and summer (bottom)
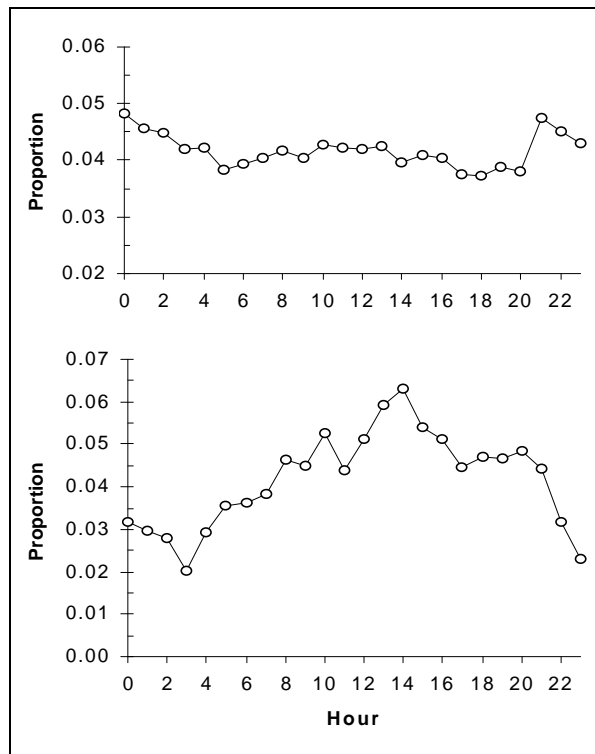
Figure 53. Diel patterns in unguided fish passage at Powerhouse 2 in spring (top) and summer (bottom)

Chapter 3   Results

There was no overlap in 80 percent confidence limits for many night and daytime hours, indicating that the mean hourly rate of fish passage through the spillway tended to be higher at night than during the day in both seasons (Figure 54). Spill volume also was higher at night than it was during the day. In spring the mean hourly rate of fish passage during night hours (2030-0540) was 17 percent higher than the mean of day hours (0800-1900), and in summer the mean hourly rate of passage during night hours (2130-0520) was 19 percent higher than the mean of day hours (0800-2000).

Figure 54. Hourly patterns in the mean number of fish spilled per hour in spring (top) and summer (bottom). Error bars represent 80 percent confidence limits on hourly means. Vertical lines indicate average times of sunrise and sunset

Fish Guidance Efficiencies
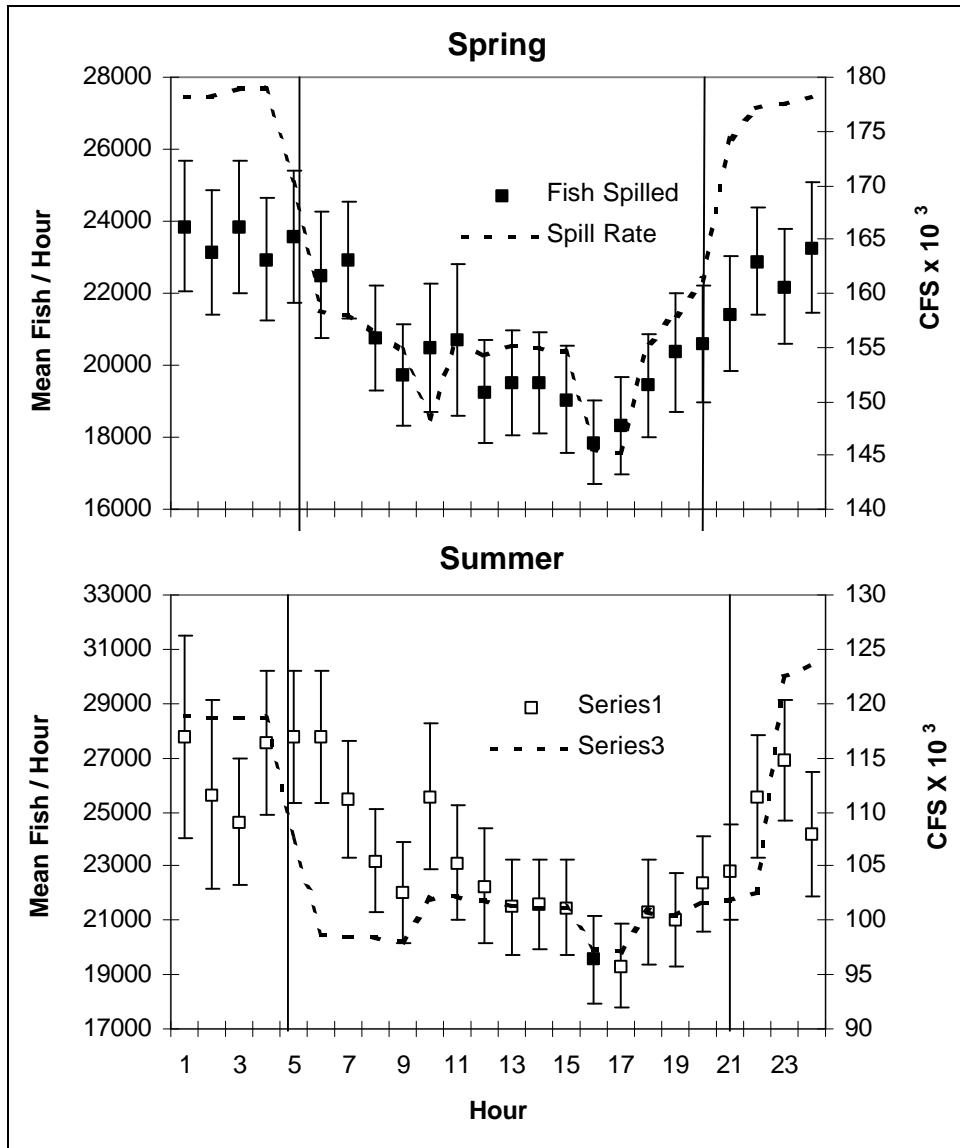
Background

Fish guidance efficiency is the ratio of the estimated number of fish passing a turbine by a non-turbine route ("guided" fish) to the estimated number of all of the fish passing that turbine ("guided" + "unguided" fish). Fish passage efficiency is the same calculation done on the scale of the PSC, a powerhouse, or the entire project. Based upon historical information, FPE and FGE are expected to be lower in summer than in spring. Results of the efficiency evaluations of fish guidance structures are presented in the following order: PSC at Units 1-6, the ESBS at Unit 8, and STS at Units 7 and 9-18.

Comparing Performance of Fish Guidance Structures

No significant correlations of hourly counts of fish were detected in turbine intakes downstream of the PSC with hourly counts of fish detected immediately upstream of corresponding 20-ft wide PSC slot entrances. Similarly, the sum of hourly counts of fish detected in Turbines 1, 2, 4, 5, and 6 was not significantly correlated with the sum of hourly counts of fish upstream of slot entrances (Figure 55). The number of fish detected upstream of PSC slots almost always was significantly higher than the number detected in turbines downstream of the PSC.
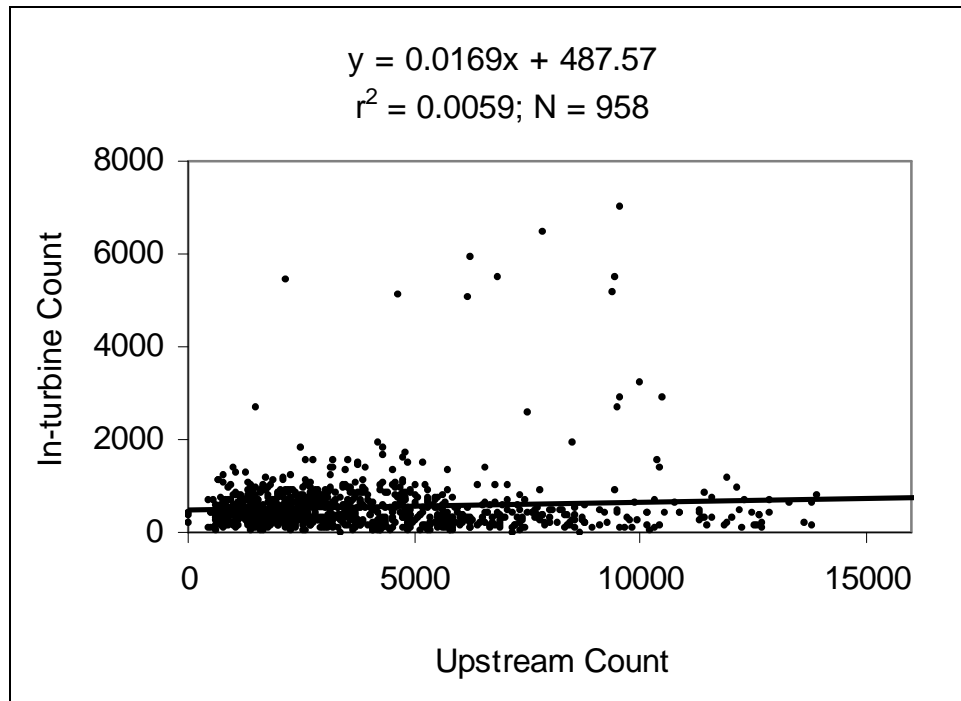

Figure 55. Scatter plot of hourly in-turbine counts of fish downstream of the PSC at Units 1, 2, 4, 5, and 6 as a function of counts upstream of the same 20-ft-wide PSC slot entrances

The expected marked decline in FGE was observed at all of the turbine units that are only equipped with screens (11 STSs or the one ESBS) for fish guidance, but it was found that FGE of the PSC remained as high in summer as it was in spring (0.72, see Figure 40). The Powerhouse 1 turbine units with STSs (Units 7, 9, and 10) had an estimated average FGE of 0.48 in spring and 0.36 in summer. FGE at the ESBS at Unit 8 in spring was 0.72, as good as the average PSC FGE, but it was only 0.50 in summer. The eight Powerhouse 2 turbine units (all with STSs) had an average FGE of 0.52 in spring and the seven turbines that operated in summer (Unit 12 did not) averaged 0.38. High FGE values for turbine units near the middle of Powerhouse 2 should be understood in light of the very brief times that they were operated in summer as described below.

Figures 56 and 57 present the mean FGEs for all of the turbine units at the dam in spring and summer, respectively. In both seasons Units 5 and 6, next to the Powerhouse 1 wing wall on the northern end of the PSC, had the highest FGEs at the project with the only estimated values over 80 percent (Table 19). In spring Unit 2 (PH-1 PSC), Unit 8 (ESBS), and Units 14 and 15 (near the center of Powerhouse 2 with STSs), shared the next highest echelon of estimated FGE values, between 0.70 and 0.80. Three PSC units (Units 1, 3, and 4) and Unit 12 (STS at south end of Powerhouse 2) had FGEs between 0.6 and 0.7. Four STS units (Units 9 and 10 on Powerhouse 1 and Units 13 and 17 on Powerhouse 2) had FGEs of 0.50-0.60. Unit 7 (STS on Powerhouse 1) and Units 16 and 18 (STSs on Powerhouse 2) had FGEs between 0.40 and 0.50, and Unit 11 (STS on the south end of Powerhouse 2) had the lowest spring FGE of 0.21. Unit 10 was off line for part of the spring and ran only about half as much as did the other turbine units.
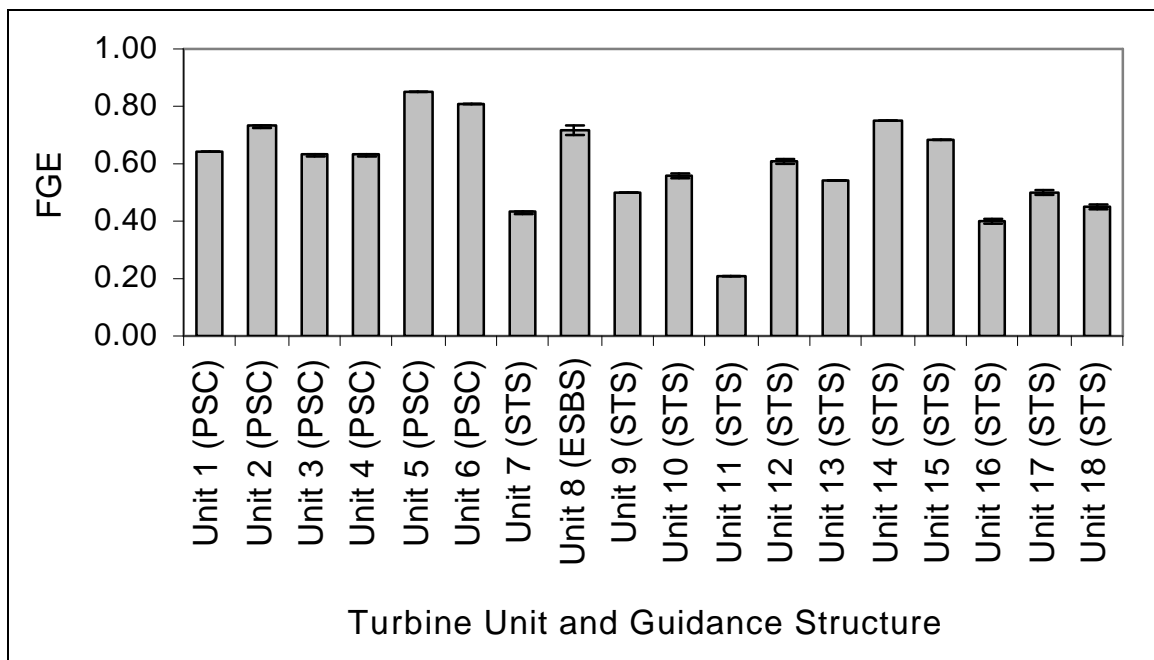

Figure 56. Estimated FGE by turbine unit in spring. Error bars are 95 percent confidence limits
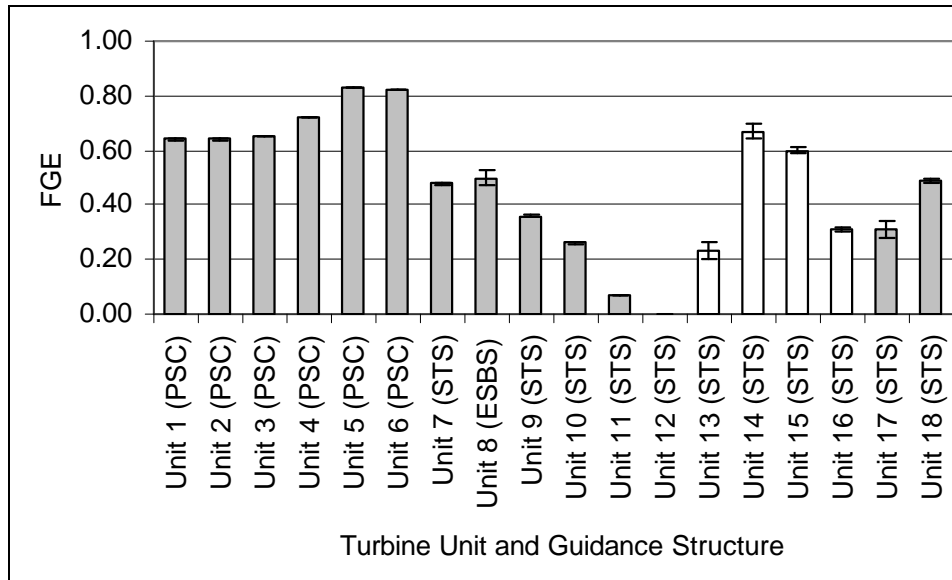
Figure 57. Estimated FGE by turbine unit in summer. Units 13-16 are shown in white because they were rarely operated in summer (i.e., they passed < 6 % of Powerhouse 2 discharge). Unit 12 did not run in summer

In summer the turbine units with the highest FGEs were again Units 5 and 6, but the overall profile of FGE across the dam was considerably different from that in spring (Figure 57). The average FGE at the PSC was the same (0.72) for summer, although the FGEs of the individual PSC turbine units were less variable than during spring. FGE estimates at Units 1-3 were similar and the lowest in the PSC (0.63-0.64), Unit 4 was slightly higher (0.72%), and Units 5 and 6 had estimated summer FGEs of 0.83 and 0.82, respectively.

Whereas the FGEs at the PSC held up well in summer, those from the screened turbine units north of the wing wall had much lower values (Figure 56). The most extreme decline from spring to summer was at Unit 10 (with an STS) where the estimated FGE dropped 30 percent from 0.56 in spring to 0.26 in summer. Unlike in spring, Unit 10 was on line about as much as were the other turbine units at Powerhouse 1 in summer. The next most severe loss in FGE was at Unit 8 (with the ESBS) where the estimate went from 0.72 in spring to 0.50 in summer, a decrease of 22 percent. Unit 9 dropped from 0.50 in spring to 0.36 in summer, but Unit 7 showed an increase of about 5 percent, from 0.43 to 0.48.

In summer, Powerhouse 2 operations were dramatically different from what they were in spring. The most obvious difference was that most of the Powerhouse 2 turbine units were operated very little or not at all (Unit 12) in summer and so Powerhouse 2 passed only about 13.6 percent as much water in summer as it did in spring. Also, about twice as much water was passed by generation during daytime than at night at Powerhouse 2 in order to provide attracting flow for upstream migrating adult salmon. The distribution of operation across turbine units was also very different in summer, with about 32 percent of Powerhouse 2's water passing Unit 11, about 27 percent each passing Units 17 and 18, about 5.4 percent passing Unit 16, and the rest of the units passing less

than 5 percent. For that reason it is of note that the rather high FGE estimates from the middle turbine units (Units 13-16) are based upon very small samples and are marked accordingly in Figure 57.

The Powerhouse 2 turbine units that ran for substantial periods (Units 11, 17, and 18) had very different FGE estimates although they all have STSs for fish guidance. Unit 11, at the north end of Powerhouse 2, had the lowest FGE estimate at the project, 0.07, whereas Unit 18 at the north end had an estimate of 0.49. It is especially surprising that Unit 17, which ran almost the same amount of water as did Unit 18 in summer, had an estimated FGE estimate 18 percent lower, or 0.32 (Figure 57).

Table 19
FGEs at Both Powerhouses in Spring and Summer

FGE Range	Spring	Summer
> 80%	Units 5 & 6 (PH-1; PSC)	Units 5 & 6 (PH-1; PSC)
70-80%	Unit 2 (PH-1; PSC) Unit 8 (PH-1; ESBS) Unit 14 (PH-2; STS)	Unit 4 (PH-1; PSC)
60-70%	Units 1, 3, & 4 (PH-1; PSC) Unit 12 & 15 (PH-2; STS)	Units 1, 2, & 3 (PH-1; PSC) Units 14 & 15 (PH-2; STS)
50-60%	Unit 9 & 10 (PH-1; STS) Unit 13 & 17 (PH-2; STS)	Unit 8 (PH-1; ESBS)
40-50%	Unit 7 (PH-1; STS) Units 16 & 18 (PH-2; STS)	Unit 7 (PH-1; STS) Unit 18 (PH-2; STS)
30-40%		Unit 9 (PH-1; STS) Units 16 & 17 (PH2; STS)
< 30%	Unit 11 (PH-1; STS)	Unit 10 (PH-1; STS) Unit 11 & 13 (PH-2; STS)

Note: Turbine units are grouped in 10% bins according to their FGE estimates. Note that, in summer, the FGE estimate for the ESBS on Unit 8 is just 50%, so it is on the line between the 40-50% and the 50-60% bins

Simultaneous examination of guided and unguided fish passage trends by turbine (Figures 58 and 59) helps put the FGE estimates (Figures 56 and 57) into perspective. In those figures, the horizontal axis at zero represents the dividing elevation of the fish guidance structure (e.g., the floor elevation of at PSC Units 1-6, the tip of the ESBS on Unit 8, or the tips of the STSs at Units 7, 9-10, and 11-18. The negative numbers indicate unguided fish below the fish guidance structures and the positive numbers indicate guided fish above that elevation.

In spring at Powerhouse 1, Unit 8's ESBS had as high an FGE estimate as the mean for the PSC units (72 percent), but it is clear from Figure 58 that many fewer fish passed at Unit 8 than passed at any of the PSC units. Also, whereas more spring fish encountered Unit 9 than any other turbine unit, Unit 9 guided only about 50 percent of them. At Powerhouse 2 the highest total (both guided and unguided) passage was at Unit 15, which also had a rather high FGE estimate

in spring (68 percent), while its nearest neighbor unit to the south, Unit 14, had an even higher estimated FGE but passed substantially fewer fish. There tended to be more guided fish passing at Units 12-15 than at other units in spring.

In summer the PSC substantially outperformed the screened units in terms of FGE estimates and was also encountered by more fish (Figure 59). A surprisingly high number of fish encountered Unit 9 in summer, as compared to the other turbine units, but relatively few were guided (Unit 9 summer FGE estimate = 36 percent). At Powerhouse 2 around three quarters of a million fish encountered Unit 11 but very few were guided (Unit 11 FGE estimate = 7 percent), whereas at the other end of the powerhouse about 1 M fish passed, about half of which were guided. Whereas Unit 17 passed almost as much water and had a lower FGE (31 percent as compared to 49 percent) as did Unit 18 in summer, it evidently had a much lower overall encounter rate (Figure 59).
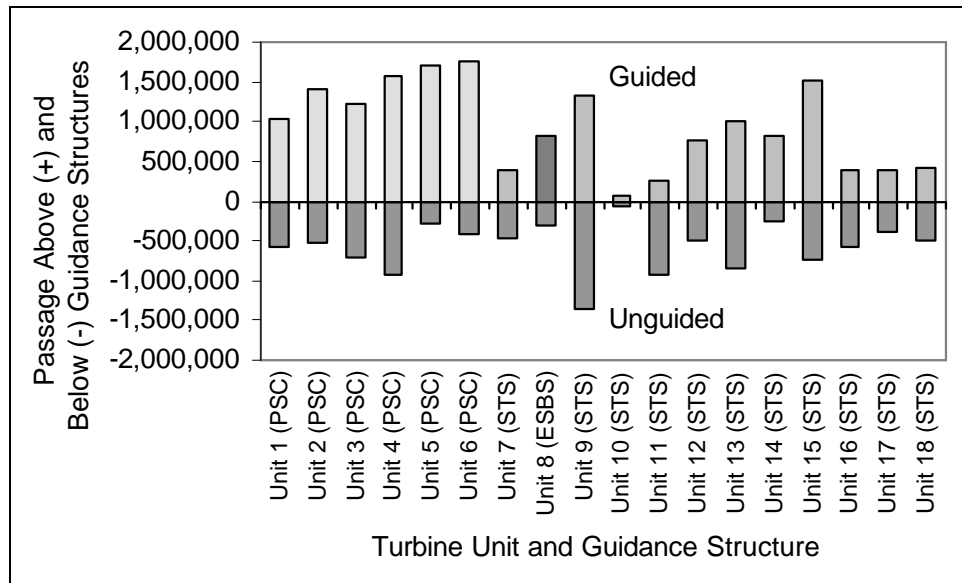

Figure 58. Estimated total fish passage above and below fish guidance structures (floor of PSC or screens) in spring. The horizontal axis at zero represents the division between guided and unguided passage (PSC floor, ESBS tip, or STS tip)
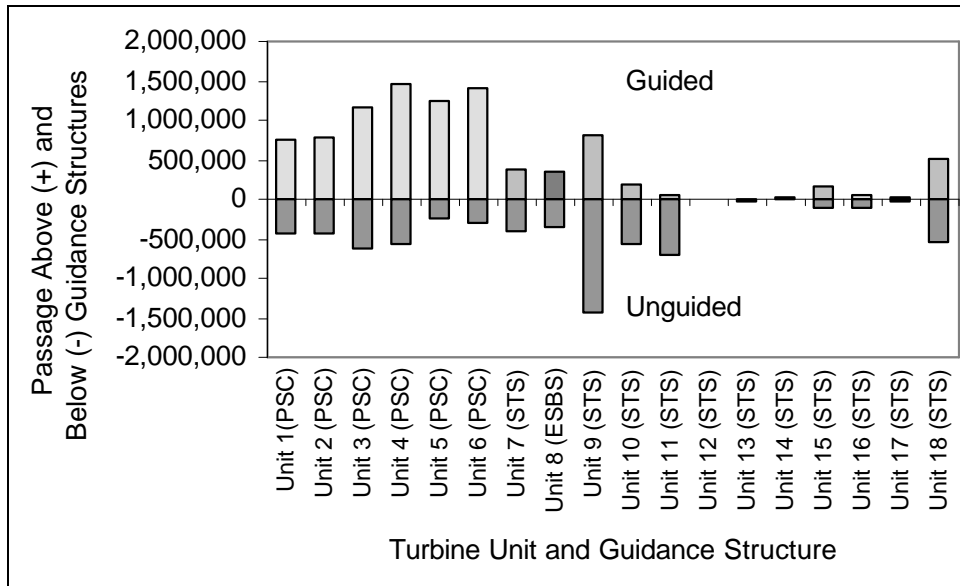
Figure 59. Estimated total fish passage above and below fish guidance structures (floor of PSC or screens) in summer. The horizontal axis at zero represents the division between guided and unguided passage (PSC floor, ESBS tip, or STS tip)

Comparing FGE Sampling Methods at Unit 8

The fish passage estimates from the up-looking and down-looking beams at Unit 8 were compared with NMFS estimates based upon gatewell dipping of guided fish and fyke netting of unguided fish. The NMFS samples were collected on 40 evenings in both spring and summer for about 2 hr each (starting at 2000 hr and ending from 2205 to 2250 hr, the mean duration being 2 hr 31 min). Hydro-acoustic samples were able to be paired up with netting samples from only 33 of the 40 days sampling in spring and summer because of equipment problems in spring (see Materials and Methods).

Hydroacoustic estimates of the number of fish guided by the ESBS were significantly correlated with the number of guided fish dipped from the gatewell (Figure 60), as were hydroacoustic estimates of unguided fish with numbers of unguided fish collected in fyke nets (Figure 61). The slopes of the correlation lines for guided and unguided fish were 0.85 and 0.93, when the intercepts were forced through zero. Only about 53 percent of the variation in netting estimates was explained by the hydroacoustic estimates.
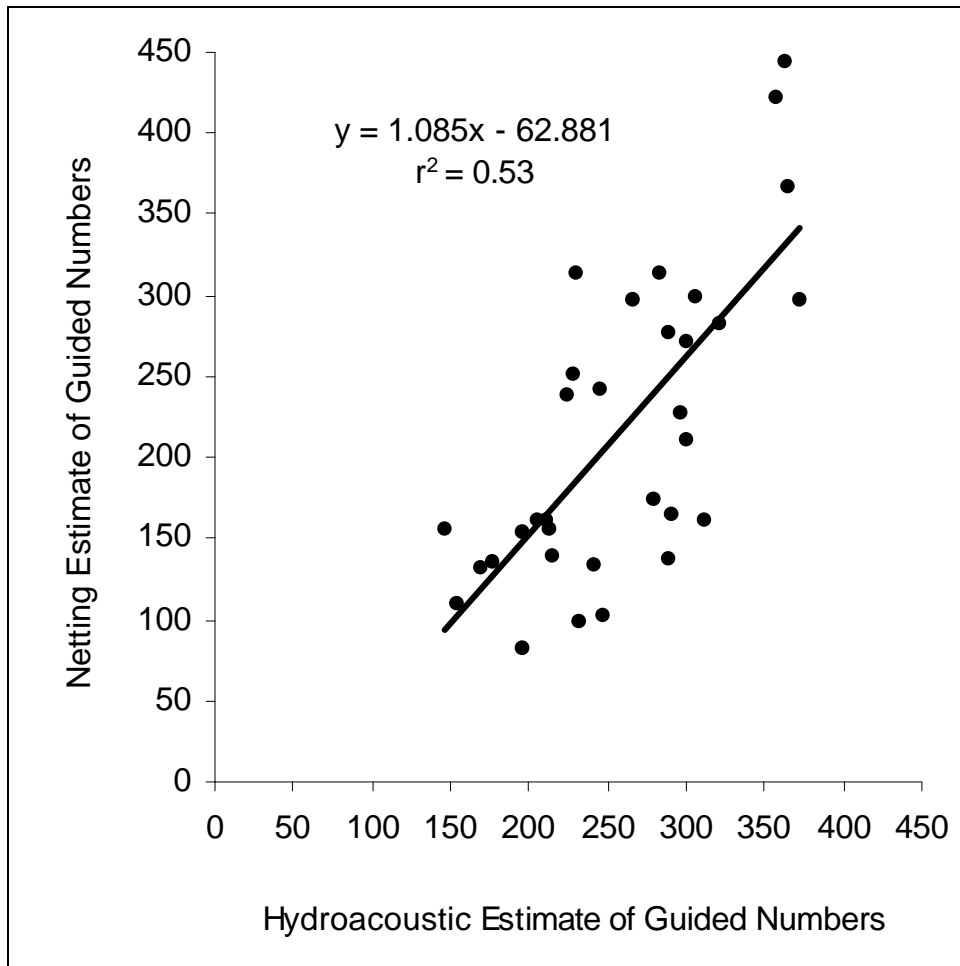
Figure 60. Correlation of gatewell-dipping estimates of the number of fish guided
by the ESBS at Unit 8 with hydroacoustic estimates

Paired t-tests of paired observations indicated that hydroacoustic and netting
estimates of FGE did not differ significantly in spring, but differences were
significant in summer despite low sample sizes (Table 20). After pooling spring
and summer observations, a t-test indicated that the means were significantly
different, although they only differed by 3 percent.

The correlation of netting and hydroacoustic estimates of FGE at Unit 8 also
were highly significant (Figure 62). A single point in the figure (x and y
coordinates 0.50, 0.24) seemed to be an obvious outlier for the correlation, but
dropping it from the analysis could not be justified. Excluding that point from the
correlation analysis increased the r^2 value by only 3 percent, from 0.65 to 0.68.
The r^2 for FGE estimates was 12 percent higher than corresponding statistics for
numbers of guided and unguided fish.
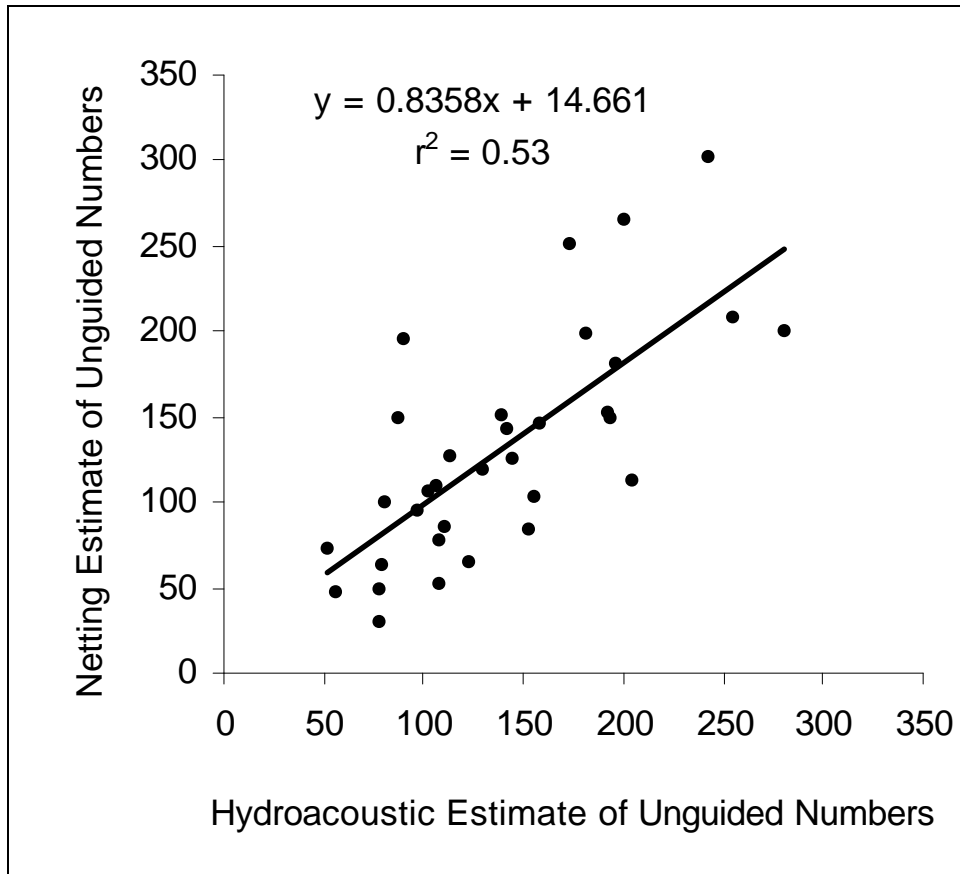
Figure 61. Correlation of fyke netting estimates of the number of fish passing under the ESBS at Unit 8 with hydroacoustic estimates

Table 20
Paired t-tests Comparing Mean Estimates of FGE by Hydroacoustics and Netting for the ESBS at Unit 8 in Spring, Summer, and Both Seasons

| Statistics | Season | | | | | |
| | Spring | | Summer | | Both | |
	Acoustic	Netting	Acoustic	Netting	Acoustic	Netting
Mean	0.70093	0.69234	0.57441	0.51119	0.65493	0.62647
Variance	0.00412	0.00335	0.01362	0.01467	0.01108	0.01497
Observations	21	21	12	12	33	33
Hypothesized Mean Difference	0		0		0	
df	20		11		32	
t Stat	0.72172		2.44805		2.24067	
P(T<=t) two-tail	0.47882		0.03236		0.03212	
t Critical two-tail	2.09		2.20		2.04	
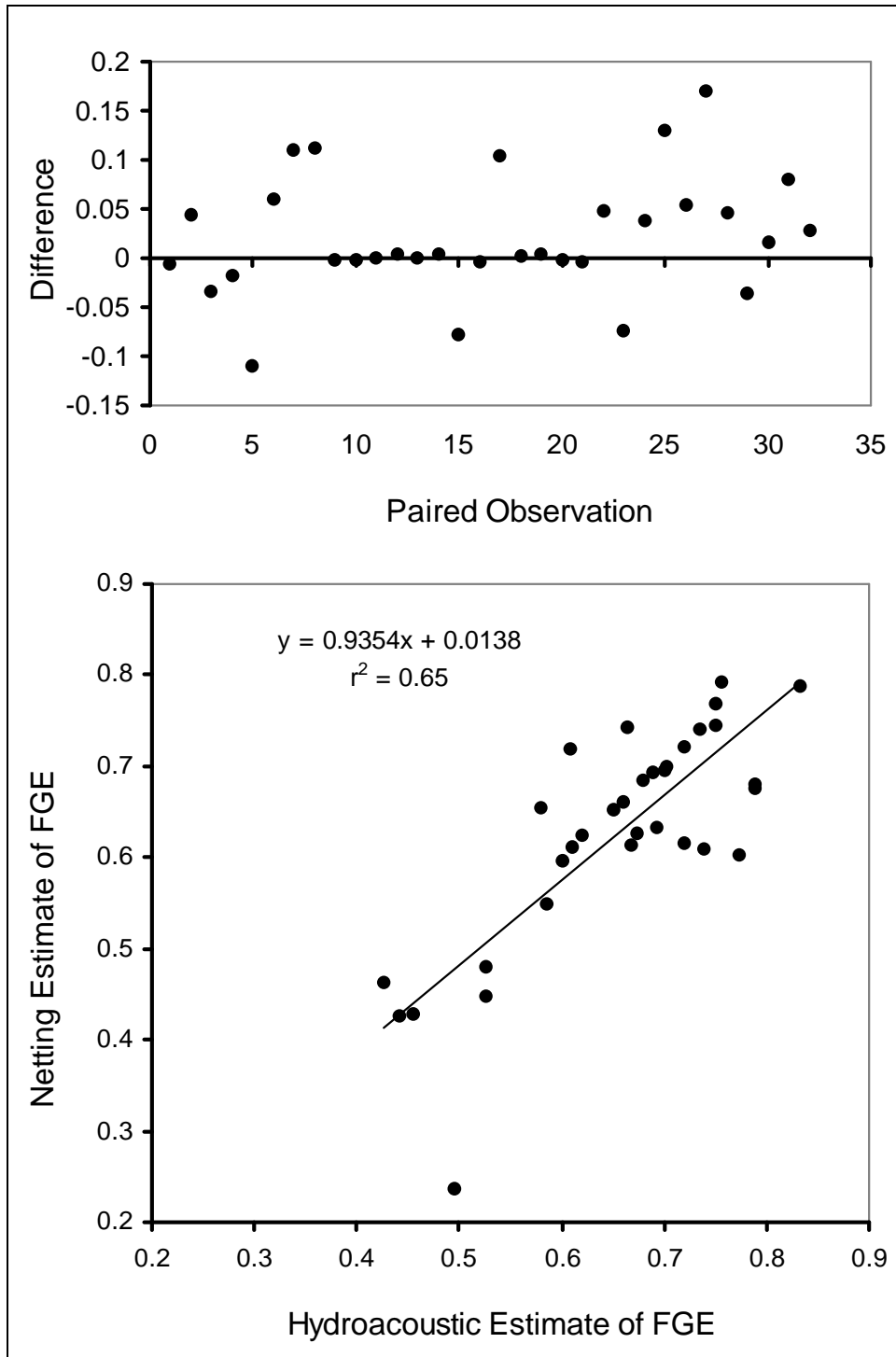
Figure 62. Plot of the difference in hydroacoustic and netting estimates of FGE for the ESBS in Unit 8 (top) and of the correlation of netting estimates of FGE at Unit 8 (bottom) with hydroacoustic estimates

4 Discussion

Hydroacoustic Detectability

The motivating force behind efforts to improve detectability modeling is the desire to provide hydroacoustic estimates that are quantitative as well as reliable relative indices to fish passage. Ratio estimators such as the FGE of the PSC, ESBSs, and STSs only require that hydroacoustic beams sampling guided and unguided fish have equal detectability so that ratios of counts, not necessarily the counts themselves, are accurate. Similarly, combining counts from different locations such as powerhouses and a spillway also requires equalization of detectability so that counts from different locations are comparable, although the counts themselves may not be accurate. Nevertheless, accurate counts estimated by proper expansion of detected fish have the potential to provide estimates with inherent quantitative value as well as providing acceptable relative estimates.

Expanded hydroacoustic counts of guided and unguided fish at Unit 8 were compared with estimates from netting by the NMFS to evaluate the reasonableness of our detectability modeling and the resulting spatial expansion factors. Preliminary hydroacoustic estimates of numbers of guided and unguided fish at Unit 8 were 3-5 times higher than NMFS netting estimates, and this suggested that the calculated effective beam angles were too narrow and spatial expansion factors were too large. On reviewing preliminary modeling efforts, it was found that average target strength had been input rather than a target strength converted from the average backscattering cross section of detected fish. This mistake caused the model to underestimate the hydroacoustic size of fish and effective beam angles. As a result, spatial expansion factors derived from fish detection ranges were overestimated. The use of revised target strength estimates calculated from the average backscattering cross section provided ratios of hydroacoustic and netting estimates that approached 1:1. These results demonstrate the value of using multiple sampling methods for calibration purposes. Ploskey and Carlson (1999) observed that hydroacoustic sampling only provides a relative index to fish passage unless calibrated against unbiased netting.

It was found that 25-47 percent increases in spill rate were associated with only modest increases in Project FPE (3-5 percent) and spill efficiency (7-8 percent), and this result raised concerns about detectability of spilled fish at the

higher spill levels that occurred at night. Maximum velocities of fish passing through hydroacoustic beams were determined from both day and night samples for every 1-m range stratum in our beams. Therefore, detectability curves, which indicated high and uniform detectability (effective beam angle) throughout the sampling range (Figures 9 and 10), were based upon worst-case velocity profiles. Much of the high detectability observed can be attributed to the rapid ping rate of 30 pings per second for all spillway transducers. In addition, both night and day samples had identical distribution statistics for the number of echoes per fish (i.e., mean = 10; median = 8; 25th percentile = 5). If detectability deteriorated with high discharge at night, one would expect fewer echoes per fish in nighttime samples than in daytime samples. Since echoes per fish did not decline at night, it was determined that fish detectability was adequate at the spillway for all time periods; therefore, the reduced spill effectiveness observed at night was a true observation rather than a detectability problem.

Quality Control on Automated Fish Tracking

Variability in Human Counts of Fish Traces

It was found that different individuals tend to have characteristic biases that manifest themselves in different counts of fish from the same hydroacoustic data sets. As in the last three seasons when the phenomenon of interpersonal bias in echogram counts of fish traces was investigated, it was found that some people tend to consistently track higher or lower numbers of fish traces than other people. This problem occurs even with experienced trackers. Human trackers were hired and trained as a group over about a month before the season started. Basic hydroacoustic theory and practice was taught, deployments were described, tracking criteria were carefully explained, data sets from previous years were tracked by all individuals, results were compared, and then problematic data were tracked again by the group. Considerable and consistent differences remained in fish counts from different people (Figures 11-14). Interpersonal bias is considered an important and persistent error that is often neglected in hydroacoustic data processing. This source of error is especially problematic because the differences among people tend to be consistently biased and are therefore additive over time (Table 15). Whenever human trackers are used to produce fish passage estimates, as is often done, or to calibrate an autotracker, as done here, this tendency for human bias should be considered.

If human trackers are used to provide counts for passage estimates, then the data should be distributed to them in such a way that the bias-induced differences are averaged over time. It is preferable that data are distributed so that each person tracks all systems and deployments for a given day, rather than one person specializing on a given system, deployment, or passage route. Personal biases will then be controlled over many days that have been tracked by the several different people. For example, a high tracking individual processing "guided" routes and a low tracking individual processing "unguided" routes would produce FGE

estimates that were too high, whereas the opposite arrangement would produce incorrectly low FGE estimates.

Human vs. Autotracker Comparisons

The autotracker's performance is considered to be acceptably close to that of the mean human tracker and a much better approximation of the mean human fish count than are some of the more biased human trackers. The autotracker was found to produce fish counts that were close to the means of individual human fish counts on five "tracker calibration days" (Figures 11, 12 and 13, Table 15), and for all of the days there was a very strong correlation between autotracker counts and the mean count by human trackers (Figure 14).

Major Passage Metrics

Project and Powerhouse FPE, Spill Efficiency, and Spill Effectiveness

For Project FPE, the summer decline in FPE at the screened units (Units 7-18) was offset by increased spillway passage and continued high PSC guidance efficiency through summer. In this first year of project-wide fish passage sampling at Bonneville Dam, the proportion of all fish to pass the dam by non-turbine routes (Project FPE) was estimated to be 0.79 in both spring and summer, which is close to the goal of 80 percent set in the Biological Opinion. Although Project FPE was the same in spring and summer, Powerhouse FPE declined by about 6 percent at Powerhouse 1 and by about 19 percent at Powerhouse 2 from the spring estimate to the summer estimate.

In both seasons, fish passage through the spillway was the largest component of Project passage (44 percent in spring, 49 percent in summer). Whereas total and daily volumes of water spilled were lower in summer than in spring (Figures 15 and 16), the proportion of the total Project discharge allotted to spill was lower in spring (average = 33 percent for spring days) than in summer (average = 49 percent for summer days), which explains summer's lower spill effectiveness (1.03 compared to 1.36 in spring). Shut down of five or six of eight Powerhouse 2 turbines in summer allowed a higher fraction of total flow for spill and reduced fish passage by the STS-equipped turbines at Powerhouse 2.

The PSC played a major role in increasing Project FPE by 6 percent in spring and 12 percent in summer over a hypothetical Project FPE provided by a combination of turbines with STSs and observed spill. The PSCs 12 percent contribution to Project FPE in summer also was greater than the modest 3 percent increase in FPE associated with the highest spill discharge rates. Figure 45 displays an adjustment of FPE based on the calculated guided passage for Units 1-6 using each day's mean FGE for the three STSs on Powerhouse 1 instead of the mean for the PSC. Under this hypothetical situation Project FPE would be reduced an average of 6 percent in spring and would continuously degrade

throughout summer until it was lowered by about 12 percent. The same exercise using the daily FGE values from Unit 8's ESBS for Units 1-6 increases project-wide FPE in late spring slightly (Unit 8 FGE average = 0.73 for spring days), but the ESBS performed nearly as poorly as the STSs in summer (Unit 8 FGE average = 0.50 for summer days).

Adjustment of PSC efficiency in spring and summer to compensate for not sampling center sluiceways in PSC units would increase mean PSC guidance efficiency to 87 percent and raise the PSC contribution to Project FPE over STS contributions from 6 to 8 percent in spring and 12 to 15 percent in summer. According to radio telemetry results, about 50 percent of tagged fish in the PSC passed through sluice gates in the center intakes of PSC units (Scott Evans, USGS, and Gary Johnson, BioAnalysts, Personal Communication) where they could not be sampled with hydroacoustics. If that 50 percent estimate held for run-of-the-river (untagged) fish, in-turbine sampling with hydroacoustics would have underestimated PSC efficiency by 15 percent. A correction for sluice passage would increase both spring and summer PSC efficiencies to about 87 percent. However, adding one half again as many fish to the PSC-guided category would further increase the southern skew in the Powerhouse 1 fish passage distribution (i.e., consider a 50 percent increase in the height of vertical bars for guided fish at PSC Units 1-6 in Figures 58 and 59). There is no doubt that many run-of-river fish passed through sluice openings at center PSC slots, but it is difficult to imagine 500,000-700,000 fish passing over each 21-ft wide weir with an average water depth of about 2 ft.

Conservative estimates of PSC performance indicate that it was a highly used route in 2000. The PSC guided an estimated 18 percent of the total Bonneville Dam passage (guided, unguided, and spilled fish combined) in spring and 21 percent of the total detected passage in summer (Table 21). These proportions are conservative in that they do not allow for any increments of shallow PSC passage that were undetected by our method, although radio telemetry studies, as mentioned above, indicate that approximately 50 percent of radio-tagged fish passed through the center sluices inside PSC units.

Table 21
Proportions of All Fish Passing by Different Turbine and Non-turbine Passage Routes in Spring and Summer

	Non-turbine Routes			Turbine Routes	
	Powerhouse 1	Powerhouse 2	Spillway	Powerhouse 1	Powerhouse 2
Spring	23% (PSC 18%)	12%	44%	12%	9%
Summer	27% (PSC 21%)	3%	49%	17%	4%

Effect of Spill Rate on Major Fish Passage Metrics

Increases in Project FPE and spill efficiency and decreases in spill effectiveness with increasing spill rate were consistent but small, which made difficult the detection of significant differences for all metrics in spring and summer at $\alpha = 0.05$. Statistically significant positive relationships were found between Project FPE and spill rate in spring and summer, and between spill efficiency and spill in spring but not in summer (although the slope was positive and significant at $\alpha = 0.10$). The slope of the relation between spill effectiveness and spill rate was negative and significant in summer ($P = 0.012$) but not in spring ($P = 0.139$). Hypothesis tests on the equality of means of the same metrics detected significant differences between "high spill" and "low spill" means for Project FPE in spring but not summer. Additionally, significant differences were detected for spill efficiency in both spring and summer, but not for spill effectiveness in either season, although the summer spill effectiveness P-value was rather close to being significant ($P = 0.088$).

Table 22 is presented to clarify these two sets of results.

Table 22 Effect of Spill Rate on Project FPE, Spill Efficiency, and Spill Effectiveness				
	Slope was significant		**Means were different**	
	Spring	**Summer**	**Spring**	**Summer**
Project FPE	Yes	Yes	Yes	No
Spill Efficiency	Yes	No	Yes	Yes
Spill Effectiveness	No	Yes	No	No

Based upon observed relations, it is reasonable to conclude that higher spill rates increased Project FPE and spill efficiency slightly, although not in direct proportion to spill-rate increases. The fish contributing to increased Project FPE and spill efficiency must have come from potentially guided fractions as well as potentially unguided fractions elsewhere at the Project. The difference between "high spill" and "low spill" mean daily Project FPE in spring was only about 5 percent and the difference between "high spill" and "low spill" spill efficiency in spring was 7.3 percent (Table 16). The related mean daily spill rates associated with those daily FPE improvements involved an increase of 45 percent from the "low spill" mean of about 86,000 ft^3/second to the "high spill" mean of 125,000 ft^3/second. Similarly, the significant difference in summer daily spill efficiency means was 8 percent and associated with a "low spill" mean to "high spill" mean increase of 25 percent (84,500 ft^3/second to 106,000 ft^3/second). The relationship between daily spill rate and daily FPE or spill effectiveness probably is not linear over the entire range of spill rates that could occur.

The case for increased spill at night resulting in increased fish passage, spill efficiency, and Project FPE cannot be made with impunity since the two different

spill levels in each season were invariably confounded with different parts of the diurnal cycle. There were essentially two different operational situations at Bonneville Dam in the 2000 passage season: A higher nighttime spill level to speed the down migration of smolts and a lower daytime spill level to reduce adult fallback. Since there is a slight increase in Project FPE and spill efficiency and since spill passage was somewhat higher during high spill periods at night in both spring and summer (Figure 46), it is tempting to assume that spill level was the cause of increased spill passage. However, fish vertical distribution changes from day to night (Tables 17 and 18) and other factors including orientation, motivation, energetic or sensory limitations, or activity level may affect a smolt's likelihood of passing by spill. Whereas fish are aware of changes in their body acceleration via their otolith organs (reviewed extensively in Fay and Popper 1999), for relatively continuous motions and gradual accelerations, visual orientation also is important. Mammals have irises that can rapidly adapt their eyes to lower light levels, but fishes rely on the migration of sensory cells and masking chemicals in the retina, a process that takes much longer than mammalian adaptation. "In general," states J.B.S. Blaxter, an internationally known fish sensory physiologist, "the fall-off in behavioral performance matches the onset of dark adaptation" (Blaxter 1988, p 205). Diel differences in the fish's distribution, condition, or behavior could affect their propensity to pass the spillway.

Descent after sunset is a behavior pattern common to many fishes. In the case of dam passage, fish that are deep are more available for turbine or spillway passage. Diel differences in smolt passage at turbine units are seen that are not a function of increased flow there. Data from this study show that a pulse of smolt passage occurs at turbines soon after sunset (Figures 42 through 45). At the spillway, it seems clear that smolts are not passive migrants at the mercy of the current (see Figures 24 and 25 that compare flow, fish passage, and fish passage density at spillway sections in spring and summer). At The Dalles Dam in 1999 it was found that spill passage increased in the evening in both 30 percent spill and 64 percent spill conditions (Ploskey et al., In Press).

This year spill levels were not selected to provide information on the relationship between spill level and spill passage. Evaluation of that relationship will require a carefully constructed experimental design with an appropriately wide range of spill levels and times so that reliable inferences can be made The best that could be done this year was to evaluate effects of spill bay discharge on hourly spill-bay passage and on total spillway passage for days and nights separately. After removing data from hours that were near sunrise and sunset and hours in which no discharge occurred for a given spill bay, estimated passage was plotted against spill bay discharge through the same spillway for day and night periods separately.

The highest estimated passage through individual spill bays rarely occurred at the lowest or highest spill rates through those bays. Those results also showed that, in either season, a wide range of fish passage estimates were associated with the same discharge level during the day or at night. That would argue for higher passage actually being a function of some factor other than discharge. In fact,

rather than higher spill correlating well with higher passage through single spill bays, it seems that the highest discharge values that are near 15,000 ft^3 / second for any spill bay are never associated with the highest passage estimates. That is consistent with our work at The Dalles Dam in 1999 (Ploskey et al., In Press) in which the highest spill was found to be associated with lower passage estimates than somewhat lower spill. It was realized then that, since higher spills produce higher passage velocities, there could be detectability problems influencing our estimates. For that reason, it was made certain that adequate detectability was available for the spillway by using deployments and multiplexing sequences that would permit increased pulse repetition rates (30 pings/second versus 24 pings/second at The Dalles Dam). It may be that increasing spill level beyond some threshold, perhaps between 10,000 and 15,000 ft^3/second per spill bay, could actually reduce fish passage through those spill bays. This issue requires more thoughtful investigation with a properly devised experimental design and sampling scheme but for now the notion that higher spill passes more fish should be viewed with some caution.

On a broader scale, managers would like to know if increasing total spill increases fish passage through the spillway. The answer appears to be that there is a significant but very modest increase in spillway fish passage from increased spill during the day or at night in spring and at night in summer (Figures 20-23). The high variation in spillway fish passage at any spill discharge results in a poor correlation fit, and spill discharge explained only 1-23 percent of the variation in spillway fish passage.

Spatial Aspect of Fish Passage Metrics

Horizontal Distribution

Relative proportional discharge through the primary passage routes was generally a poor indicator of the relative proportion of fish passage among those same routes. The overall lateral distribution of fish passage through Bonneville Dam during the spring was not consistently related to project flow patterns except that about 35 percent of the fish and 32 percent of the water that passed the Project passed through Powerhouse 1. Fish passage through Powerhouse 2 and the spillway, by contrast, was not closely related to the flow through each respective structure. Powerhouse 2 passed 21 percent of the fish with 36 percent of the flow, and the spillway passed 44 percent of the fish with only 32 percent of the flow in spring.

Since fish passage more nearly matched project discharge patterns in summer than during spring, it is possible that the higher spill discharge prevalent during spring combined with channel morphology to divert a greater proportion of fish away from Powerhouse 2 and to the spillway. It is also possible that behavioral differences inherent in changing species compositions, sizes, and ages of spring and summer smolt populations resulted in varying responses to project flow patterns.

Horizontal passage patterns at Powerhouse 1 were consistent between seasons, although the horizontal distribution of fish passage for the entire project varied between spring and summer. Fish passage by spill bay was not entirely a function of discharge by spill bay. Although both fish passage and discharge were lowest through Spill Bays 5-7, the bays that passed the most water did not pass the most fish (Figures 24-27). More water was spilled through Bays 2-4, relative to other sections of the spill bay, yet the density of fish passage was highest at Bays 11-14 during both spring and summer.

Vertical Distribution

The vertical distribution of fish in front of the PSC at Powerhouse 1 was conducive for successful surface collection with a deep slot configuration. Sample volumes upstream of the PSC were located only about 1-3 m from the face of the PSC. From 92 to 99 percent of fish detected immediately upstream of the PSC in spring and from 85 to 96 percent of summer fish were above the elevation of the PSC floor. Based on these fish distributions, a surface collector located upstream of Units 1-6 at Powerhouse 1 would likely be highly effective.

Most of the fish 100 ft upstream of Powerhouse 2 were distributed above the elevation of the top of the turbine intakes during both spring and summer. In spring a large eddy was observed extending from the north shoreline to upstream of Intake 17c. This eddy would not influence vertical distributions of fish near the north end of the powerhouse unless the probability of detecting a fish multiple times was uniform with depth. In summer reduced discharge through Powerhouse 2 would permit even sub-yearling fish to swim anywhere in the forebay, and they could have been detected multiple times by hydroacoustic beam. Multiple detections at locations 100 ft upstream of TIEs would not affect vertical distribution estimates unless the probability of obtaining multiple detections varied with depth.

Immediately upstream of the trash racks at Intakes 14b and 17c, summertime fish distributions were lower in the water column than those observed 100 ft upstream, but most fish were still in a favorable position for diversion by the submerged traveling screens. From 66 to 72 percent of all fish were detected above the elevation of the top of the intake, and from 85 to 93 percent of detected fish were higher in the water column than the tip of the screens (Figure 38). These observations are consistent with observations in 1996 and 1997 in mobile hydroacoustic surveys (Ploskey et al. 1998; BioSonics 1998, respectively).

Temporal Trends in Fish Passage

The temporal correspondence of major peaks in the proportion of fish passing Bonneville Dam in spring and of two of three peaks in summer by hydroacoustic sampling and Powerhouse 2 smolt sampling in the JBS by the NMFS was reassuring. Some correspondence would be expected if most of the fish detected by hydroacoustics were juvenile salmon. The third peak that was detected by hydroacoustics but not by sampling in the JBS in late June could be explained in one of two ways. First, the hydroacoustic sample was of all fish passing through the project whereas the smolt-trap sample was only of guided fish passing 2-3 units operating at Powerhouse 2. Given the low percent guidance efficiency of screens in late summer (mean hydroacoustic estimate = 0.16), one would not expect JBS sampling to capture that peak. Second, the third summer peak detected by hydroacoustics but not by JBS sampling may have been composed of a greater proportion of shad than earlier peaks detected by both methods. Larger fish were filtered out in late summer by not counting any fish with echo or target strengths $> - 45$ dB, but that filtering is less than perfect. Large fish like American shad can have an apparent acoustic size less than -45 dB when detected off axis in the sample volume of a single-beam transducer. Adult shad have greater swimming abilities and are less likely to be routed through the JBS than are juvenile salmonids.

There are four reasons why Project FPE did not decline precipitously in summer as did the FGE of turbines with screens (Units 7-18). First, Powerhouse 2 with poor FGE in summer was only operating at 25-38 percent of capacity because 5-6 of the units were off most of the time. Second, the efficiency of the PSC did not decline in summer and contributed more to Project FPE in late spring and summer than it did most of spring (Figure 45). Third, on some days in summer, spill efficiency accounted for a greater proportion of FPE than it did in spring, although overall seasonal trends in both Project FPE and spill efficiency were relatively stable throughout both seasons. Fourth, the proportion of fish relative to the proportion of water passed was relatively constant in spring and summer at the PSC, although the spill effectiveness declined slightly during summer (Figure 46).

Perhaps the most significant finding of this study was the summer decline in FGE of turbines with screens while the efficiency of the PSC remained high and relatively stable (Figure 44). Even the efficiency of the ESBS in Unit 8 was as poor as that of STSs in other turbines in late summer. Two factors may contribute to the continued success of the PSC in summer. First, the interception location of the PSC was upstream of the powerhouse and, second, the PSC was open to the sky and passed relatively more fish during the day than at night. In contrast, most fish passage through Powerhouse 1 turbines occurred at night. It is assumed that willingness of fish to enter a collector during the daytime would be greater when ambient lighting does not change abruptly at the entrance. The success of the PSC also probably has a lot to do with depth (45 ft), entrance velocities, and upstream hydraulics. The diel pattern of smolt passage through Powerhouse 2 turbines was more crepuscular in spring and summer than it was nocturnal. It has

been speculated that the peak in fish passage through turbines around sunset results from passage of individuals that have lost visual cues and the ability to hold in the upper water column. The daytime dominated passage at the PSC suggests that fish will readily enter the PSC during the day whereas they generally resist passing into turbines during the day and end up passing more at sunset.

The problem with concluding that increased spill increased the number of fish passing the spillway is that spill rates and day-night effects were confounded in 2000 because increased spill usually occurred at night. For this reason, an evaluation of spill rate on spill effectiveness and fish passage could provide valuable information for optimizing spill at Bonneville Dam. Spilling more water at night increased the proportion of fish passing the spillway, but the increase was not directly proportional to spill rate (i.e., 26-47 percent more water passed only 17-19 percent more fish). In addition, spill effectiveness tended to be lower than the effectiveness of the PSC in 2000 and of the sluice chute at Powerhouse 2 when it was last tested in 1998. Unfortunately, it is not known where benefits to juvenile salmon are on the spill curve. The data acquired suggest that there may be diminishing returns with increasing spill rate and that there may be more effective ways to spill. However, only by purposefully manipulating spill over a wide range of discharge can one hope to identify optimum spill patterns and rates.

Fish Guidance Efficiencies

The most important contribution from this work on FGEs at Bonneville Dam is the high level of performance of Powerhouse 1's PSC, especially in summer. Summer passage has proven to be a serious challenge for smolt guidance at lower Columbia River dams, and this first year of project-wide sampling shows that Bonneville Dam is no exception.

The STSs performed worse than either the ESBS at Unit 8 or the PSC on Units 1-6 in spring. The FGE of the STSs on Powerhouse 2 averaged only 52 percent in spring although most of the interior units on that powerhouse were somewhat higher. Unit 11's STS performed most poorly. On Powerhouse 1 the PSC and the ESBS performed equally well in spring with estimated FGEs of 72 percent. The southernmost two units of the PSC performed best with FGEs of over 80 percent.

The in-turbine sampling shows that the PSC performed as well as the ESBS did in spring and much better than the ESBS or STSs in summer. At Powerhouse 1, the PSC and the ESBS performed equally well in spring with estimated FGEs of 72 percent. The two southernmost units of the PSC performed best with FGEs of over 80 percent. The FGE of the STSs in Powerhouse 2 averaged only 52 percent in spring, although most of the interior units on that powerhouse were somewhat higher. Unit 11's FGE was the lowest in spring. In summer the average FGE of STSs were 36 percent at Powerhouse 1 and 35 percent at Powerhouse 2, and the FGE of the ESBS in Unit 8 had dropped to 50 percent. Powerhouse 2 was largely idle in summer, but when interior units were operated, the STSs produced relatively high FGEs. Unit 11, which ran most of the summer,

had the lowest FGE, but Unit 18 at the northern end did better with an FGE of about 50 percent.

To get a more complete picture of the passage seasons, viewing FGE in combination with horizontal distribution is suggested (see Figures 56 and 57). These show that a large proportion of the spring migrants and an even larger proportion of the summer migrants passed south of the wing wall that extends upstream between Units 6 and 7 and that most of those fish were guided by the PSC.

Comparing FGE Sampling Methods for the PSC

No significant correlations were found between fish counts in turbine intakes downstream of the PSC with fish counts upstream of 20-ft wide PSC slots, unlike a significant correlation observed for a 5-ft wide slot in 1999. The most likely explanation for the differences is that the linear flow velocity at the 5-ft wide slot (5 fps) in 1999 was 39 percent higher than the velocity at the 20-ft wide slots in 2000 (3.5 fps). Given the wallowing of fish in split-beams immediately upstream of the 20-ft wide PSC slots, it seems logical that those fish were not committed to passing into the PSC and in fact may have been counted multiple times. By contrast, the probability of a fish in 5 fps flow passing into the PSC was likely significantly greater than it was for fish in the 3.5 fps flows observed in this study. If fish were not entrained or committed to passing into the 20-ft slot, they could be detected moving toward an entrance and still swim away after passing through the hydroacoustic beam. It was believed that differences in the probability of detected fish passing into the PSC may explain why significant correlations were found in 1999 but not in 2000. It also is possible that the model used to classify fish as passing into the PSC was not accurate. The acoustic screen model used to expand fish is best applied when the acoustic beams are between two structures or the flow through the beam is fast enough to preclude fish from being counted more than once.

Although counts from split-beam sampling upstream from the PSC were not correlated with the in-turbine single-beam counts, those data can still be used to evaluate the availability of fish for collection. Many more fish were found just upstream from the PSC face above the level of the PSC floor than below the level of the PSC floor in all hours of the day in summer. Expanded counts showed that there were twice as many fish above the level of the floor at night and an even higher proportion above the floor during the daytime hours. Even though the numbers of fish that actually entered the slots and passed through the PSC from those data cannot be confidently estimated, the data indicate that a large proportion of the fish were available to be collected by the PSC in summer.

By segregating range bins in forebay transducer beams, expanded estimates of fish abundance just upstream from the top halves and the bottom halves of the PSC slots were determined. During all hours of the day and particularly during daylight hours there were many more fish upstream of the top halves of the PSC slots than there were upstream of the bottom halves of the slots. Mobile hydroacoustics at Bonneville Dam (Ploskey et al. 1998; BioSonics Inc. 1998)

have shown that upstream of the dam most fish are higher in the water column than screen FGEs would indicate. Current data suggest that, at the face of the surface collector, fish have not begun the descent that brings them under the screens and delivers them to the turbine intakes because the PSC intercepts fish before they are entrained.

Comparing FGE Sampling Methods for Unit 8

Netting and hydroacoustics both provide imperfect estimates of FGE because of gear and sampling limitations, and unexplained variability and bias adversely affects the fit of correlations to these data. Nevertheless, comparison of sampling methods provides the opportunity to identify potential biases and highlights strengths and weaknesses of both methods. Bias cannot be measured with a single method and is therefore more insidious and difficult to quantify than sampling precision.

The correlation of hydroacoustic and netting estimates of FGE (r^2=0.65) was better than those for guided and unguided components of FGE because of compensating errors in the numerator and denominator of the ratio estimator during simultaneous hydroacoustic sampling of both FGE components. The assumption of equal detectability of guided and unguided smolts must have been reasonable most of the time given correlations between hydroacoustic and netting estimates of FGE with a correlation slope approaching 1. The near 1:1 ratio of numbers of guided fish netted in the gatewell to hydroacoustic counts above the ESBS and of numbers of unguided, fyke-netted fish to hydroacoustic counts below the ESBS was reassuring, despite substantial scatter in the correlation plots and $r^2 = 0.53$. The near 1:1 ratios for guided and unguided fish estimates by the two methods suggest that hydroacoustic detectability was not just equal but also relatively accurate, yielding appropriate expansion factors.

Many factors could contribute to scatter in the correlations, particularly when both the dependent and independent variables have error and potential bias associated with them. Both netting methods that were considered as a ground truth are less than 100 percent efficient, particularly for young salmon. Unless known numbers of fish were marked, introduced, and netted, the two types of nets were not calibrated and could have had different efficiencies. The assumption of equal net efficiencies may be incorrect and result in biased FGE estimates because the gatewell and turbine intake environments are dramatically different, as are the methods used to sample the two areas. Gessel et al. (1991) reported > 95 percent efficiency for gatewell dip-netting at Bonneville Dam. However, Steig and Ransom (1993) reported that many juvenile salmon guided by a bar screen at Rocky Reach Dam on the Columbia River were not sampled by a dip basket. They estimated that net-based FGE estimates would have more than doubled if net efficiency had been 100 percent. Fish also may remain in the gatewell slot before a test, may be lost through orifices during the test, or may be lost out the bottom of the gatewell during and particularly at the end of a test. Fish also may accumulate in an intake while the turbine is off and, depending upon their vertical distribution at startup, may bias estimates of numbers of guided or unguided fish.

Paired t-tests indicated that mean estimates of FGE by the two sampling methods did not differ significantly in spring, and although differences were significant for both seasons combined, means only differed by 3 percent and probably were biologically meaningless. In summer the mean hydroacoustic estimate was 6 percent higher than the mean netting estimate, but even that difference is not too bothersome given problems encountered trying to exclude shad from the sample in summer.

Hydroacoustic sampling provides only a relative index to fish passage, unless correlated against unbiased physical capture estimates. However, significant correlations between hydroacoustic and netting estimates indicate that the hydroacoustic data could be scaled by correlation coefficients to increase the accuracy of passage estimates. Ideally, nets would be calibrated to account for net efficiency bias. The significance of calibrating hydroacoustics to netting is that the nondestructive nature of hydroacoustic sampling permits it to be used much more extensively than netting.

Correlations between estimates of FGE derived from netting and hydroacoustic sampling are reassuring and useful because both methods have advantages that can be exploited to improve overall sampling effectiveness at a project. Netting can provide estimates of fish passage and guidance efficiency by species but is labor intensive, injures or kills fish, and cannot be used for more than a few hours per day at one or two intakes. This restriction to one or two intakes prevents biologists from evaluating spatial variation in fish passage and FGE among intakes. Hydroacoustic sampling can be applied to all turbine units, 24 hr/day, without adversely affecting fish. However, hydroacoustic sampling provides only a relative index to fish passage unless calibrated against unbiased netting and cannot provide species-specific estimates without netting to accurately estimate species composition. If the goal is to determine the efficiency of many screens or other fish guidance structures during spring and summer runs, hydroacoustics can provide a meaningful index. Some netting should be required to calibrate hydroacoustic estimates, however, if fish passage estimates are important or if species-specific estimates of FGE are desired.

PSC Guidance Efficiency by Different Methods

Average collection efficiency of the PSC was 83 percent in spring and 84 percent in summer after it was adjusted by radio-telemetry estimates of the proportion of smolts in the PSC that passed into the center-slot sluiceways, and the adjusted estimates agree favorably with estimates by other methods. Sluice gates in center slots of PSC Units 1-6 were open throughout spring and summer 2000 but could not be sampled with hydroacoustics. Nevertheless, radio-telemetry data indicated that approximately 50 percent of radio-tagged fish in the PSC passed through the sluiceway (Scott Evans, USGS, and Gary Johnson, BioAnalysts, Personal Communication). Therefore, hydroacoustic estimates of total passage at the PSC were at least 15 percent low in 2000. Radio-telemetry and acoustic-telemetry estimates of PSC efficiency for all species combined in spring 2000 were 83 and 92 percent, respectively (Johnson and Carlson 2000), and those estimates agree well with an 87 percent hydroacoustic estimate

corrected for sluiceway passage. In 1998, hydroacoustic estimates of PSC collection efficiency for 20-ft slot openings in PSC Units 3 and 5 were 87.8 percent in spring and 92 percent in summer. A radio-telemetry estimate for 1998 was 97.5 percent for the 20-ft slot treatment. In 1999, hydroacoustic estimates for a 20-ft slot entrance at Unit 5 were 84.4 percent in spring and 75.2 percent in summer. Radio-telemetry studies in 1999 estimated 20-ft slot efficiency at 65 percent, the lowest of any estimates by any method (Johnson and Carlson 2000).

References

BioSonics, Incorporated. (1998). "Hydroacoustic evaluation and studies at Bonneville Dam, Spring/Summer 1997." Contract Report to the U.S. Army Corps of Engineers District, Portland, OR.

Blaxter, J. H. S. (1988). "Sensory performance, behavior, and ecology of fish," *The sensory biology of aquatic animals*. J. Atema, R.R. Fay, A.N. Popper, and W.N. Tavolga, ed. Springer-Verlag. New York, 203-232.

Fay, R. R., and Popper, A. N. (ed). (1999). *Comparative hearing: Fish and amphibians*. Springer-Verlag. New York.

Gessel, M. H., Monk, B. H., and Williams, J. G. (1988). "Evaluation of the juvenile fish collection and bypass systems at Bonneville Dam 1987." Annual Report by the U.S. Department of Commerce, National Oceanic and Atmospheric Administration, National Marine Fisheries Service, Coastal Zone and Estuarine Studies Division, to the U.S. Army Engineer District, Portland, OR.

Gessel, M. H., Williams, J. G., Brege, D. A., and Krcma, R. F. (1991). "Juvenile salmonid guidance at the Bonneville Dam Second Powerhouse, Columbia River, 1983-1989." *North American Journal of Fisheries Management* 11, 400-412.

Giorgi, A. E., and Stevenson, J. R. (1995). "A review of biological investigations describing smolt passage behavior at Portland District Corps of Engineer Projects: Implications in surface collection systems," Contract Report prepared by Don Chapman Consultants, Inc., for the U.S. Army Engineer District, Portland, OR.

Hawkes, L. A., Martinson, R. D., Absolon, R. F., and Killins, S. (1991). "Monitoring of downstream salmon and steelhead at Federal hydroelectric facilities," Annual Report 1990 by the U.S. Department of Commerce, National Oceanic and Atmospheric Administration, National Marine Fisheries Service, Environmental and Technical Services Division, to the U.S. Department of Energy, Bonneville Power Administration, Portland, OR.

Johnson, G. E., and Carlson, T. J. (2000). "Monitoring and evaluation of the prototype surface collector at Bonneville First Powerhouse in 2000: Synthesis of information on PSC Performance," U.S. Army Corps of Engineers Draft Report prepared by BioAnalysts, Inc and Battelle.

Krcma, R. F., DeHart, D., Gessel, M., Long, C., and Sims, C. W. (1982). "Evaluation of submersible traveling screens, passage of juvenile salmonids through the ice-trash sluiceway, and cycling of gatewell-orifice operations at the Bonneville first powerhouse, 1981," Final Report by the U.S. Department of Commerce, National Oceanic and Atmospheric Administration, National Marine Fisheries Service, Coastal Zone and Estuarine Studies Division, to the U.S. Army Engineer District, Portland, OR.

Love, R. H. (1977). "Target strength of an individual fish at any aspect," *Journal of the Acoustical Society of America* 62(6), 1397-1403.

Magne, R. A. (1987). "Hydroacoustic monitoring at the Bonneville Dam Project in 1987," Fishery Field Unit, U.S. Army Engineer District, Portland, OR.

Magne, R. A., Rawding, D. J., and Nagy, W. T. (1986). "Hydroacoustic monitoring at the Bonneville Dam second powerhouse during 1986 fish guiding efficiency tests," Fishery Field Unit, U.S. Army Engineer District, Portland, OR.

Magne, R. A., Stansell, R. J., and Nagy, W. T. (1989). "A summary of hydroacoustic monitoring at the Bonneville Dam Second Powerhouse in 1988," Fishery Field Unit, U.S. Army Engineer District, Portland, OR.

Muir, W. D., Giorgi, A. E., Zaugg, W. S., and Beckman, B. R. (1989). "An assessment of the relationship between smolt development and fish guidance efficiency at Bonneville Dam," Annual Report by the National Marine Fisheries Service, Coastal Zone and Estuarine Studies Division, Northwest Fisheries Center, Seattle, WA.

Ploskey, G. R., and Carlson, T. J. (1999). "Comparison of hydroacoustic and net estimates of fish guidance efficiency of an extended submersible bar screen at John Day Dam," *North American Journal of Fisheries Management* 19, 1066-1079.

Ploskey, G. R., Johnson, P. N., Nagy, W. T., Burczinski, M. G., and Lawrence, L. R. (1998). "Hydroacoustic evaluations of smolt passage at Bonneville Dam including surface collection simulations," Technical Report EL-98-4, U.S. Army Engineer Waterways Experiment Station, prepared for the U.S. Army Engineer District, Portland, OR.

Ploskey, G. R., Nagy, W. T., Lawrence, L. R., Hanks, M. E., Schilt, C. R., Johnson, G. E., Patterson, D. S., and Skalski, J. R. (2001). "Hydroacoustic evaluation of juvenile salmon passage at The Dalles Dam: 1999," ERDC/EL TR-01-11, U.S. Army Engineer Research and Development Center, Vicksburg, MS.

Skalski, J. R., and Robson, D. S. (1992). *Techniques for wildlife investigations: Design and analysis of capture data*. Academic Press, San Diego, CA.

Stansell R. J., Magne, R. A., Nagy, W. T., and Beck, L. M. (1990). "Hydroacoustic monitoring of downstream migrant juvenile salmonids at Bonneville Dam, 1989," Fishery Field Unit, U.S. Army Engineer District, Portland, OR.

Steig, T. W., and Ransom, B. H. (1993). "Long term hydroacoustic evaluations of a fixed in-turbine fish diversion screen at Rocky Reach Dam on the Columbia River, Washington," *Waterpower '93, Proceedings of the International Conference on Hydropower*, American Society of Civil Engineers, D. W. Hall, ed., New York, 219-228.

Thorne, R. E., and Kuehl, E. S. (1989). "Evaluation of hydroacoustics techniques for assessment of juvenile fish passage at Bonneville Powerhouse I," Final Report by BioSonics Inc., Seattle, WA, for the U.S. Army Engineer District, Portland, OR.

Uremovich, B. L., Cramer, S. P., Willis, C. F., and Junge, C. O. (1980). "Passage of juvenile salmonids through the ice-trash sluiceway and sqawfish predation at Bonneville Dam, 1980," Oregon Dep. Fish. Wildl. Annual progress report prepared for the U.S. Army Engineer District, Portland, OR.

Willis, C. F., and Uremovich, B. L. (1981). "Evaluation of the ice and trash sluiceway at Bonneville Dam as a bypass system for juvenile salmonids, 1981," Oregon Department of Fish and Wildlife. Annual progress report prepared for the U.S. Army Engineer District, Portland, OR.

Wood, L. A., Martinson, R. D., Graves, R. J., Carroll, D. R., and Killins, S. D. (1994). "Monitoring of downstream salmon and steelhead at Federal hydroelectric facilities," Annual Report 1993 by the U.S. Department of Commerce, National Oceanic and Atmospheric Administration, National Marine Fisheries Service, Environmental and Technical Services Division, to the U.S. Department of Energy, Bonneville Power Administration, Portland, OR.

REPORT DOCUMENTATION PAGE

Form Approved
OMB No. 0704-0188

1. REPORT DATE *(DD-MM-YYYY)*	2. REPORT TYPE	3. DATES COVERED *(From - To)*
May 2002	Final report	

4. TITLE AND SUBTITLE

Hydroacoustic Evaluation of Fish Passage Through Bonneville Dam in 2000

5a. CONTRACT NUMBER

5b. GRANT NUMBER

5c. PROGRAM ELEMENT NUMBER

6. AUTHOR(S)

Gene R. Ploskey, Carl R. Schilt, Michael E. Hanks, John R. Skalski, William T. Nagy, Peter N. Johnson, Deborah S. Patterson, Jina Kim, and Larry R. Lawrence

5d. PROJECT NUMBER

5e. TASK NUMBER

5f. WORK UNIT NUMBER

7. PERFORMING ORGANIZATION NAME(S) AND ADDRESS(ES)

See reverse.

8. PERFORMING ORGANIZATION REPORT NUMBER

ERDC/EL TR-02-8

9. SPONSORING / MONITORING AGENCY NAME(S) AND ADDRESS(ES)

U.S. Army Engineer District, Portland
Portland, OR 97208-2946

10. SPONSOR/MONITOR'S ACRONYM(S)

11. SPONSOR/MONITOR'S REPORT NUMBER(S)

12. DISTRIBUTION / AVAILABILITY STATEMENT

Approved for public release; distribution is unlimited.

13. SUPPLEMENTARY NOTES

14. ABSTRACT

This study was one of many investigations of the U.S. Army Engineer District, Portland, involving monitoring and assessment of juvenile fish passage at Bonneville Dam. It was a joint study by the ERDC Environmental Laboratory and Pacific Northwest National Laboratory to evaluate the performance of a Prototype Surface Collector and the fish passage efficiency (FPE) of the extended length bar screen at Unit 8.

The goal of this study was to report the first project-wide estimates of FPE, spill efficiency, and spill effectiveness for the Bonneville Project. These data provide a valuable baseline for evaluating the performance of future management efforts to improve juvenile fish passage. Detailed statistical methods are presented.

15. SUBJECT TERMS

Hydroacoustic
Bonneville Dam
Fish passage

16. SECURITY CLASSIFICATION OF:			17. LIMITATION OF ABSTRACT	18. NUMBER OF PAGES	19a. NAME OF RESPONSIBLE PERSON
a. REPORT	**b. ABSTRACT**	**c. THIS PAGE**			**19b. TELEPHONE NUMBER** *(include area code)*
UNCLASSIFIED	UNCLASSIFIED	UNCLASSIFIED		140	

7. (CONTINUED).

Pacific Northwest National Laboratory
902 Battelle Boulevard
Richland, WA   99352

Mevatec Corporation
1525 Perimeter Parkway
Huntsville, AL   35806

U.S. Army Engineer District, Portland
P.O. Box 2946
Portland, OR   97208-2946

DynTel Corporation
3530 Manor Drive, Suite 4
Vicksburg, MS   39180

U.S. Army Engineer Research and Development Center
Environmental Laboratory
3909 Halls Ferry Road
Vicksburg, MS   39180-6199